GROTHENDIECK SHENANIGANS: PERMUTONS FROM PIPE DREAMS VIA INTEGRABLE PROBABILITY

A. H. MORALES, G. PANOVA, L. PETROV, D. YELIUSSIZOV

Abstract. We study random permutations corresponding to pipe dreams. Our main model is motivated by the Grothendieck polynomials with parameter $\beta = 1$ arising in the K-theory of the flag variety. The probability weight of a permutation is proportional to the principal specialization (setting all variables to 1) of the corresponding Grothendieck polynomial. By mapping this random permutation to a version of TASEP (Totally Asymmetric Simple Exclusion Process), we describe the limiting permuton and fluctuations around it as the order n of the permutation grows to infinity. The fluctuations are of order $n^{\frac{1}{3}}$ and have the Tracy–Widom GUE distribution, which places this algebraic (K-theoretic) model into the Kardar–Parisi–Zhang universality class. As an application, we find the expected number of inversions in this random permutation, and contrast it with the case of non-reduced pipe dreams.

Inspired by Stanley's question for the maximal value of principal specializations of Schubert polynomials, we resolve the analogous question for $\beta = 1$ Grothendieck polynomials, and provide bounds for general β. This analysis uses a correspondence with the free fermion six-vertex model, and the frozen boundary of the Aztec diamond.

1. Introduction

1.1. **A story from Algebra to Probability.** Algebraic Combinatorics established itself as a field that uses combinatorial methods to understand algebraic behavior in problems ranging from Group Theory to Algebraic Geometry. It started with stark exact formulas, like the celebrated hook-length formula for the dimension of irreducible modules of the symmetric group S_n; beautiful interpretations, such as the Littlewood–Richardson rule for the structure constants of representations of the general linear group GL_n; powerful and intricate bijections, such as the Robinson–Schensted–Knuth correspondence. However, exact answers only go so far, leaving room for questions like "approximately how many", "what are the typical objects", and "what is the typical behavior". These questions lead us into the realm of Asymptotic Algebraic Combinatorics, which aims to answer them with the help of tools originating outside of Combinatorics. In the present work, we employ Integrable Probability, a rapidly evolving field focused on developing and analyzing interacting particle systems and random growth models possessing a certain degree of structure or symmetry. The arising probabilistic models exhibit rich structure leading to new permutons representing the typical permutations. The connection between the algebraic model and statistical mechanics is multi-fold via a correspondence between the so-called bumpless pipe dream models for Schubert/Grothendieck and the six-vertex model. The well studied free fermion six-vertex model and the frozen boundary of the Aztec diamond are key to understanding the maximal permutations.

On the algebro-combinatorial side, many significant questions concerning exact formulas and combinatorial interpretations in the cohomology and K-theory of the flag variety remain open. Understanding their asymptotic behavior is thus even more natural. Stanley [Sta17] asked the most basic question on the principal specializations of Schubert polynomials $\mathfrak{S}_w$ (representing

cohomology classes of the flag variety): does the following limit exist

$$\lim_{n\to\infty} \frac{1}{n^2} \log_2 \max_{w\in S_n} \mathfrak{S}_w\big(\underbrace{1,\dots,1}_{n}\big),$$

and if so, what is it and for which permutations w is this achieved. This question (including the existence of the limit) is still open. In [MPP19], a lower bound of about 0.29 was established for *layered permutations*. An upper bound of about 0.37 comes from a remarkable connection with Alternating Sign Matrices and the six-vertex model (see Remark 6.8). As we shall see later, this question has an even more interesting interpretation from the Probability/Statistical Mechanics side as it is asking for the asymptotic growth of the energy in a model with *long-range interactions* (pipes are not allowed to cross more than once), and for such models no general tools are known.

A natural one-parameter generalization of Schubert polynomials are the Grothendieck polynomials $\mathfrak{G}_w^\beta$, which represent K-theoretic classes of the flag variety. Extending Stanley's questions, we would like to understand the asymptotic behavior of maximal principal specializations $\max_{w\in S_n} \mathfrak{G}_w^\beta(1^n)$ of Grothendieck polynomials. This question was first touched on in [MPP22], [Den22]. Establishing a family of such maximal permutations would shed light on the Schubert questions as $\beta \to 0$, as well as on the corresponding long-range interaction model.

Thanks to a combinatorial model for Grothendieck and Schubert polynomials, these questions have very natural statistical mechanics interpretations. Namely, both polynomials are partition functions of tilings into crosses and elbows of a size n triangle (staircase) shape, which result in a configuration of n "pipes". Such pipe configurations are often called *pipe dreams*. In the Schubert case, the only valid tilings are the ones where no two pipes cross more than once. This is a global (long-range interaction) condition, which makes the model much less tractable. In the Grothendieck case for $\beta = 1$, all tilings are allowed, but the pipes must be resolved (reduced) to obtain a permutation. One of the key ideas leading to our analysis is that this model can be mapped to a colored stochastic six-vertex model (and furter to TASEP, the Totally Asymmetric Simple Exclusion Process). The resulting interacting particle systems have only local (short-range) interactions, and are amenable to techniques from Integrable Probability.

In this work, we investigate the asymptotics of the *typical* $\beta = 1$ *Grothendieck random permutations* and characterize their limit shape which is described by a permuton. We also study fluctuations of Grothendieck random permutations around the limiting permuton. They are of order $n^{\frac{1}{3}}$ and asymptotically have the Tracy–Widom GUE distribution. This distribution was first observed in the fluctuations of the largest eigenvalue of Gaussian random matrices with unitary symmetry. By now, having Tracy–Widom fluctuations is an indication that a model is within the Kardar–Parisi–Zhang (KPZ) universality class [Cor12], which includes a wide range of random growth models and interacting particle systems. We also derive the expected number of inversions, which are of order n^2.

We also study the natural, yet not as algebraically motivated, model, where the staircase is tiled with crosses with probability p and elbows with probability $1-p$, and the pipes follow the tiles without any reductions or reassignments. Using simple random walks, we show that the resulting random permutation is close to the identity, and, moreover, that the total displacement $\sum_{i=1}^n |i - w_i|$ and length (number of inversions) of this permutation are of order $n^{3/2}$. This was motivated by, and partially resolves, an open problem of Colin Defant.

Returning to the original question, we investigate the asymptotics of $\max_{w\in S_n} \mathfrak{G}_w^\beta(1^n)$. When $\beta = 1$, this maximum is known to be $O(2^{\binom{n}{2}})$. Using the correspondence with 2-enumerated

Alternating Sign Matrices (equivalently, the six-vertex model with domain wall boundary conditions and free-fermion weights; or the model of uniform domino tilings of the Aztec diamond), we show that a large family of layered permutations also achieve this asymptotic maximum. For general β, we establish certain bounds for the maximal principal specialization.

1.2. **Pipe dreams and permutations.** We denote by S_n the set permutations of $\{1, 2, \dots, n\}$ that we write in the one-line notation $w = w_1 w_2 \cdots w_n$ unless indicated otherwise. We also denote the image of i under w by $w(i)$, and use the notation $w_i = w(i)$ interchangeably when this does not lead to confusion. The longest permutation $n\, n-1 \dots 2\, 1$ is denoted by $w_0 = w_0(n)$. For a permutation w of length ℓ, we denote by $R(w)$ the set of *reduced words* of w, that is, tuples $(r_1, \dots, r_\ell)$ such that $s_{r_1} \cdots s_{r_\ell}$ is a reduced decomposition of w, where $s_i = (i, i+1)$ are the simple transpositions.

Grothendieck polynomials can be defined combinatorially via pipe dreams (equivalently, rc-graphs), as partition functions of the following model.

A *pipe dream* of order n is a tiling of the staircase shape (having $n-1$ boxes in the first row, $n-2$ boxes in the second row, and so on, with boxes left-justified) by tiles of two types: *bumps*  and *crossings*  . The n-th diagonal below the staircase is equipped with half bumps  (whose boundary we do not draw). Each of the boxes can have a tile of any type, so there are $2^{\binom{n}{2}}$ pipe dreams of order n. See Figure 1, left, for an example of a pipe dream of order 6.

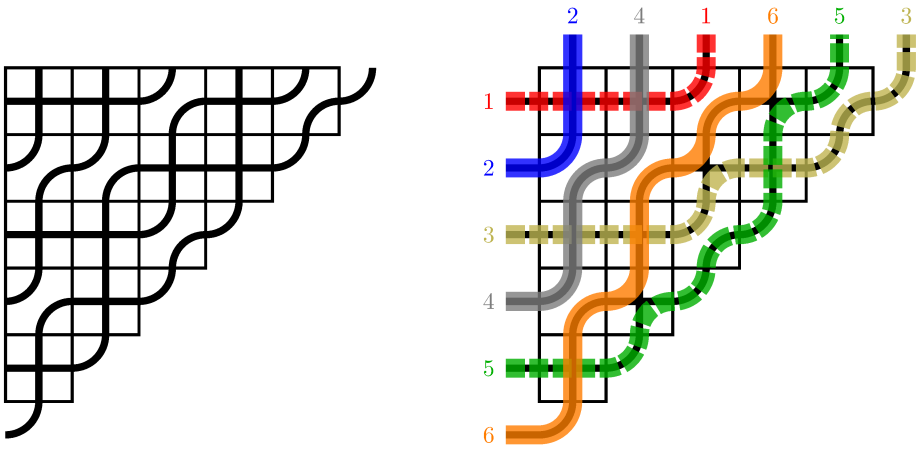

FIGURE 1. **Left**: A pipe dream D of order 6. **Right**: A reduction of the pipe dream leading to the permutation $w(D) = 241653$. The right image appears in color online. Dashing is added for the printed version and accessibility.

A pipe dream (a tiling of the staircase shape) forms a collection of strands (or *pipes*) labeled 1 to n from the row where they start. A pipe dream is called *reduced* if any two pipes cross through each other at most once.

Definition 1.1 (Reduction of a pipe dream)**.** Given a pipe dream D that is not necessarily reduced, the *reduction* of D is a unique reduced pipe dream D' obtained as follows: starting at the bottom left tile traverse the pipe dream upwards along columns and to the right. For each encountered crossing, replace it with a bump if the pipes have already crossed in the already traversed squares. The labeling of pipes together with a reduction is indicated by colored paths in Figure 1, right.

Definition 1.2 (Permutation from a pipe dream)**.** One can associate a permutation $w(D) \in S_n$ to a pipe dream of order n as follows. If D is reduced then $w(D)_j^{-1}$ is the column where the pipe j ends up in.[1] Equivalently, the column j contains the exiting pipe of color $w(D)_j$. Note that to capture the column number for the pipe j, we need the inverse permutation $w(D)^{-1}$.

If D is not reduced, then $w(D)$ is the permutation associated to the reduction D' of D.

Remark 1.3. Alternatively, the permutation $w(D)$ from a non-reduced pipe dream can be defined using the *Demazure product* [Dem74]. Namely, for an elementary transposition $s_i = (i, i+1)$ (with $1 \leqslant i \leqslant n-1$) and a permutation $w \in S_n$, the Demazure (or 0-Hecke) product is defined as

$$s_i \star w := \begin{cases} ws_i, & \text{if } \ell(ws_i) > \ell(w), \\ w, & \text{otherwise.} \end{cases} \tag{1.1}$$

Here $\ell(\cdot)$ is the length of a permutation, that is, its number of inversions.

To each cross in D, associate a transposition s_i. Reading from the bottom left to top right, we obtain a (not necessarily reduced) word. For example, the pipe dream in Figure 1, left, corresponds to the word $s_5 s_5 s_3 s_4 s_1 s_2 s_4 s_5 s_4$. Replacing this product of elementary transpositions by the Demazure product, we obtain the permutation $w(D)^{-1}$. For our example, the Demazure product is

$$s_5 \star s_5 \star s_3 \star s_4 \star s_1 \star s_2 \star s_4 \star s_5 \star s_4 = s_5 s_2 s_1 s_4 s_3 s_5 = 316254,$$

which is the inverse of $w(D)$ given in Figure 1, right.

Let $\mathrm{PD}(n)$ and $\mathrm{RPD}(n)$ be the sets of pipe dreams and reduced pipe dreams of size n. For each $w \in S_n$, let $\mathrm{PD}(w)$ and $\mathrm{RPD}(w)$ be, respectively, the sets of pipe dreams and reduced pipe dreams D such that $w(D) = w$. Note that $\#\,\mathrm{PD}(n) = 2^{\binom{n}{2}}$, whereas there is no simple known formula for $\#\,\mathrm{RPD}(n)$ [OEI, A331920]. Given a pipe dream D, let $\mathrm{cross}(D)$ be the set of coordinates (i, j) of the cross tiles. The *weight* of D is the monomial $\mathrm{wt}(D) := \prod_{(i,j)\in \mathrm{cross}(D)} x_i$. For example, for the pipe dream in Figure 1, left, we have $\mathrm{wt}(D) = x_1^3 x_2^2 x_3^2 x_4 x_5$.

The nonsymmetric Grothendieck polynomials generalize the Schubert and the Schur polynomials, and capture the K-theory of the flag variety. They can be defined or interpreted in a number of ways, including via divided difference operators [Las90], see Section 1.3, pipe dreams [BB93], bumpless pipe dreams [Wei21], [LLS23], and solvable lattice models [BFH+23], [BS22]. We can also define them as the partition functions of this model, via the the following result due to [FK96], [FK94], and [BB93].

Theorem 1.4 (Grothendieck polynomials as sums over pipe dreams)**.** *For any $w \in S_n$, we have*

$$\mathfrak{G}_w^{\beta}(x_1, \ldots, x_n) = \sum_{D \in \mathrm{PD}(w)} \beta^{\#\,\mathrm{cross}(D) - \ell(w)}\, \mathrm{wt}(D). \tag{1.2}$$

In particular, setting $\beta = 0$ forbids non-reduced pipe dreams, so the Schubert polynomial is

$$\mathfrak{S}_w(\mathbf{x}) = \sum_{D \in \mathrm{RPD}(w)} \mathrm{wt}(D). \tag{1.3}$$

[1] Throughout the paper, the column coordinate j increases from left to right, and the row coordinate i increases from top to bottom.

1.3. **The origins of Grothendieck polynomials.** The *(single) Grothendieck polynomials* were introduced by Lascoux and Schützenberger [LS82], [Las90] to study the K-theory of flag varieties. Their original recursive definition is as follows. Let $\pi_i : \mathbb{Z}[\beta][\mathbf{x}] \to \mathbb{Z}[\beta][\mathbf{x}]$ denote the *isobaric divided difference operator*:

$$\pi_i f := \frac{(1-\beta x_{i+1})\, f - (1-\beta x_i)\, s_i \cdot f}{x_i - x_{i+1}},$$

where s_i acts on a polynomial f by permuting x_i and x_{i+1}. The Grothendieck polynomials $\mathfrak{G}_w^\beta$ are recursively determined by the following conditions:

- For the longest permutation, we have $\mathfrak{G}^\beta_{w_0(n)} = x_1^{n-1} x_2^{n-2} \cdots x_{n-1}$.
- For all $w \in S_n$ and $i = 1, \ldots, n-1$ such that $\ell(ws_i) = \ell(w) + 1$, we have $\mathfrak{G}_w^\beta = \pi_i \mathfrak{G}^\beta_{ws_i}$.

Setting $\beta = 0$ in $\mathfrak{G}_w^\beta$, we obtain a Schubert polynomial $\mathfrak{S}_w$ which represents cohomology classes of Schubert cycles in the flag variety [BGG73], [Dem74], [LS82]. Note that some authors use the parameter $(-\beta)$ instead of β. Our choice of the sign of β is dictated by having positive coefficients in combinatorial formulas for the Grothendieck polynomials.

1.4. **Grothendieck random permutations from reduced pipe dreams.** Fix $p \in [0,1]$. Equip the set of all pipe dreams with a probability measure by independently placing the tiles in each box:

 with probability p,  with probability $1-p$. (1.4)

In particular, for $p = \frac{1}{2}$, we have the uniform measure on the set of pipe dreams.

By reducing this random pipe dream as in Definition 1.1, we obtain a random permutation $\mathbf{w} \in S_n$ which we call the *Grothendieck random permutation* (of order n and with parameter p; we suppress the dependence on n and p in the notation). The name is justified by a connection with the polynomials $\mathfrak{G}_w^{\beta=1}$. Indeed, we have for any $w \in S_n$:

$$\mathbb{P}(\mathbf{w} = w) = \sum_{D \in \mathrm{PD}(w)} p^{\mathrm{cross}(D)} (1-p)^{\mathrm{elbow}(D)} = (1-p)^{\binom{n}{2}}\, \mathfrak{G}_w^{\beta=1}\left(\frac{p}{1-p}, \ldots, \frac{p}{1-p}\right), \tag{1.5}$$

where the first equality is simply the definition of the measure (1.4), and the second immediately follows from Theorem 1.4 with $\beta = 1$. In Section 6.2 below, we explain how the same distribution on permutations arises from the six-vertex model with domain wall boundary conditions and free-fermion weights (corresponding to 2-enumeration of Alternating Sign Matrices).

When $p = 0$ or $p = 1$, we almost surely have $\mathbf{w} = \mathrm{id}$ or $\mathbf{w} = (n, n-1, \ldots, 1)$, respectively. These cases are trivial, and in the rest of the paper we assume that $p \in (0,1)$. Individual samples of Grothendieck random permutations with $p = \frac{4}{5}$ and $p = \frac{1}{2}$ and a plot constructed from averaging over many samples are given in Figure 2.

1.5. **Asymptotics of Grothendieck random permutations.** For $w \in S_n$, define its *height function* by

$$H(x,y) := \#\left(\left\{w^{-1}(x), w^{-1}(x+1), \ldots, w^{-1}(n)\right\} \cap \{y, y+1, \ldots, n\}\right),$$

where $1 \leqslant x, y \leqslant n$. In terms of the pipe dream as in Figure 1, right, $H(x,y)$ is the number of pipes of color $\geqslant x$ which exit through the positions $\geqslant y$ at the top. In the example in Figure 1, right, we have $H(4,3) = 2$. See also Figure 5 for an interpretation in terms of the permutation matrix of w, where $H(x,y)$ gives the number of 1s in the rectangle with lower left corner at (x,y).

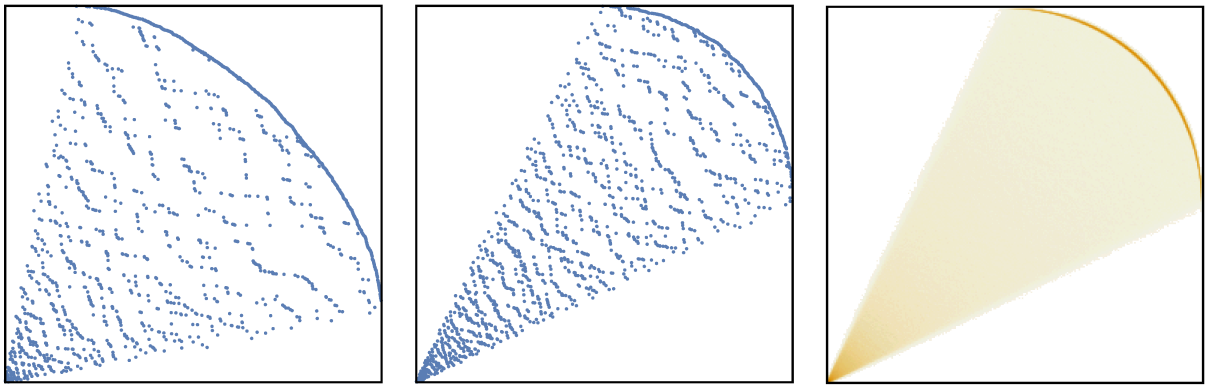

FIGURE 2. **Left and center**: A sample of a Grothendieck random permutation of order $n = 2000$ with $p = \frac{4}{5}$ and $p = \frac{1}{2}$, respectively. **Right**: An average of Grothendieck random permutations with $n = 2000$ and $p = \frac{1}{2}$ over 2000 samples. We take a sum of permutation matrices, and coarse-grain the result into 8×8 blocks. The plot is the heat map of the resulting matrix, which approximates the Grothendieck permuton. The `C` code for these simulations is available on the `arXiv` as an ancillary file. An interactive simulation is available at [Pet25].

Let now $\mathbf{w} \in S_n$ be the Grothendieck random permutation with parameter $p \in (0,1)$ which we assume fixed. This makes the height function $H(x,y)$ random, too. We show that $H(x,y)$ satisfies the law of large numbers, and characterize its asymptotic fluctuations:

Theorem 1.5. 1. *There exists a limiting height function* h° *such that*

$$\lim_{n\to\infty} n^{-1} H(\lfloor n\mathsf{x}\rfloor, \lfloor n\mathsf{y}\rfloor) = \mathsf{h}^\circ(\mathsf{x},\mathsf{y}), \qquad (\mathsf{x},\mathsf{y}) \in [0,1]^2,$$

where the convergence is in probability. The function $\mathsf{h}^\circ(\mathsf{x},\mathsf{y})$ *is explicit, see* (4.5). *It is continuous and depends only on* p. *The graph of* h° *is given in Figure 10, right.*

2. *The fluctuations of* $H(x,y)$ *around* h° *belong to the KPZ universality class:*

$$\lim_{n\to\infty} \mathbb{P}\left(\frac{H(\lfloor n\mathsf{x}\rfloor, \lfloor n\mathsf{y}\rfloor) - n\mathsf{h}^\circ(\mathsf{x},\mathsf{y})}{\mathsf{v}(\mathsf{x},\mathsf{y})\, n^{1/3}} \le r \right) = F_2(r), \qquad r \in \mathbb{R},$$

where F_2 *is the cumulative distribution function of the Tracy–Widom GUE distribution, and* $\mathsf{v}(\mathsf{x},\mathsf{y})$ *is given in* (4.16).

Theorem 1.5 justifies the simulations in Figure 2. We prove it in Section 4 by realizing $H(x,y)$ as an observable of a discrete time TASEP with parallel geometrically distributed jumps started from the densely packed (step) initial configuration. Here we omit the technical details of this coupling, and refer to Theorem 3.2 in the text. By employing known techniques from Integrable Probability and passing back to the Grothendieck random permutation, we obtain the limit shape and fluctuations.

The law of large numbers in the first part of Theorem 1.5 means that the Grothendieck random permutations $\mathbf{w} \in S_n$ converge to a deterministic *permuton*. Recall that permutons are Borel probability measures μ on $[0,1]^2$ with uniform marginals, that is, $\mu([0,1] \times [a,b]) = \mu([a,b] \times [0,1]) = b - a$. For details on permutons and their connection to pattern frequencies in permutations, we refer to [HKM+13], [BBF+20], and the survey [Grü24]. Our limiting

Grothendieck permuton is completely determined by the limiting height function via

$$\mu([\mathsf{x},1]\times[\mathsf{y},1]) = \mathsf{h}^{\circ}(\mathsf{x},\mathsf{y}).$$

Note that the "complementary" function $\mu([0,\mathsf{x}]\times[0,\mathsf{y}])$ is often referred to as *copula* in the literature, cf. [Grü24]. Our limiting permuton has a singular part, that is, a positive portion of its mass is concentrated along the curve

$$\mathcal{E}_p := \left\{(\mathsf{x},\mathsf{y})\colon (\mathsf{y}-\mathsf{x})^2/p + (\mathsf{y}+\mathsf{x}-1)^2/(1-p) = 1,\ 1-p \leqslant \mathsf{x} \leqslant 1\right\} \subset [0,1]^2.$$

The total mass supported on this curve is equal to (Proposition 4.4)

$$\gamma_p := 1 - \sqrt{\frac{1-p}{p}}\arccos\sqrt{1-p}. \tag{1.6}$$

In particular, $\gamma_{\frac{1}{2}} = 1 - \frac{\pi}{4}$.

As a corollary of the permuton convergence of Theorem 1.5, one can also obtain laws of large numbers for arbitrary pattern counts in Grothendieck random permutations. The simplest example is the number of inversions:

Proposition 1.6 (Proposition 4.5)**.** *Let $\mathbf{w} = \mathbf{w}(n) \in S_n$ be the Grothendieck random permutations with a fixed parameter $p \in (0,1)$. We have*

$$\lim_{n\to\infty} \frac{\operatorname{inv}(\mathbf{w}(n))}{\binom{n}{2}} = \gamma_p, \tag{1.7}$$

where γ_p is given by (1.6).

The fact that the scaled number of inversions converges to γ_p, the singular part of the Grothendieck permuton, is surprising. Besides exact computations given in Section 4.2, we do not have a conceptual explanation for this phenomenon.

Remark 1.7. In Sections 6.1 and 6.2, we connect Grothendieck random permutations to 2-enumerated Alternating Sign Matrices (bijectively corresponding to the six-vertex model with domain wall boundary conditions and free-fermion weights, and also to domino tilings of the Aztec diamond). The connection between Grothendieck polynomials and the six-vertex model goes back to [Las02], see also [Wei21]. Equivalences between 2-enumerated Alternating Sign Matrices, six-vertex models, and domino tilings of the Aztec diamond are well-known in statistical mechanics and integrable probability, see, for example, [CEP96], [CKP01], and [EKLP92], [ZJ00], [FS06].

Via this connection, our asymptotic results (Theorem 1.5) can be recast as results about a random permutation coming from the free-fermion six-vertex model with domain wall boundary conditions. Moreover, there is a vast amount of asymptotic results about domino tilings and free-fermion six-vertex models, and in Section 6.2 we show how some of them lead to further asymptotic properties of Grothendieck random permutations.

1.6. **A deformation and random non-reduced pipe dreams.** Let us discuss a deformation of the Grothendieck random permutation by means of a new parameter $q \in [0,1]$. Take a pipe dream of order n obtained by randomly placing the tiles in the same way as in (1.4) (depending on $p \in (0,1)$). However, instead of reduction (Definition 1.1), let us apply a modified (q-randomized) procedure:

Definition 1.8 (q-Reduction of a pipe dream)**.** Assume that D is a pipe dream that is not necessarily reduced. For each crossing tile, consider the incoming pipes. There are two cases:

- If the lower colored pipe enters from the left (and the higher colored one from the bottom), then the pipes cross through each other with probability 1.
- Otherwise, if the lower colored pipe enters from the bottom (and the higher colored one from the left), then the pipes cross through each other with probability q. That is, with probability $1-q$ we replace the crossing with a bump.

The random q-reduction steps are done independently at each crossing tile when reading the staircase diagonal by diagonal starting from the bottom left. See Section 2.2 below for a detailed definition of the Markov process for $q=0$, which has the same order of reduction steps. Denote the random permutation obtained by the q-reduction of a random pipe dream with the measure (1.4) by $\mathbf{w}^{(q)} \in S_n$. See Figure 3 for simulations.

Remark 1.9. For $q=0$, the q-reduction procedure becomes the usual reduction from Definition 1.1. For $q>0$, the q-reduction no longer tracks whether the pipes have crossed before. Instead, it simply applies the local q-reduction rule at each crossing tile, based on the relative colors of the incoming pipes.

Remark 1.10. The q-reduction of a pipe dream can be viewed as applying the q-Hecke product instead of the Demazure (0-Hecke) product as in Remark 1.3. Now, instead of the symmetric group S_n, we need to pass to the corresponding (Iwahori-)Hecke algebra $\mathcal{H}_n(q)$, and the q-reduction of a pipe dream becomes a linear combination of the Hecke elements T_w corresponding to various permutations $w \in S_n$. By choosing the Hecke product in a "stochastic" way (as in [Buf20]), namely,

$$T_{s_i} T_w = \begin{cases} (1-q)T_w + qT_{ws_i}, & \text{if } \ell(ws_i) > \ell(w), \\ T_w, & \text{otherwise,} \end{cases}$$

the linear combination of the elements T_w becomes convex, and thus corresponds to a probability distribution on S_n. This distribution is the law of the inverse $(\mathbf{w}^{(q)})^{-1}$.

The asymptotic analysis of $\mathbf{w}^{(q)}$ for $q \in (0,1]$ may be performed similarly to the case $q=0$. The underlying particle system is a certain q-deformation of TASEP which allows both left and right jumps (governed by different rules). Setting $q=1$ removes the asymmetry, which changes the normalization in the law of large numbers and fluctuations (as well as the fluctuation distribution). This behavior parallels the different scales of laws of large numbers in the KPZ and the Edwards–Wilkinson (EW) universality classes. The KPZ class asymptotics arise in TASEP and its asymmetric deformations, while symmetric versions of TASEP fall into the EW class. We refer to [Cor12] for a detailed discussion of these two universality classes.

In this paper, we mainly focus on the case $q=0$, and obtain results outlined in Section 1.5. In Section 5, we also treat the case $q=1$. In the latter model, the q-reduction does not change the pipe dream at all. Probabilistically, this is the most natural way to associate a permutation to a random pipe dream with distribution (1.4). On the other hand, the $q=1$ model apparently lacks a rich algebraic underpinning.

Finding the asymptotic number of inversions of $\mathbf{w}^{(1)} = \mathbf{w}^{(1)}(n) \in S_n$ as $n \to \infty$ was posed as an open problem by Colin Defant at the Richard Stanley's 80th birthday conference.[2] We show the following asymptotics:

[2]Conference "The Many Combinatorial Legacies of Richard P. Stanley: Immense Birthday Glory of the Epic Catalonian Rascal," https://www.math.harvard.edu/event/math-conference-honoring-richard-p-stanley/. Accessed: 07/23/2024.

Theorem 1.11 (Theorem 5.4 and Proposition 5.6)**.** *For $p \in [0,1)$ and any $\varepsilon > 0$, the expected number of inversions satisfies for all sufficiently large n:*

$$\frac{2}{3\sqrt{\pi}}(1-\varepsilon)n^{3/2}\sqrt{\frac{p}{1-p}} \le \mathbb{E}\big[\operatorname{inv}\big(\mathbf{w}^{(1)}(n)\big)\big] \le \frac{4}{3\sqrt{\pi}}(1+\varepsilon)n^{3/2}\sqrt{\frac{p}{1-p}}. \tag{1.8}$$

Moreover, the random permutations $\mathbf{w}^{(1)}(n)$ converge in distribution to the identity permuton supported on the diagonal of $[0,1]^2$.

Based on simulations (see Figure 3 for examples) and supporting numerics, we make further conjectures about the behavior of $\mathbf{w}^{(q)}$. (1.8):

Conjecture 1.12 (Conjecture 5.5; settled in [Def24])**.** *For any $p \in [0,1)$, we have convergence in probability:*

$$n^{-3/2}\operatorname{inv}(\mathbf{w}^{(1)}) \to \varkappa\sqrt{\frac{p}{1-p}}, \qquad n \to \infty,$$

where $\varkappa$ is a constant independent of p whose value is near 0.53.[3]

Theorem 1.11 implies that $\varkappa$ (if it exists) must satisfy $2/(3\sqrt{\pi}) \leqslant \varkappa \leqslant 4/(3\sqrt{\pi})$, and the approximate value 0.53 is conjectured based on numerical data.

We also expect that as $p = p(n) \to 1$ with n, the random permutations $\mathbf{w}^{(1)}(n)$ converge in distribution to a nontrivial deterministic permuton (which depends on the speed and the parameters in $p(n) \to 1$).

In the intermediate cases $q \in (0,1)$, let $H^{(q)}(x,y)$ be the height function of $\mathbf{w}^{(q)}$, defined in the same way as in Section 1.5 above.

Conjecture 1.13. *For any fixed $p, q \in (0,1)$, the random permutations $\mathbf{w}^{(q)}(n) \in S_n$ converge to a permuton determined by a height function $\mathsf{h}^{(q)}(\mathsf{x},\mathsf{y})$ on $[0,1]^2$. That is, we have the limit in probability:*

$$\lim_{n\to\infty} n^{-1} H^{(q)}(\lfloor n\mathsf{x}\rfloor, \lfloor n\mathsf{y}\rfloor) = \mathsf{h}^{(q)}(\mathsf{x},\mathsf{y}), \qquad (\mathsf{x},\mathsf{y}) \in [0,1]^2.$$

Fluctuations of $H^{(q)}(x,y)$ around $\mathsf{h}^{(q)}$ should be governed by one of the laws appearing in the KPZ universality class in the presence of a boundary (Tracy–Widom GUE distribution, its GOE/GSE counterparts and crossovers, or Gaussian fluctuations on scale $n^{1/2}$). We refer to [BBCS18], [BBCW18] for further discussion of fluctuations in half-space models from the KPZ universality class.

1.7. **Asymptotics and maxima of Grothendieck principal specializations.** We are interested in the following *principal specializations* of the Grothendieck polynomials:

$$\Upsilon_w(\beta) := \mathfrak{G}_w^{\beta}\big(\underbrace{1,1,\dots,1}_{n}\big), \qquad w \in S_n. \tag{1.9}$$

In particular, $\Upsilon_w(0)$ is the principal specialization of the Schubert polynomial. For $\beta = 1$, these quantities are the (unnormalized) probability weights of the Grothendieck random permutation $\mathbf{w}$ with $p = \frac{1}{2}$, see (1.5).

Set

$$v_n(\beta) := \sum_{w\in S_n} \Upsilon_w(\beta), \qquad u_n(\beta) := \max_{w\in S_n} \Upsilon_w(\beta). \tag{1.10}$$

[3] After this article appeared on the `arXiv`, Defant settled this conjecture in [Def24] and showed that $\varkappa = \dfrac{2\sqrt{2}}{3\sqrt{\pi}}$.

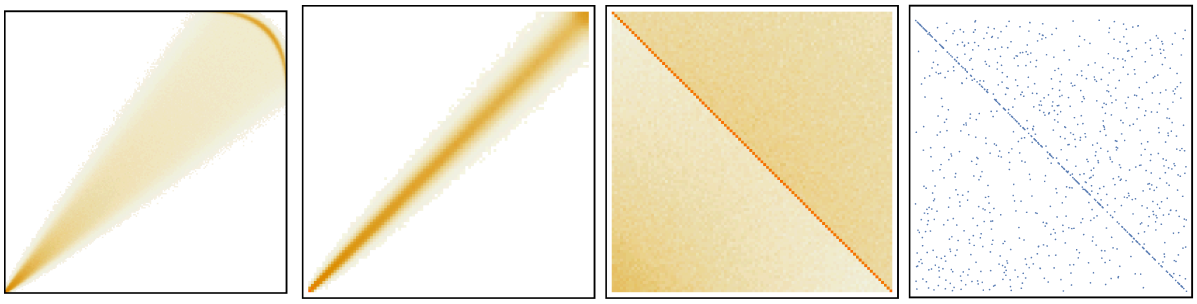

FIGURE 3. Simulations of $\mathbf{w}^{(q)}$, from left to right: (1) An average over 2000 samples with $n = 1000$, $p = 0.7$, and $q = 0.5$. We see curved boundary in the top right, similarly to $q = 0$. (2) An average over 2000 samples with $n = 1000$, $p = 0.5$, and $q = 1$. The random permutation $\mathbf{w}^{(1)}$ is close to the identity (and converges to it, see Theorem 1.11). (3) An average over 2000 samples with $n = 1000$, $p = 0.9985$, and $q = 1$. The permutation has a positive mass close to the anti-diagonal. (4) A single sample with $n = 1000$, $p = 0.9985$, and $q = 1$, with the anti-diagonal clearly visible. The latter two simulations suggest a permuton limit as $p = p(n) \to 1$. The `C` code for these simulations is available on the `arXiv` as an ancillary file.

From Theorem 1.4, we have:

$$v_n(1) = 2^{\binom{n}{2}}, \qquad u_n(1) = 2^{\binom{n}{2}-o(n^2)}, \qquad n \to \infty. \tag{1.11}$$

The first equality is exact, while the second one is asymptotic. This asymptotic behavior follows from the cardinality $n! \sim e^{n \log n + O(n)} \ll 2^{\binom{n}{2}}$ of the set over which we take the maximum.

For $u \in S_k, w \in S_m$, we denote

$$u \times w := (u(1), \ldots, u(k), w(1) + k, \ldots, w(m) + k) \in S_{k+m}. \tag{1.12}$$

For a composition $b = (b_\ell, \ldots, b_1)$ of $n = b_1 + \cdots + b_\ell$, the *layered permutation* $w(b) \in S_n$ is defined as follows:

$$w(b) = w_0(b_\ell) \times \cdots \times w_0(b_1), \tag{1.13}$$

where $w_0(k)$ is the full reversal permutation of order k. Denote by $L_n \subset S_n$ the subset of layered permutations, and let

$$u'_n(1) := \max_{w \in L_n} \Upsilon_w(1). \tag{1.14}$$

In Section 6.4, we prove that on layered permutations, the $\beta = 1$ Grothendieck polynomials attain their asymptotic maximum:

Theorem 1.14 (Theorem 6.16)**.** *There are sequences of layered permutations $w(b^{(n)}) \in S_n$ so that*

$$\lim_{n \to \infty} \frac{1}{n^2} \log_2 \Upsilon_{w(b^{(n)})}(1) = \frac{1}{2}.$$

Theorem 1.14 implies that in leading order, $u'_n(1)$ asymptotically behaves in the same way as $v_n(1)$ and $u_n(1)$ (1.11).

Explicit constructions of such sequences of layered permutations are given in Theorem 6.16. In particular, we can take the parts of the compositions $b^{(n)} = (\ldots, b_2, b_1)$ to be geometric $b_i \sim (1 - \alpha)\alpha^{i-1}n$ for any $\alpha \in [1/\sqrt{2}, 1)$. See Figure 4 for an illustration. Note, however that we do not know in the limit what compositions b of size n yield the global maximum of $\Upsilon_{w(b)}$ over all

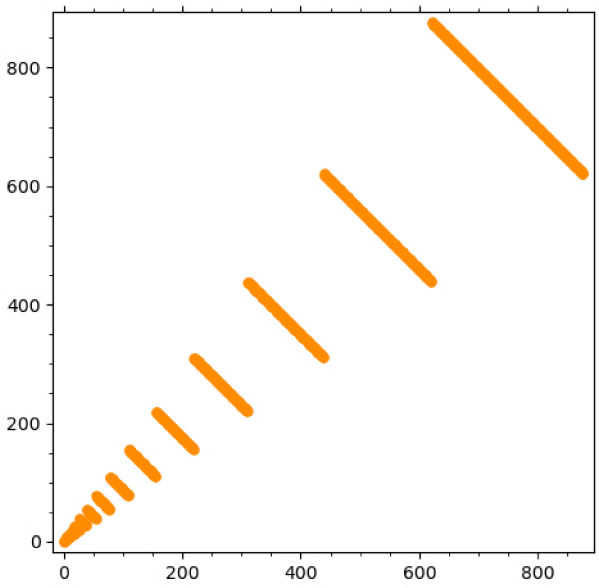

$\sum_{i=1}^{k} b_i$	b_1	$f(n)$
4	2	0.175460
6	2	0.215599
9	3	0.279931
13	4	0.328982
19	6	0.375242
27	8	0.406540
39	12	0.433385
55	16	0.450935
78	23	0.464651
110	32	0.474448
156	46	0.481823
220	64	0.486974
311	91	0.490735
439	128	0.493404
621	182	0.495329
877	256	0.496684

FIGURE 4. **Left**: Permutation matrix of a layered permutation $w(b) \in S_{877}$, where the composition is $b = (256, 182, 128, 91, 64, 46, 32, 23, 16, 12, 8, 6, 4, 3, 2, 2, 1, 1)$. Note that $b_i/b_{i+1} \approx 1/\sqrt{2}$. **Right**: Table of exact values for $3 \leqslant k \leqslant 19$ of layered permutations $w(b)$ with $b_i/b_{i+1} \approx 1/\sqrt{2}$. The third column is $f(n) := \frac{1}{n^2} \log_2 \Upsilon_{w(b)}(1)$, where $n = \sum_i b_i$.

layered permutations. For Schubert polynomials, the analogous question was settled in [MPP19]. We present numerics for principal specializations of the $\beta = 1$ Grothendieck polynomials in Appendix A, and explain the difference between the (numerically) optimal layered permutations and the ones constructed in the proof of Theorem 6.16.

Regarding Stanley's problem on permutations achieving the maximal Schubert specialization $u_n(0)$ (the case $\beta = 0$), the Merzon–Smirnov conjecture [MS16] states that *the maximum is attained on layered permutations*. On one hand, our Theorem 1.14 establishes that an asymptotic analog of this conjecture holds for the $\beta = 1$ Grothendieck polynomials. On the other hand, the typical shape of Grothendieck random permutations (Figure 2, center and right; see also Theorem 1.5) suggests that the global maximum $u_n(1)$ may be achieved on permutations whose shape is far from layered. In Section 6.5, we obtain new bounds on the quantities $v_n(\beta)$ and $u_n(\beta)$ for general values of β, but do not consider the relation of maximal principal specializations to layered permutations.

1.8. **Outline.** In the Introduction, we defined the model and formulated our main results. In Section 2, we explain how the Grothendieck random permutation $\mathbf{w}$ from Section 1.4 is sampled by running a Markov chain, more precisely, the colored stochastic six-vertex model. In Section 3, we connect the vertex model to a discrete time TASEP with parallel update and geometrically distributed jumps. This process is well-studied within Integrable Probability, which leads to law of large numbers and Tracy–Widom fluctuation results. In Section 4, we recast the asymptotic results about TASEP into limiting properties of Grothendieck random permutations. In Section 5, we consider a variant of our model coming from non-reduced pipe dreams (described in Section 1.6). In Section 6, we address the question of asymptotics of principal specializations

of $\beta = 1$ Grothendieck polynomials, and show that they are asymptotically the largest on layered permutations. We also obtain new bounds on the principal specializations for general β, based on an interpretation of Grothendieck polynomials in terms of Alternating Sign Matrices. In Section 7, we discuss further directions and a few open problems.

In Appendix A, we provide tables of maximal principal specializations of $\beta = 1$ Grothendieck polynomials on layered permutations. In Appendix B, we provide the steepest descent computations leading to the asymptotics in TASEP. While these computations are standard by now, we include them to justify the exact values of the constants in TASEP limit shape and fluctuations.

Acknowledgments. We are very grateful to Jehanne Dousse for her valuable insights in the development of this project and doing experiments in Sage. We thank Igor Pak for bringing us together and initiating our collaboration. We thank Daoji Huang, Mark Shimozono and Tianyi Yu for sharing an early version of [HSY24]. We would also like to thank Dave Anderson, Philippe Biane, Jacopo Borga, Filippo Colomo, Colin Defant, Philippe DiFrancesco, Rick Kenyon, Matthew Nicoletti, Khaydar Nurligareev, Mikhail Tikhonov, and Anna Weigandt for helpful discussions.

The project was begun at the SQuaRE "Young Tableaux Asymptotics" at the American Institute of Mathematics. The authors thank AIM for providing a supportive and mathematically rich environment. Part of this research was performed in Spring 2024 while some of the authors were visiting the program "Geometry, Statistical Mechanics, and Integrability" at the Institute for Pure and Applied Mathematics (IPAM), which is supported by the NSF grant DMS-1925919.

AM was partially supported by the NSF grant DMS-2154019, the NSERC Discovery Grant RGPIN-2024-06246, and the FRQNT Team grant 341288. GP was partially supported by the NSF grant CCF-2302174. LP was partially supported by the NSF grant DMS-2153869 and the Simons Collaboration Grant for Mathematicians 709055. DY was partially supported by the MSHE RK grant AP23489146.

2. From pipe dreams to the colored stochastic six-vertex model

2.1. Colored stochastic six-vertex model.

Introduce the vertex weights

$$w_p(a,b;c,d) = w_p\Big(\ b \xrightarrow{\ c\ } \atop \xrightarrow[\ a\ ]{}\ d\ \Big),$$

where $a, b, c, d \in \{0, 1, \dots, n\}$. Here 0 represents the absence of a pipe, and positive numbers indicate the pipes' colors. We view (a, b) and (c, d) as incoming and outgoing pipes, respectively. The weights are defined as follows:

$$\begin{aligned} &w_p(a,a;a,a) = 1; \\ &w_p(b,a;b,a) = p, \qquad w_p(b,a;a,b) = 1-p; \\ &w_p(a,b;a,b) = 0, \qquad w_p(a,b;b,a) = 1, \end{aligned} \tag{2.1}$$

where $0 \leqslant a < b \leqslant n$. The weights of all other configurations not listed in (2.1) are zero. Let us indicate a few crucial properties of the weights:

- The weights *conserve* the pipes: $w_p(a,b;c,d) = 0$ unless $\{a,b\} = \{c,d\}$ as sets.
- The weights are *stochastic*:

$$w_p(a,b;c,d) \geqslant 0, \qquad \sum_{c,d=0}^{n} w_p(a,b;c,d) = 1 \quad \text{for all } a, b.$$

Remark 2.1. The weights w_p come from the fundamental stochastic R-matrix for the quantum group $U_q(\widehat{\mathfrak{sl}_{n+1}})$ [Jim86], see also [BW22, Section 2.1] for a brief overview. For the application to random pipe dreams, we specialize the *quantum parameter* q to zero (equivalently, to infinity in the normalization of [BW22] — this choice depends only on the order in which colors correspond to basis vectors of the fundamental representation of $\mathfrak{sl}_{n+1}$). The remaining parameter p is related to the *spectral parameter* in an integrable vertex model.

2.2. **Matching random pipe dreams to the stochastic vertex model.** Attach coordinates $(i,j) \in \mathbb{Z}^2_{\geqslant 1}$ to boxes of the staircase shape, with i increasing down, and j increasing to the right. The staircase shape is then $\delta_n := \{(i,j)\colon i+j \leqslant n\}$.

Place a stochastic vertex with the weight w_p at each box $(i,j) \in \delta_n$. Let the initial condition along the left boundary of δ_n be the *rainbow* one, with colors 1 to n from top to bottom. Then we can sample a random configuration of pipes as in Figure 1, right, by running a discrete time Markov chain with time $\tau = j - i$, where $-(n-1) \leqslant \tau \leqslant n-1$. At each step $\tau \to \tau+1$, the configuration with $j - i \leqslant \tau$ is already sampled, which determines the incoming colors at all boxes $(i,j) \in \delta_n$ with $j - i = \tau + 1$. The next step $\tau \to \tau+1$ consists in an independent update of the outgoing colors at all boxes $(i,j) \in \delta_n$ with $j - i = \tau + 1$, using the stochastic vertex weights $w_p(a,b;\cdot,\cdot)$ (2.1), $1 \leqslant a, b \leqslant n$. Here we view each $w_p(a,b;\cdot,\cdot)$ as a probability distribution on possible outputs, (a,b) or (b,a). Reading off the outgoing colors at the top boundary of δ_n, we arrive at a random permutation $\mathbf{w} \in S_n$.

Proposition 2.2. *The random permutation $\mathbf{w} \in S_n$ obtained from the colored stochastic six-vertex model as described above has the same distribution as the Grothendieck random permutation defined in Section 1.4.*

Proof. The Markov evolution of the stochastic vertex model is equivalent to a simultaneous exploration of a random pipe dream (that is, determining the state  or  at each box), and its reduction by following the pipes. Indeed, in the evolution of the stochastic vertex model, in each box (i,j), two strands of different colors meet as incoming pipes. There are two possibilities:

- If the pipe of the lower numbered color is below, then these pipes have already met and crossed through each other (which is allowed only once in a reduced pipe dream). Thus, regardless of the state  or  at (i,j), the pipes *must* bump off each other. In (2.1), this corresponds to the vertex weight $w_p(a,b;b,a) = 1$, where $1 \leqslant a < b \leqslant n$.
- If the pipe of the lower numbered color is to the left, then the pipes have not yet crossed through each other (but they may have bumped off at an elbow). Then, we place the tile  or  at (i,j) with probability p or $1-p$, respectively. After placing the tile, the strands deterministically follow the paths drawn on it. The choice of the tile is equivalent to using the stochastic vertex weights $w_p(b,a;b,a) = p$ or $w_p(b,a;a,b) = 1-p$, where $1 \leqslant a < b \leqslant n$.

We see by induction that the vertex model (2.1) produces the same random permutation as reducing the random pipe dream. □

2.3. **Height function and color forgetting.** Let $x, y \in \{1,\dots,n\}$. For a fixed pipe dream D and the corresponding permutation $w = w(D)$ (see Definition 1.2), define the *permutation height function* as

$$\begin{aligned} H(x,y) &:= \#\big\{\text{pipes of colors} \geqslant x \text{ which exit through positions } j \geqslant y \text{ at the top}\big\} \\ &= \#\left(\big\{w^{-1}(x), w^{-1}(x+1), \dots, w^{-1}(n)\big\} \cap \{y, y+1, \dots, n\}\right). \end{aligned} \tag{2.2}$$

Observe that $H(x,y)$ depends only on the permutation w and not on the structure of crossings and bumps in the pipe dream. For a fixed w, the function $H(x,y)$ decreases in x and y. When the pipe dream and the permutation $\mathbf{w}$ are random, the height function $H(x,y)$ becomes a random variable.

In the permutation matrix of $w \in S_n$, $H(x,y)$ is the number of entries in the rectangle $[y,n] \times [x,n]$. Recall that the pipe of color i exits at $w^{-1}(i)$, so the rectangle is transposed. See Figure 5 for an illustration. This interpretation of $H(x,y)$ implies that

$$H(x,y) \leqslant \min(n-x, n-y). \tag{2.3}$$

In colored stochastic six-vertex models, quantities like $H(x,y)$ are referred to as *colored height functions*, cf. [BW20].

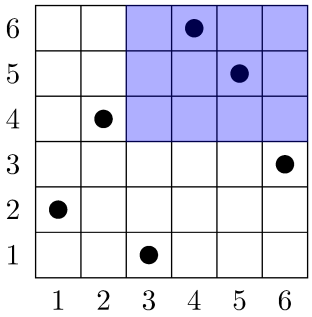

FIGURE 5. Permutation matrix of $w = (2,4,1,6,5,3)$ coming from the pipe dream in Figure 1, right (dots indicate 1's). The highlighted rectangle has $H(4,3) = 2$ entries.

Remark 2.3. The color-position symmetry [BB21] of the colored stochastic six-vertex model implies that the distribution of $H(x,y)$ corresponding to the Grothendieck random permutation $\mathbf{w}$ is symmetric in x,y. Indeed, by the color-position symmetry, $\mathbf{w}$ and $\mathbf{w}^{-1}$ have the same distribution. Therefore,

$$H(x,y) = \sum_{i=x}^{n}\sum_{j=y}^{n} \mathbf{1}_{\mathbf{w}^{-1}(i)=j} \overset{d}{=} \sum_{i=x}^{n}\sum_{j=y}^{n} \mathbf{1}_{\mathbf{w}(i)=j} = H(y,x).$$

However, we can access the distribution of $H(x,y)$ directly using color forgetting (Proposition 2.4 below), and do not rely on color-position symmetry.

Consider an *uncolored* (*color-blind*) stochastic vertex model with all pipes of the same color. We indicate pipes and empty edges by 0 and 1, respectively. The weights of the color-blind model are defined as

$$\begin{aligned} &w_p^\bullet(0,0;0,0) = 1, \qquad && w_p^\bullet(1,1;1,1) = 1,\\ &w_p^\bullet(1,0;1,0) = p, \qquad && w_p^\bullet(1,0;0,1) = 1-p,\\ &w_p^\bullet(0,1;0,1) = 0, \qquad && w_p^\bullet(0,1;1,0) = 1. \end{aligned} \tag{2.4}$$

Proposition 2.4. *Fix $1 \leqslant x \leqslant n$. In the colored stochastic vertex model of Sections 2.1 and 2.2, erase all pipes of colors $< x$, and identify all the remaining pipes for colors $\geqslant x$. The resulting random configuration of uncolored pipes evolves according to the color-blind stochastic vertex model $w_p^\bullet$ (2.4).*

Proof. This is a standard property of the colored stochastic six-vertex model, see [BW22, Section 2.4] and references therein. In interacting particle systems, this property is known as the basic coupling, cf. [Lig76], [Lig05]. Let us provide an idea of the proof.

The crucial property is that the weights w_p (2.1) depend only on the relative order of colors of the incoming pipes, and not the actual colors. Therefore, when we identify all colors $\geqslant x$, the resolution of the pipe crossings does not affect the behavior of the color-blind system. In detail, one can consider four cases for the incoming pipes (a,b), $1 \leqslant a,b \leqslant n$, depending on whether $a \geqslant x$ and/or $b \geqslant x$. The resulting probability distribution on possible outputs, (a,b) or (b,a), depends only on these cases, and not on the actual values of a,b. These four cases correspond to the color-blind incoming pipes in $w_p^{\bullet}$ (2.4). □

By Proposition 2.4, the permutation height function $H(x,y)$ can be identified with an observable of the model $w_p^{\bullet}$ with initial occupied configuration $\{x, x+1, \dots, n\}$ along the left boundary (that is, the sites $\{1,\dots,x-1\}$ are empty). Indeed, in this color-blind model, $H(x,y)$ is simply the number of pipes exiting through the top boundary at positions $\geqslant y$. We see that under the color forgetting, the color parameter x in $H(x,y)$ became a parameter of the initial configuration.

Remark 2.5. One can similarly forget the colors $> x$, and the resulting color-blind system evolves according to different weights (obtained from $w_p^{\bullet}$ by swapping $0 \leftrightarrow 1$). It is more convenient for us to work with the model $w_p^{\bullet}$, which we directly relate to an interacting particle system in the next Section 3.2.

3. From vertex models to TASEP

3.1. TASEP with moving exit boundary.

Definition 3.1. Let $k \geqslant 1$. Let $\xi(t) := \big(\xi_1(t) > \ldots > \xi_k(t)\big) \subset \mathbb{Z}$ be the k-particle discrete time TASEP (Totally Asymmetric Simple Exclusion Process) having parallel updates and geometrically distributed jumps. In detail, $\xi(t)$, $t \in \mathbb{Z}_{\geqslant 0}$, is a discrete time Markov chain on particle configurations in $\mathbb{Z}$ which at each time step $t \to t+1$ evolves as follows:

$$\xi_i(t+1) = \xi_i(t) + \min\left(G_i(t+1), \xi_{i-1}(t) - \xi_i(t) - 1\right), \qquad 1 \leqslant i \leqslant k, \tag{3.1}$$

where $G_i(t+1)$ are independent geometric random variables with parameter $p \in (0,1)$, that is,

$$\mathbb{P}\left(G_i(t+1) = m\right) = (1-p)p^m, \qquad m \in \mathbb{Z}_{\geqslant 0}. \tag{3.2}$$

The update (3.1) occurs in parallel for all particles $1 \leqslant i \leqslant k$, that is, the new positions $\xi_i(t+1)$ depend only on the configuration $\xi(t)$ at the previous time step, and new independent random variables. By agreement, we have $\xi_0(t) \equiv +\infty$, so that the first particle $\xi_1(t)$ performs an independent random walk with geometrically distributed jumps. See Figure 6 for an illustration.

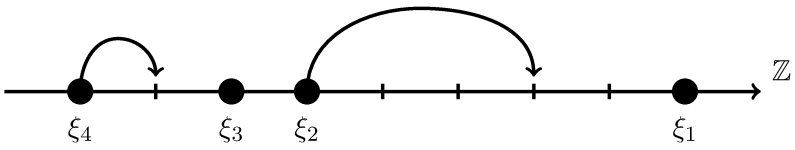

Figure 6. One step of the TASEP with parallel updates and geometric jumps. Here the independent geometric random variables could be $G_1 = 0$, $G_2 = 3$, $G_3 = 1$, $G_4 = 2$ (there is more than one choice of the G_i's leading to the same update). For these G_i's, the jumps of ξ_3 and ξ_4 are blocked by the preceding particles.

Start the TASEP from the *densely packed* (also called *step*) initial configuration $\{1, 2, \dots, k\}$, that is, $\xi_i(0) = k + 1 - i$, $1 \leqslant i \leqslant k$. Fix $n \geqslant k$, and introduce a *moving exit boundary* which starts at $n + \frac{1}{2}$, and deterministically moves to the left with speed 1. The *exit time* of a particle $\xi_i(t)$ is defined by

$$T_{\mathrm{exit}}(i) := \min\{t : \xi_i(t) \geqslant n + 1 - t\}. \tag{3.3}$$

For example, if $n = k$, then the first particle starting at n exits at time $t = 1$ (but have not exited at the initial time $t = 0$). The exit times are almost surely ordered:

$$1 \leqslant T_{\mathrm{exit}}(1) < T_{\mathrm{exit}}(2) < \ldots < T_{\mathrm{exit}}(k) \leqslant n. \tag{3.4}$$

Note that tor any $n \geqslant k$, all particles have exited the system by the time $t = n$. See Figures 7 and 8 for an illustration and simulations.

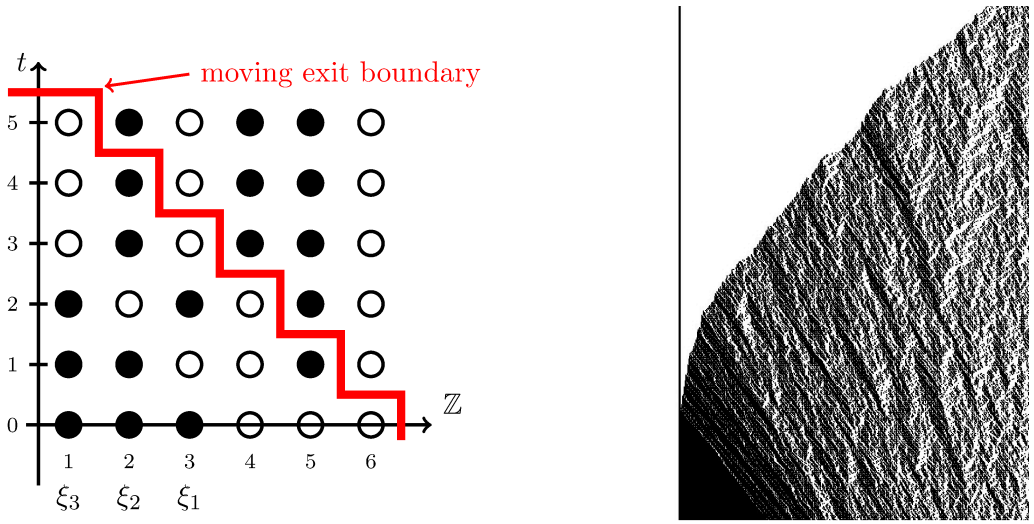

FIGURE 7. **Left**: Trajectory of TASEP with moving exit boundary for $k = 3$ and $n = 6$. Particles do not jump anymore after they exit (though the behavior beyond the boundary is irrelevant). The exit times are $T_{\mathrm{exit}}(1) = 2$, $T_{\mathrm{exit}}(2) = 3$, and $T_{\mathrm{exit}}(3) = 5$. **Right**: A fragment (close to the left boundary) of the simulation with $n = 2000$, $k = 400$, and $p = 0.8$. The last particle $\xi_k(t)$ globally follows a nonlinear trajectory that is a quadratic parabola near the point of tangence with the left boundary.

Integrability of TASEP with parallel updates, geometric jumps, and densely packed initial configuration can be traced back to [VK86], see also [DMO05], [DW08, Case C], and [BF14]. We recall the necessary integrability results in Section 3.3 below after connecting TASEP to vertex models and Grothendieck random permutations in the next Section 3.2.

3.2. **Identification with vertex models.** Fix n and $1 \leqslant x, y \leqslant n$. Recall the observables $H(x, y)$ defined by (2.2). That is, $H(x, y)$ are random variables which are functions of the Grothendieck random permutation (equivalently, of the colored stochastic six-vertex model). In Proposition 2.4, we identified $H(x, y)$ with observables of a color-blind vertex model with weights $w_p^{\bullet}$ (2.4).

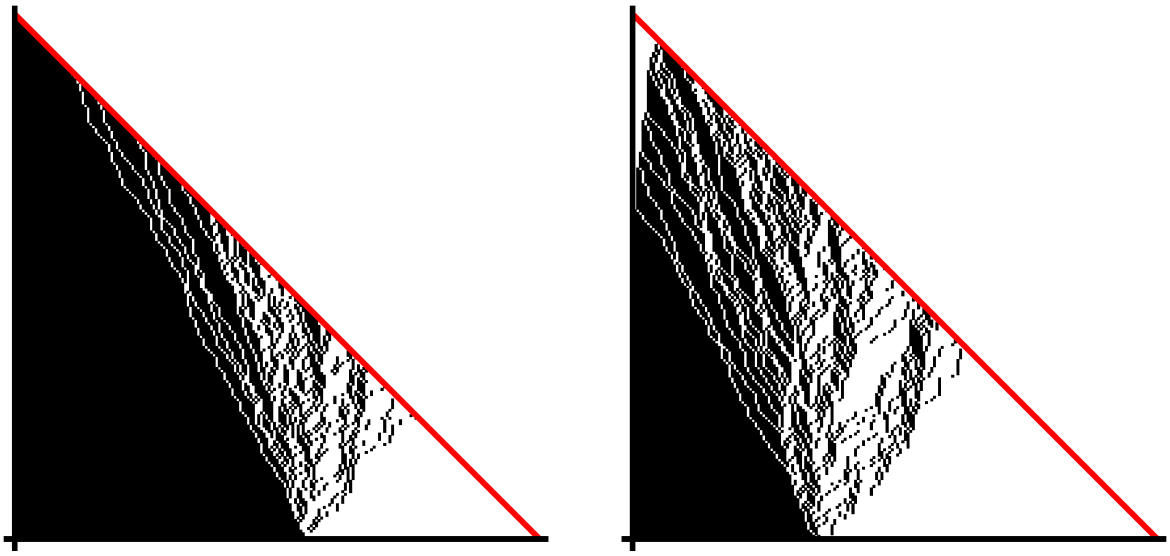

FIGURE 8. Simulations of TASEP with moving exit boundary for $n = 200$, $p = 0.5$, and $k = 110$ (**left**) or $k = 70$ (**right**). Particles beyond the diagonal exit boundary are not shown. In both cases, the first particle $\xi_1(t)$ (performing a random walk) globally follows a linear trajectory. In the left simulation, the last particle ξ_k did not have time to move before the exit boundary caught up with it. In the right simulation, the last particle ξ_k follows a nonlinear trajectory. See also Figure 7, right, for a close-up in a larger simulation.

Theorem 3.2. *For any $1 \leqslant x, y \leqslant n$ and $0 \leqslant h \leqslant n - x + 1$, we have*

$$\begin{aligned} \mathbb{P}_{\mathbf{w}}\big(H(x,y) \leqslant h\big) &= \mathbb{P}_{\mathrm{TASEP}}\big(T_{\mathrm{exit}}(n-x+1-h) \leqslant y-1\big) \\ &= \mathbb{P}_{\mathrm{TASEP}}\big(\xi_{n-x+1-h}(y-1) \geqslant n-y+2\big). \end{aligned} \tag{3.5}$$

Here $\mathbb{P}_{\mathbf{w}}$ corresponds to the Grothendieck random permutation of order n, and $\mathbb{P}_{\mathrm{TASEP}}$ is the probability distribution of the TASEP with $k = n - x + 1$ particles and moving exit boundary. In (3.5) we have, by agreement, $T_{\mathrm{exit}}(m) = 0$ and $\xi_m(t) = +\infty$ for all $m \leqslant 0$.

Proof. The second identity in (3.5) immediately follows from the definition of the exit times (3.3). Let us focus on the first identity.

By Proposition 2.4, let us consider the color-blind vertex model with $k = n - x + 1$ identical pipes entering the left boundary of the staircase shape δ_n at locations $\{x, x+1, \dots, n\}$. The event $\{H(x,y) \leqslant h\}$ means that at most h of these pipes exit the top boundary at positions $\geqslant y$. Note that the color-blind model has indistinguishable pipes, and thus the "resolution" of their crossings does not change the behavior of the system (see the proof of Proposition 2.4 for more detail).

View the horizontal coordinate j as time $t = 0, 1, \dots, n$, and record the pipes' coordinates as

$$\eta_1(t) < \ldots < \eta_k(t), \qquad t = 0, 1, \dots, n.$$

The initial condition is $\eta_{k-m+1}(0) = n - m + 1$, $1 \leqslant m \leqslant k$.

At each time step, according to the $w_p^{\bullet}$ (2.4), each pipe first deterministically turns up. When a pipe faces up, it can travel up a further distance distributed as a geometric random variable with parameter p, see (3.2). However, during a time step $t \to t+1$, each pipe η_m cannot travel

further than the previous pipe' location $\eta_{m-1}(t)$ (this is the exclusion mechanism). When a pipe stops moving up, it turns right and waits till the next time step. Once a pipe reaches the top boundary, it exits the system. See Figure 9, left, for an illustration.

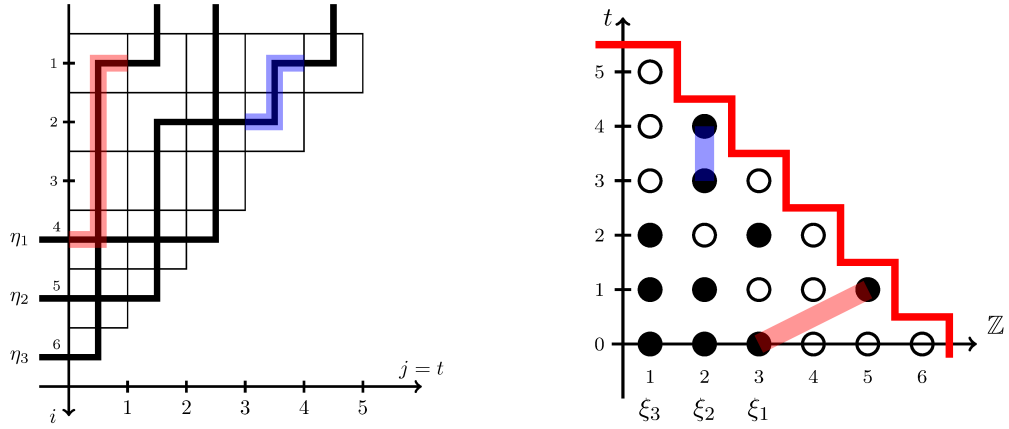

FIGURE 9. **Left**: The evolution of the uncolored pipes $\eta(t)$. Here $n = 6$ and $x = 4$, so $k = 3$. At time $t = 2$, we have $\eta_2(2) = 2$, $\eta_3(2) = 4$, and the pipe η_1 has exited before $t = 2$. We have $H(4, 3) = 2$. **Right**: The evolution of the process $\xi(t)$ which is in bijection with the pipe configuration on the left (that is, $\xi_m(t) = n + 1 - t - \eta_m(t)$). In detail, a move of the particle ξ_ℓ by $r \geqslant 0$ steps corresponds to the pipe moving $r + 1$ steps up (at the same time increment). Two pairs of corresponding moves are highlighted.

Setting $\xi_m(t) := n+1-t-\eta_m(t)$, one readily verifies that the evolution of $\xi_1(t) > \ldots > \xi_k(t)$ is the same as that of the TASEP with $k = n - x + 1$ particles defined in Section 3.1. In particular, subtracting t from $n + 1 - \eta_m(t)$ eliminates the deterministic up movement of the pipes by one at each time step.

The top boundary for pipes (as in Figure 9, left) becomes the moving exit boundary for TASEP. The event $\{H(x, y) \leqslant h\}$ for pipes is equivalent to the event that at least $k - h = n - x + 1 - h$ of the TASEP particles have exited before time $y - 1$. Because the exit times are ordered as in (3.4), we get the desired first identity in (3.5). □

3.3. **Integrability of TASEP.** Fix $m \geqslant 0$, and let $\lambda = (\lambda_1 \geqslant \ldots \geqslant \lambda_m \geqslant 0)$ be a partition with at most m parts. The *Schur symmetric polynomial* in m variables indexed by λ is defined as

$$s_\lambda(a_1, \ldots, a_m) := \frac{\det[a_i^{\lambda_j+m-j}]_{i,j=1}^m}{\det[a_i^{m-j}]_{i,j=1}^m},$$

where a_i are variables. The denominator is the Vandermonde determinant $\prod_{1\leqslant i<j\leqslant m}(a_i - a_j)$.

Let $m, t \geqslant 1$. The *Schur measure* [Oko01] is a probability measure on partitions with at most $\min(m, t)$ parts depending on parameters $a_1, \ldots, a_m, b_1, \ldots, b_t$. Its probability weights are defined as

$$\mathbb{P}(\lambda) := \prod_{i=1}^{m}\prod_{j=1}^{t}(1 - a_i b_j) \cdot s_\lambda(a_1, \ldots, a_m)\, s_\lambda(b_1, \ldots, b_t). \tag{3.6}$$

When $m = t = 1$, the weights (3.6) define the geometric distribution on $\lambda = (\lambda_1 \geqslant 0)$ with parameter $a_1 b_1$. In general, the form of the normalizing constant in (3.6) follows from the Cauchy

summation identity for Schur polynomials. The infinite sum for the normalizing constant runs over all λ of length $\leqslant \min(m,t)$ and converges if $|a_i b_j|<1$ for all i,j.

The next statement connects TASEP to Schur measure, which provides the necessary integrability structure for the former.

Proposition 3.3. *For any $t,m\geqslant 1$, the displacement of the m-th particle in the TASEP with parallel updates, geometric jumps with parameter p, and densely packed initial configuration (as in Section 3.1) has the same distribution as λ_m, the last part of a partition under the Schur measure (3.6) with $a_1=\ldots=a_m=1$ and $b_1=\ldots=b_t=p$:*

$$\xi_m(t)-\xi_m(0)\overset{d}{=}\lambda_m,\qquad \lambda\sim (1-p)^{mt}s_\lambda(\underbrace{1,\ldots,1}_{m})\,s_\lambda(\underbrace{p,\ldots,p}_{t}). \tag{3.7}$$

Proposition 3.3 is a well-known result in Integrable Probability. It follows either from the Robinson–Schensted–Knuth (RSK) correspondence with column insertion, or by representing the TASEP as a marginally Markovian evolution of a process on the space of semistandard Young tableaux (equivalently, interlacing arrays / Gelfand–Tsetlin patterns).

For the simpler continuous time TASEP (when each particle waits an exponentially distributed time and jumps to the right by 1 if the destination is unoccupied), the connection to Schur measures is exploited in the celebrated work [Joh00] via last-passage percolation, which is related to the row RSK. The RSK approach can be traced back to [VK86]. Dynamics on interlacing arrays are constructed later in [BF14] using a non-RSK approach.

For our discrete time TASEP with geometric jumps, the RSK was explicitly used in [DMO05, Section 5] to establish Proposition 3.3. A systematic treatment of discrete time dynamics on interlacing arrays connected to Schur measures leading to various TASEPs and PushTASEPs may be found in [MP17, Section 4]. It includes RSK-type and other dynamics on interlacing arrays under one roof, as well as a generalization of the Schur structure to the level of q-Whittaker symmetric polynomials.

3.4. **Determinantal structure.** The connection to Schur measures (Proposition 3.3) allows to extract law of large numbers and fluctuation results for the TASEP particles. The key property of Schur measures which makes this possible is the fact that they form a *determinantal point process.*

Fix $m,t\geqslant 1$, and define a random point configuration $X(\lambda):=\{\lambda_j+m-j\}_{j=1}^m$ on $\mathbb{Z}_{\geqslant 0}$, where λ is distributed as (3.7). If λ has less parts than m, append it by zeros. These zeros translate into a part of $X(\lambda)$ of the form $\{0,1,\ldots,l\}$ for some l.

Proposition 3.4. *The random point configuration $X(\lambda)$ on $\mathbb{Z}_{\geqslant 0}$ is a determinantal point process. This means that for any $r\geqslant 1$ and pairwise distinct points $u_1,\ldots,u_r\in\mathbb{Z}_{\geqslant 0}$, the correlation functions have the form*

$$\mathbb{P}(X(\lambda)\text{ contains all of the points }u_1,\ldots,u_r)=\det\left[K(u_i,u_j)\right]_{i,j=1}^r. \tag{3.8}$$

The correlation kernel K is given by a double contour integral:

$$K(u_1,u_2)=\frac{1}{(2\pi\mathbf{i})^2}\oiint\frac{dz\,dw}{z-w}\frac{w^{u_2-m}}{z^{u_1-m+1}}\frac{(1-p/z)^m}{(1-z)^t}\frac{(1-w)^t}{(1-p/w)^m},\qquad u_1,u_2\in\mathbb{Z}_{\geqslant 0}, \tag{3.9}$$

where the contours are positively oriented simple closed curves satisfying $p<|w|<|z|<1$.

Proposition 3.4 is due to [Oko01], see also [BR05]. General discussions and many examples of determinantal point processes may be found in [Sos00], [Bor11], or [HKPV06].

3.5. **Asymptotics of TASEP.** Determinantal structure powers the asymptotic behavior of the TASEP particles. We are interested in probabilities of the form

$$\mathbb{P}_{\mathrm{TASEP}}(\bar{\xi}_m(t) \geqslant u), \qquad \text{where} \quad \bar{\xi}_m(t) \coloneqq \xi_m(t) - \xi_m(0). \tag{3.10}$$

Indeed, since Theorem 3.2 reduces the distribution of $H(x, y)$ to probabilities of the form (3.10), we can forget about the moving exit boundary in TASEP. Indeed, the parameter n of the moving boundary is absorbed into m and u.

Let the parameters t, m, u grow to infinity proportionally to each other:

$$m = \lfloor L\mathsf{m} \rfloor, \qquad t = \lfloor L\mathsf{t} \rfloor, \qquad u = \lfloor L\mathsf{u} \rfloor, \qquad L \to \infty. \tag{3.11}$$

First, let us heuristically discuss the law of large numbers and fluctuations of $\mathbb{P}_{\mathrm{TASEP}}(\bar{\xi}_m(t) \geqslant u)$, without providing exact constants. The latter are given in Definition 3.6 below, and we formulate the asymptotic results in Theorem 3.7. The proof of Theorem 3.7 using the determinantal structure is a standard application of the steepest descent method for double contour integrals. We provide the computations (leading to the constants in Definition 3.6) in Appendix B.

At the "hydrodynamic" scale (3.11), TASEP has a limit shape (first observed in the continuous time TASEP in [Ros81], see also [AD95]). That is, there exists a function $\mathsf{c}(\mathsf{m}, \mathsf{t})$ such that for any $\varepsilon > 0$, we have

$$\lim_{L\to\infty} \mathbb{P}_{\mathrm{TASEP}}\big(\bar{\xi}_m(t) \geqslant L\mathsf{c}(\mathsf{m}, \mathsf{t}) + \varepsilon\big) = 0, \qquad \lim_{L\to\infty} \mathbb{P}_{\mathrm{TASEP}}\big(\bar{\xi}_m(t) \geqslant L\mathsf{c}(\mathsf{m}, \mathsf{t}) - \varepsilon\big) = 1. \tag{3.12}$$

In other words, we have convergence in probability:

$$\lim_{L\to\infty} L^{-1}\bar{\xi}_{\lfloor L\mathsf{m} \rfloor}(\lfloor L\mathsf{t} \rfloor) = \mathsf{c}(\mathsf{m}, \mathsf{t}). \tag{3.13}$$

Let us note a certain a priori property of the limit shape:

Lemma 3.5. *If* $\mathsf{t} < \mathsf{m}/p$, *we have* $\mathsf{c}(\mathsf{m}, \mathsf{t}) = 0$.

Proof. This follows from the fact that the leftmost hole in the TASEP configuration (which starts immediately to the right of $\xi_1(0)$ at time $t = 0$) travels left by at most 1 at each time step. The probability that the hole moves is $p = \mathbb{P}(G > 0)$, where G is the geometric random variable (3.2). Therefore, if $\mathsf{t} < \mathsf{m}/p$, then the hole has not reached the m-th particle by time t with probability $1 - e^{-CL}$ for some $C > 0$. This implies the claim. □

Next, since TASEP belongs to the Kardar–Parisi–Zhang (KPZ) universality class [Cor12], we expect fluctuations of order $L^{1/3}$ provided that $\mathsf{t} > \mathsf{m}/p$. More precisely, modifying m and u on the scale $L^{\frac{1}{3}}$ probes the scaling window in the law of large numbers (3.12). That is, there exist constants $\mathsf{v}_1(\mathsf{m}, \mathsf{t}), \mathsf{v}_2(\mathsf{m}, \mathsf{t}) > 0$, such that

$$\lim_{L\to\infty} \mathbb{P}_{\mathrm{TASEP}}\left(\bar{\xi}_{\lfloor L\mathsf{m} - L^{1/3}\alpha\mathsf{v}_1(\mathsf{m},\mathsf{t}) \rfloor}(\lfloor L\mathsf{t} \rfloor) \geqslant L\mathsf{c}(\mathsf{m}, \mathsf{t}) - L^{1/3}\beta\mathsf{v}_2(\mathsf{m}, \mathsf{t})\right) = F_2(\alpha + \beta) \tag{3.14}$$

for all $\alpha, \beta \in \mathbb{R}$. Here, F_2 denotes the cumulative distribution function of the Tracy–Widom GUE distribution. The plus signs by α and β in the right-hand side of (3.14) are straightforward from the monotonicity of the pre-limit probabilities.

The distribution function F_2 was first discovered in connection with the fluctuations of the largest eigenvalue in large complex Hermitian random matrices exhibiting unitary symmetry [TW93]. Subsequently, F_2 was put into a larger class of limiting distributions arising in random growth models and interacting particle systems, known as the KPZ universality class. We refer to the surveys [Cor12], [QS15], [HT15] for a detailed exposition. The appearance of F_2 in the

fluctuations (out of several candidates in the KPZ universality class) is a feature of the step initial configuration in our TASEP.

Definition 3.6. Let $\mathsf{m},\mathsf{t}>0$. Define

$$\mathsf{c}(\mathsf{m},\mathsf{t}) := \begin{cases} 0, & \text{if } \mathsf{t}\leqslant \mathsf{m}/p;\\ \dfrac{(\sqrt{p\mathsf{t}}-\sqrt{\mathsf{m}})^2}{1-p}, & \text{if } \mathsf{t}\geqslant \mathsf{m}/p. \end{cases} \tag{3.15}$$

If $\mathsf{t}>\mathsf{m}/p$, set

$$\mathsf{v}_1(\mathsf{m},\mathsf{t}) := \frac{\sqrt{p}\mathsf{m}^{1/3}}{\mathsf{t}^{1/6}}\frac{(\sqrt{\mathsf{t}/p}-\sqrt{\mathsf{m}})^{2/3}}{(\sqrt{p\mathsf{t}}-\sqrt{\mathsf{m}})^{1/3}}, \qquad \mathsf{v}_2(\mathsf{m},\mathsf{t}) := \frac{\sqrt{p}(\sqrt{p\mathsf{t}}-\sqrt{\mathsf{m}})^{2/3}(\sqrt{\mathsf{t}/p}-\sqrt{\mathsf{m}})^{2/3}}{(\mathsf{m}\mathsf{t})^{1/6}(1-p)}. \tag{3.16}$$

Theorem 3.7. *Let the constants* $\mathsf{c}(\mathsf{m},\mathsf{t})$ *and* $\mathsf{v}_{1,2}(\mathsf{m},\mathsf{t})$ *be given in Definition 3.6. Then*

- *The law of large numbers* (3.13) *holds for all* $\mathsf{m},\mathsf{t}>0$.
- *The Tracy–Widom fluctuation result* (3.14) *holds under the condition* $\mathsf{t}>\mathsf{m}/p>0$.

The proof of Theorem 3.7 is given in Appendix B.

4. Limit behavior of Grothendieck random permutations

4.1. **Law of large numbers for the permutation height function.** In this section, we obtain the asymptotic behavior of Grothendieck random permutations of growing order via the the pre-limit identity in distribution (Theorem 3.2) and TASEP asymptotics (Theorem 3.7). As a result, we complete the proof of Theorem 1.5 formulated in the Introduction. First, we focus on computations involving the law of large numbers, and then add the fluctuation terms. By Theorem 3.2, we have

$$\mathbb{P}_{\mathbf{w}}\big(H(x,y)\leqslant h\big)=\mathbb{P}_{\mathrm{TASEP}}\big(\xi_{n-x+1-h}(y-1)\geqslant n-y+2\big),$$

where H is the height function of the Grothendieck random permutation $\mathbf{w}$, and $\xi_i(t)$ are the TASEP particles with the step initial configuration $\xi_i(0)=n-x-i+2$, $1\leqslant i\leqslant n-x+1$. Therefore,

$$\mathbb{P}_{\mathbf{w}}\big(H(x,y)\leqslant h\big)=\mathbb{P}_{\mathrm{TASEP}}\big(\bar{\xi}_{n-x+1-h}(y-1)\geqslant n-y+1-h\big), \tag{4.1}$$

where $\bar{\xi}_i(t)=\xi_i(t)-\xi_i(0)$ is the displacement.

Let $h=\lfloor n\mathsf{h}\rfloor$, where h is the scaled permutation height function. Let also $x=\lfloor n\mathsf{x}\rfloor$, $y=\lfloor n\mathsf{y}\rfloor$, where $\mathsf{x},\mathsf{y}\in[0,1]$ are the scaled coordinates in the permutation matrix. Note that by (2.3), we have $0\leqslant\mathsf{h}\leqslant\min(1-\mathsf{x},1-\mathsf{y})$.

For each $\mathsf{x},\mathsf{y},\mathsf{h}$, the asymptotic location of $n^{-1}\bar{\xi}_{n-x+1-h}(y-1)$ is determined from the TASEP law of large numbers (3.13), (3.15). Namely, this location is equal to

$$\mathsf{c}(1-\mathsf{x}-\mathsf{h},\mathsf{y})=\frac{(\sqrt{p\mathsf{y}}-\sqrt{1-\mathsf{x}-\mathsf{h}})^2}{1-p}\mathbf{1}_{p\mathsf{y}\geqslant 1-\mathsf{x}-\mathsf{h}}.$$

There are two cases. If

$$\mathsf{c}(1-\mathsf{x}-\mathsf{h},\mathsf{y})>1-\mathsf{y}-\mathsf{h}, \tag{4.2}$$

then the probability (4.1) goes to 1. If the inequality is reversed, then this probability goes to 0. As h increases, the left- and the right-hand sides of (4.2) increase and decrease, respectively. Therefore, we should define

$$\mathsf{h}^{\circ}(\mathsf{x},\mathsf{y}) := \inf\left\{\mathsf{h}\in[0,\min(1-\mathsf{x},1-\mathsf{y})]\colon \mathsf{c}(1-\mathsf{x}-\mathsf{h},\mathsf{y})>1-\mathsf{y}-\mathsf{h}\right\}. \tag{4.3}$$

If the set in (4.3) is empty, we take the maximal possible value, $\mathsf{h}^\circ(\mathsf{x},\mathsf{y}) = \min(1-\mathsf{x}, 1-\mathsf{y})$.

To describe h° more explicitly, introduce the northeast part of the ellipse

$$\mathcal{E}_p := \big\{(\mathsf{x},\mathsf{y})\colon (\mathsf{y}-\mathsf{x})^2/p + (\mathsf{y}+\mathsf{x}-1)^2/(1-p) = 1,\ \ 1-p \leqslant \mathsf{x} \leqslant 1\big\} \subset [0,1]^2. \tag{4.4}$$

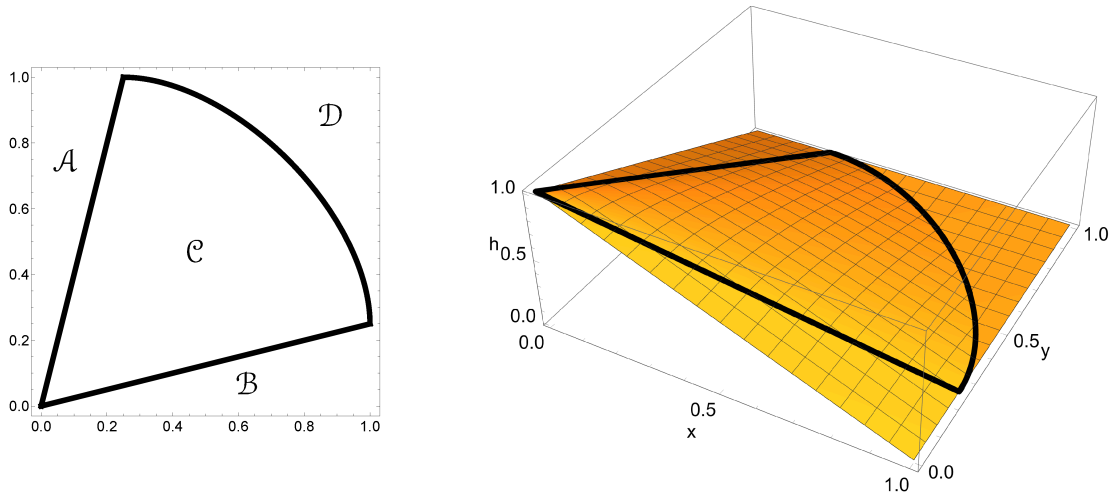

FIGURE 10. **Left:** The subsets (4.5) of the unit square. **Right:** Graph of the limit shape $\mathsf{h}^\circ(\mathsf{x},\mathsf{y})$ defined by (4.3) and given explicitly by (4.5). The function h° is linear outside of the curved triangle $\mathcal{C}$. In both figures, the parameter is $p = 3/4$.

Lemma 4.1. *The function* h° (4.3) *is given by*

$$\mathsf{h}^\circ(\mathsf{x},\mathsf{y}) = \begin{cases} 1-\mathsf{y}, & (\mathsf{x},\mathsf{y}) \in \mathcal{A} := \{0<\mathsf{x}<1-p,\ \mathsf{x}/(1-p)<\mathsf{y}<1\}; \\ 1-\mathsf{x}, & (\mathsf{x},\mathsf{y}) \in \mathcal{B} := \{0<\mathsf{x}<1,\ 0<\mathsf{y}<(1-p)\mathsf{x}\}; \\ 1+\dfrac{2}{p}\sqrt{(1-p)\mathsf{x}\mathsf{y}} - \dfrac{\mathsf{x}+\mathsf{y}}{p}, & (\mathsf{x},\mathsf{y}) \in \mathcal{C} := \begin{Bmatrix} 0<\mathsf{x}<1,\ (1-p)\mathsf{x}<\mathsf{y}<\mathsf{x}/(1-p), \\ (\mathsf{x},\mathsf{y}) \text{ below } \mathcal{E}_p \end{Bmatrix}; \\ 0, & (\mathsf{x},\mathsf{y}) \in \mathcal{D} := \{(\mathsf{x},\mathsf{y}) \text{ above } \mathcal{E}_p\}. \end{cases} \tag{4.5}$$

It is continuous on $[0,1]^2$.

See Figure 10, left, for an illustration of the subsets $\mathcal{A},\mathcal{B},\mathcal{C},\mathcal{D}$ in (4.5). The graph of the function h° is given in Figure 10, right.

Proof. In $\mathcal{A}$ and $\mathcal{C}$, we have $\mathsf{c}(1-\mathsf{x}-\mathsf{h}^\circ,\mathsf{y}) = 1-\mathsf{y}-\mathsf{h}^\circ$. Solving this for h° leads to the result. In $\mathcal{D}$, we have $\mathsf{c}(1-\mathsf{x}-\mathsf{h},\mathsf{y}) > 1-\mathsf{y}-\mathsf{h}$ for all $\mathsf{h} \geqslant 0$, so $\mathsf{h}^\circ(\mathsf{x},\mathsf{y}) = 0$. In $\mathcal{B}$, we have $\mathsf{c}(1-\mathsf{x}-\mathsf{h},\mathsf{y}) < 1-\mathsf{y}-\mathsf{h}$ for all $0 \leqslant \mathsf{h} \leqslant 1-\mathsf{x}$. This means that the set over which we take the infimum in (4.3) is empty. This implies that $\mathsf{h}^\circ(\mathsf{x},\mathsf{y}) = 1-\mathsf{x}$ in $\mathcal{B}$, which completes the proof. □

Lemma 4.1 and identity (4.1) immediately imply the law of large numbers for the height function:

$$\lim_{n\to\infty} n^{-1} H\left(\lfloor n\mathsf{x}\rfloor, \lfloor n\mathsf{y}\rfloor\right) = \mathsf{h}^\circ(\mathsf{x},\mathsf{y}), \qquad \mathsf{x},\mathsf{y} \in [0,1], \tag{4.6}$$

with convergence in probability. This completes the proof of the first part of Theorem 1.5 from the Introduction.

4.2. **Properties of the limiting permuton.** The law of large numbers (4.6) implies that the Grothendieck random permutations $\mathbf{w} \in S_n$ converge, as $n \to \infty$, to a (deterministic) *permuton* prescribed by $\mathsf{h}^\circ(\mathsf{x},\mathsf{y})$. Recall that a permuton is a probability measure on $[0,1]^2$ with uniform marginals. We refer to [HKM+13], [BBF+20], [Grü24] for detailed treatment of permutons.

In detail, the permuton is connected to the height function as

$$\mathsf{h}^\circ(\mathsf{x},\mathsf{y}) = \mathbb{P}\left(X > \mathsf{x}, Y > \mathsf{y}\right), \qquad \mathsf{x},\mathsf{y} \in [0,1],$$

where $(X,Y) \in [0,1]^2$ is a random point distributed according to the permuton. Note that both X and Y are uniformly distributed on $[0,1]$, while their joint distribution is nontrivial. Indeed, from (4.5) if follows that $\mathsf{h}^\circ(\mathsf{x},0) = 1-\mathsf{x}$, $\mathsf{h}^\circ(0,\mathsf{y}) = 1-\mathsf{y}$, as it should be for uniform marginals of a permuton.

Let is find the part of the permuton that is concentrated on the curve $\mathcal{E}_p$ (4.4) (this concentration is visible in simulations, see Figure 2). For small $\varepsilon > 0$, we have

$$\mathsf{h}^\circ(\mathsf{x},\mathsf{y}-\varepsilon) - \mathsf{h}^\circ(\mathsf{x},\mathsf{y}) = \mathbb{P}\left(X > \mathsf{x},\ \mathsf{y}-\varepsilon < Y \leqslant \mathsf{y}\right).$$

Dividing this by $\varepsilon = \mathbb{P}(\mathsf{y}-\varepsilon < Y \leqslant \mathsf{y})$, taking the limit as $\varepsilon \to 0$, and passing to the complement event, we obtain the conditional cumulative distribution function (cdf) of X given $Y = \mathsf{y}$:

$$\mathbb{P}(X \leqslant \mathsf{x} \mid Y = \mathsf{y}) = 1 + \frac{\partial}{\partial \mathsf{y}} \mathsf{h}^\circ(\mathsf{x},\mathsf{y}) = \begin{cases} 0, & (\mathsf{x},\mathsf{y}) \in \mathcal{A}; \\ 1, & (\mathsf{x},\mathsf{y}) \in \mathcal{B} \cup \mathcal{D}; \\ \dfrac{p-1}{p} + \dfrac{\sqrt{(1-p)\mathsf{x}\mathsf{y}}}{p\mathsf{y}}, & (\mathsf{x},\mathsf{y}) \in \mathcal{C}. \end{cases} \tag{4.7}$$

This function has a jump discontinuity along the ellipse $\mathcal{E}_p$ (4.4), that is, at the point

$$\mathsf{x}_p(\mathsf{y}) := \left(\sqrt{p(1-\mathsf{y})} + \sqrt{\mathsf{y}(1-p)}\right)^2, \qquad \mathsf{y} > 1-p. \tag{4.8}$$

We conclude:

Proposition 4.2. *Let $\mathsf{y} > 1-p$. The unique discontinuity of the conditional distribution of X given $Y = \mathsf{y}$ is an atom at $\mathsf{x} = \mathsf{x}_p(\mathsf{y})$, and the atom's mass is*

$$\mathbb{P}(X = \mathsf{x}_p(\mathsf{y}) \mid Y = \mathsf{y}) = \frac{1}{p} - \frac{\sqrt{(1-p)\mathsf{x}_p(\mathsf{y})\mathsf{y}}}{p\mathsf{y}} = \frac{1}{p} - \frac{\sqrt{1-p}\left(\sqrt{p(1-\mathsf{y})} + \sqrt{\mathsf{y}(1-p)}\right)}{p\sqrt{\mathsf{y}}}, \tag{4.9}$$

where $1-p < \mathsf{y} \leqslant 1$.

In particular, from (4.9) we have $\mathbb{P}(X = 1-p \mid Y = 1) = 1$, as it should be.

Remark 4.3. While conditionally on $Y = \mathsf{y}$ (where $\mathsf{y} > 1-p$), the distribution of X has an atom, the permuton (that is, the joint distribution of X and Y) does not have atoms. This follows from the fact that $\mathsf{h}^\circ(\mathsf{x},\mathsf{y})$ (4.5) is continuous on $[0,1]^2$.

By integrating (4.9) in y from $1-p$ to 1 (which is straightforward), we obtain the "singular" mass of the permuton, that is, the mass concentrated on the curve $\mathcal{E}_p$ (4.4):

Proposition 4.4. *Let $(X,Y) \in [0,1]^2$ be a random point distributed according to our permuton. Then we have*

$$\mathbb{P}\left[(X,Y) \in \mathcal{E}_p\right] = \mathbb{P}\left[X = \mathsf{x}_p(Y)\right] = 1 - \sqrt{\frac{1-p}{p}}\arccos\sqrt{1-p}, \qquad p \in [0,1].$$

In particular, for $p = \frac{1}{2}$, this expression is equal to $1 - \frac{\pi}{4}$.

As an application, let us consider the law of large numbers of the number of inversions $\mathrm{inv}(\mathbf{w}) := \#\{i < j \colon \mathbf{w}(i) > \mathbf{w}(j)\}$, where $\mathbf{w} \in S_n$ is the Grothendieck random permutation. By a result of [HKM+13] (see also Theorem 1 in the survey [Grü24] or [BBF+20, Theorem 2.5]), the convergence of $\mathbf{w} \in S_n$ to a permuton is equivalent to the convergence (in probability) of all pattern counting statistics of $\mathbf{w}$. The limiting pattern counts are determined by the permuton. In particular, for inversions, we have

$$\lim_{n\to\infty} \frac{\mathrm{inv}(\mathbf{w})}{\binom{n}{2}} = \gamma_p := \mathbb{P}\left[(X_1 > X_2,\, Y_1 < Y_2) \text{ or } (X_1 < X_2,\, Y_1 > Y_2)\right], \qquad p \in (0,1), \tag{4.10}$$

where (X_1, Y_1) and (X_2, Y_2) are independent points of $[0,1]^2$ sampled from the limiting permuton.

Proposition 4.5 (Proposition 1.6 in the Introduction)**.** *We have* $\gamma_p = 1 - \sqrt{\frac{1-p}{p}} \arccos\sqrt{1-p}$.

The fact that the scaled number of inversions is the same as the singular mass of the permuton is surprising, but we do not have a conceptual explanation for this coincidence.

Proof of Proposition 4.5. Fix $(\mathsf{x},\mathsf{y}) \in [0,1]^2$, and let $(X,Y) \in [0,1]^2$ be a random point sampled from the permuton. We have

$$\mathbb{P}\left[(X > \mathsf{x},\, Y < \mathsf{y}) \text{ or } (X < \mathsf{x},\, Y > \mathsf{y})\right] = 1 - \mathsf{h}^\circ(\mathsf{x},\mathsf{y}) - \mathsf{h}^\bullet(\mathsf{x},\mathsf{y}), \tag{4.11}$$

where $\mathsf{h}^\circ(\mathsf{x},\mathsf{y}) = \mathbb{P}(X > \mathsf{x},\, Y > \mathsf{y})$ is given by (4.5), and

$$\mathsf{h}^\bullet(\mathsf{x},\mathsf{y}) := \mathbb{P}(X \leqslant \mathsf{x},\, Y \leqslant \mathsf{y})$$

is the *copula* [Grü24] corresponding to the permuton.

In (4.11), we used the absence of atoms (Remark 4.3) and ignored the difference between strict and weak inequalities. The function $\mathsf{h}^\bullet$ can be computed using the conditional distribution (4.7):

$$\mathsf{h}^\bullet(\mathsf{x},\mathsf{y}) = \int_0^{\mathsf{y}} \mathbb{P}(X \leqslant \mathsf{x} \mid Y = w)\, dw = \begin{cases} \mathsf{x}, & (\mathsf{x},\mathsf{y}) \in \mathcal{A};\\ \mathsf{y}, & (\mathsf{x},\mathsf{y}) \in \mathcal{B};\\ \dfrac{p-1}{p}(\mathsf{x}+\mathsf{y}) + \dfrac{2}{p}\sqrt{(1-p)\mathsf{x}\mathsf{y}}, & (\mathsf{x},\mathsf{y}) \in \mathcal{C};\\ \mathsf{x}+\mathsf{y}-1, & (\mathsf{x},\mathsf{y}) \in \mathcal{D}. \end{cases}$$

By (4.11), the constant γ_p (for general p) is given by

$$\gamma_p = \mathbb{E}\left[1 - \mathsf{h}^\circ(X,Y) - \mathsf{h}^\bullet(X,Y)\right],$$

where the expectation is taken with respect to the permuton. To evaluate this expectation, we use the conditional density of X given $Y = y$ which is obtained from (4.7):

$$f_{X|Y=\mathsf{y}}(\mathsf{x}) = \frac{1}{2p}\sqrt{\frac{1-p}{\mathsf{x}\mathsf{y}}}\,\mathbf{1}_{(\mathsf{x},\mathsf{y})\in\mathcal{C}}.$$

Recalling that for $Y = \mathsf{y} > 1-p$ the conditional distribution of X has an atom, we can express the expectation as follows:

$$\begin{aligned} \gamma_p = 1 &- \iint_{\mathcal{C}} \left(\mathsf{h}^\circ(\mathsf{x},\mathsf{y}) + \mathsf{h}^\bullet(\mathsf{x},\mathsf{y})\right) f_{X|Y=\mathsf{y}}(\mathsf{x})\, d\mathsf{x}\, d\mathsf{y}\\ &- \int_{1-p}^1 \left(\mathsf{h}^\circ(\mathsf{x}_p(\mathsf{y}),\mathsf{y}) + \mathsf{h}^\bullet(\mathsf{x}_p(\mathsf{y}),\mathsf{y})\right) \mathbb{P}\left(X = \mathsf{x}_p(\mathsf{y}) \mid Y = \mathsf{y}\right) d\mathsf{y}. \end{aligned} \tag{4.12}$$

In the single integral in (4.12), one can check that $\mathsf{h}^\circ(\mathsf{x}_p(\mathsf{y}),\mathsf{y})+\mathsf{h}^\bullet(\mathsf{x}_p(\mathsf{y}),\mathsf{y})=\mathsf{x}_p(\mathsf{y})+\mathsf{y}-1$, and so the integral takes the form

$$\int_{1-p}^{1}(\mathsf{x}_p(\mathsf{y})+\mathsf{y}-1)\left(\frac{1}{p}-\frac{\sqrt{(1-p)\mathsf{x}_p(\mathsf{y})\mathsf{y}}}{p\mathsf{y}}\right)d\mathsf{y}=\frac{1}{2}\left(p-1+\sqrt{\frac{1}{p}-1}\Big(\frac{\pi}{2}-\arctan\sqrt{\frac{1}{p}-1}\Big)\right).$$

The integral is expressed in a closed form since the integrand has an explicit antiderivative.[4] In the double integral, we have

$$\begin{aligned}(\mathsf{h}^\circ(\mathsf{x},\mathsf{y})+\mathsf{h}^\bullet(\mathsf{x},\mathsf{y}))\,f_{X|Y=\mathsf{y}}(\mathsf{x})&=\left(1+\frac{4\sqrt{1-p}}{p}\sqrt{\mathsf{xy}}+\left(1-\frac{2}{p}\right)(\mathsf{x}+\mathsf{y})\right)\frac{1}{2p}\sqrt{\frac{1-p}{\mathsf{xy}}}\\&=\frac{\sqrt{1-p}}{2p\sqrt{\mathsf{xy}}}+\frac{2(1-p)}{p^2}+\left(1-\frac{2}{p}\right)\frac{\sqrt{1-p}}{2p}\cdot\frac{\mathsf{x}+\mathsf{y}}{\sqrt{\mathsf{xy}}}.\end{aligned}$$

For integrating over $\mathcal{C}$, we split the $d\mathsf{y}$ integral into two, and can readily compute the $d\mathsf{x}$ integral in both cases. Denote the x-antiderivative by

$$I(t):=\frac{\sqrt{1-p}\sqrt{t}}{p\sqrt{\mathsf{y}}}+\frac{2(1-p)}{p^2}t+\left(1-\frac{2}{p}\right)\frac{\sqrt{1-p}}{p}\cdot\frac{\frac{1}{3}t^{\frac{3}{2}}+\mathsf{y}\sqrt{t}}{\sqrt{\mathsf{y}}}.$$

Then the double integral in (4.12) is equal to

$$\begin{aligned}\int_0^{1-p}\Big(I(\mathsf{y}/(1-p))-I(\mathsf{y}(1-p))\Big)d\mathsf{y}+\int_{1-p}^{1}\Big(I(\mathsf{x}_p(\mathsf{y}))-I(\mathsf{y}(1-p))\Big)d\mathsf{y}&=\frac{1}{3}\left(p+\frac{2}{p}-3\right)\\&+\frac{3\pi\sqrt{(1-p)p^3}-3\sqrt{(1-p)p^3}\left(\arctan\sqrt{\frac{1}{p}-1}+\frac{\pi}{2}\right)+p((9-5p)p-4)}{6p^2},\end{aligned}$$

where the second line is the integral $\int_{1-p}^{1}I(\mathsf{x}_p(\mathsf{y}))d\mathsf{y}$, whose integrand has an explicit antiderivative. Putting all the computed integrals together and using basic trigonometric identities, we arrive at the result. □

4.3. **Fluctuations of the permutation height function.** Let us now apply the second part of Theorem 3.7 to the Grothendieck random permutations, and obtain fluctuations of the height function around its limit shape $\mathsf{h}^\circ(\mathsf{x},\mathsf{y})$. Throughout this subsection, we assume that the point (x,y) belongs to the curved triangle $\mathcal{C}$ where the height function h° is not linear.

Recall that by $H(x,y)$ we denote the random height function of the Grothendieck random permutation $\mathbf{w}\in S_n$. By (4.1), we have for all $r\in\mathbb{R}$:

$$\begin{aligned}&\mathbb{P}_{\mathbf{w}}\big(H(\lfloor n\mathsf{x}\rfloor,\lfloor n\mathsf{y}\rfloor)\leqslant n\mathsf{h}^\circ+rn^{1/3}\big)\\&\qquad=\mathbb{P}_{\mathrm{TASEP}}\big(\bar{\xi}_{\lfloor n(1-\mathsf{x}-\mathsf{h}^\circ-rn^{1/3})\rfloor}(\lfloor n\mathsf{y}\rfloor)\geqslant n(1-\mathsf{y}-\mathsf{h}^\circ-rn^{1/3})\big)+o(1),\end{aligned}\tag{4.13}$$

where we used the shorthand notation

$$\mathsf{h}^\circ=\mathsf{h}^\circ(\mathsf{x},\mathsf{y})=1+\frac{2}{p}\sqrt{(1-p)xy}-\frac{x+y}{p}.\tag{4.14}$$

The term $o(1)$ in (4.13) is due to the fact that we removed shifts by $(+1)$, and combined the integer parts. These modifications are negligible because fluctuations live on the scale $n^{1/3}$.

[4] Antiderivatives throughout this proof are expressed through elementary functions. They are tedious but explicit, and were obtained by a computer algebra system (namely, `Mathematica`).

By the fluctuation result for TASEP, the probability in the right-hand side of (4.13) has the following behavior:

$$\lim_{n\to\infty} \mathbb{P}_{\mathrm{TASEP}}\big(\bar{\xi}_{\lfloor n(1-\mathsf{x}-\mathsf{h}^\circ - r n^{1/3})\rfloor}(\lfloor n\mathsf{y}\rfloor) \geqslant n(1-\mathsf{y}-\mathsf{h}^\circ - r n^{1/3})\big) \\ = F_2\left(r\Big(\frac{1}{\mathsf{v}_1(1-\mathsf{x}-\mathsf{h}^\circ,\mathsf{y})} + \frac{1}{\mathsf{v}_2(1-\mathsf{x}-\mathsf{h}^\circ,\mathsf{y})}\Big)\right), \tag{4.15}$$

where F_2 is the Tracy–Widom GUE cumulative distribution function, and the constants $\mathsf{v}_1, \mathsf{v}_2$ are given by (3.16). We have

$$\frac{1}{\mathsf{v}_1(\mathsf{m},\mathsf{t})} + \frac{1}{\mathsf{v}_2(\mathsf{m},\mathsf{t})} = \frac{(\sqrt{\mathsf{t}} - \sqrt{\mathsf{m}p})\mathsf{t}^{1/6}}{\mathsf{m}^{1/3}(\sqrt{\mathsf{t}/p} - \sqrt{\mathsf{m}})^{2/3}(\sqrt{\mathsf{t}p} - \sqrt{\mathsf{m}})^{2/3}}.$$

Let us denote the above expression with $\mathsf{m} = 1-\mathsf{x}-\mathsf{h}^\circ(\mathsf{x},\mathsf{y})$ and $\mathsf{t} = \mathsf{y}$ by

$$\mathsf{v}(\mathsf{x},\mathsf{y}) := \frac{(\sqrt{\mathsf{y}} - \sqrt{p(1-\mathsf{x}-\mathsf{h}^\circ(\mathsf{x},\mathsf{y}))})\mathsf{y}^{1/6}}{(1-\mathsf{x}-\mathsf{h}^\circ(\mathsf{x},\mathsf{y}))^{1/3}(\sqrt{\mathsf{y}/p} - \sqrt{1-\mathsf{x}-\mathsf{h}^\circ(\mathsf{x},\mathsf{y})})^{2/3}(\sqrt{\mathsf{y}p} - \sqrt{1-\mathsf{x}-\mathsf{h}^\circ(\mathsf{x},\mathsf{y})})^{2/3}}, \tag{4.16}$$

where $\mathsf{h}^\circ(\mathsf{x},\mathsf{y})$ is given in (4.14). While it is not evident from (4.16), inside $\mathcal{C}$ the function $\mathsf{v}(\mathsf{x},\mathsf{y})$ is symmetric in x,y.

With the constant $\mathsf{v}(\mathsf{x},\mathsf{y})$, the convergence in (4.15) implies the desired Tracy–Widom GUE fluctuations of the height function $H(x,y)$. This completes the proof of Theorem 1.5.

5. Random permutations from non-reduced pipe dreams

Here we consider a different family of random permutations which is obtained by sampling a non-reduced pipe dream and not resolving any double crossings. This corresponds to setting $q = 1$ in Definition 1.8 from the Introduction. For shorter notation, throughout this section we denote these random permutations $\mathbf{w}^{(1)}$ by $\mathbf{w}$.

5.1. **Exact formula.** Consider the staircase shape $\delta_n = \{(i,j)\colon i+j \leqslant n\}$ (where i and j are the row and column indices, respectively) and place tiles ⊞ or ◪ in each box of δ_n independently with probabilities p and $1-p$, respectively. Let the random permutation $\mathbf{w} \in S_n$ is obtained by following the pipes starting at $(i,0)$, and ending at $(0,\mathbf{w}_i^{-1})$, $i = 1,\dots,n$. For example, for the pipe dream in Figure 1, this procedure gives $w = 241635$.

Observe that each pipe is a random walk in the bulk of δ_n, equipped with the mandatory turns by 90° at the elbows at the diagonal boundary $i+j=n$. We begin by deriving an exact formula for the probability distribution of $\mathbf{w}_i^{-1}$, the outgoing position of the i-th pipe. For general p, this distribution involves two Gauss hypergeometric functions ${}_2F_1$, which for $p = \frac{1}{2}$ simplifies to a sum of binomial coefficients. We do not use these exact formulas for asymptotic analysis, but instead, in Section 5.2 below, we obtain bounds on the expected number of inversions using the random walk approach.

Recall the Gauss hypergeometric function

$${}_2F_1(a,b;c;z) = \sum_{k\geq 0} \frac{(a)_k (b)_k}{(c_k)} \frac{z^k}{k!},$$

where $(a)_k = a(a+1)\cdots(a+k-1)$. Set

$$\begin{aligned} F_1(i,j) &:= (1-p)p^{i+j-2}\,{}_2F_1\left(-i+1,-j+1;1;(1/p-1)^2\right) \\ &= \sum_{k=0}^{\infty}\binom{i-1}{k}\binom{j-1}{k}(1-p)^{2k+1}p^{i+j-2-2k}; \\ F_2(s,n) &:= n(1-p)^2p^{n+s-3}\,{}_2F_1\left(-s+2,-n+1,2,(1/p-1)^2\right) \\ &= \sum_{k=0}^{\infty}\binom{s-2}{k}\binom{n}{k+1}(1-p)^{2k+2}p^{n+s-3-2k}. \end{aligned}$$

Note that both hypergeometric series terminate after finitely many terms. For $p=\frac{1}{2}$, these functions simplify to binomial coefficients:

$$F_1(i,j)\big|_{p=1/2} = 2^{-i-j+1}\binom{i+j-2}{j-1}, \qquad F_2(s,n)\big|_{p=1/2} = 2^{-s-n+1}\binom{n+s-2}{n-1}.$$

Proposition 5.1. *We have for all $i,j=1,\dots,n$:*

$$\mathbb{P}(\mathbf{w}_i^{-1}=j) = F_1(i,j) + p^n\mathbf{1}_{i+j=n+1} + F_2(i+j-n,n)\,\mathbf{1}_{i+j>n+1}. \tag{5.1}$$

Proof. We proceed by induction on i. For $i=1$, we have

$$\mathbb{P}(\mathbf{w}_1^{-1}=j) = \begin{cases}(1-p)p^{j-1}, & \text{if } 1\le j<n;\\ p^{n-1}, & \text{if } j=n,\end{cases}$$

which coincides with the proposed formula. Now let $i>1$. Let $X_i^{(n)}$ denote the exit position of the pipe started at $(i,0)$, assuming that all squares on the diagonal $i+j=n+1$ are elbows. By considering where this pipe crosses the first row, we can represent $X_i^{(n)} = X_{i-1}^{(n-1)} + Y$, where Y depends on $X_{i-1}^{(n-1)}$ and has the following conditional distribution given $X_{i-1}^{(n-1)}$:

$$\mathbb{P}\big(Y=m \mid X_{i-1}^{(n-1)}\big) = \begin{cases}p, & m=0;\\ (1-p)^2p^{m-1}, & 1\leqslant m<n-X_{i-1}^{(n-1)};\\ (1-p)p^{n-X_{i-1}^{(n-1)}-1}, & m=n-X_{i-1}^{(n-1)}.\end{cases}$$

Since $\mathbf{w}_i^{-1}=X_i^{(n)}$, we can write

$$\begin{aligned} &\mathbb{P}(X_{i-1}^{(n-1)}=j)\cdot p + \sum_{r<j}\mathbb{P}(X_{i-1}^{(n-1)}=r)\cdot\mathbb{P}(\mathbf{w}_i^{-1}=j) \\ &\qquad = \begin{cases}(1-p)^2p^{j-r-1}, & j<n;\\ \sum_{r<n}\mathbb{P}(X_{i-1}^{(n-1)}=r)\cdot(1-p)p^{n-r-1}, & j=n.\end{cases} \end{aligned} \tag{5.2}$$

Using the induction hypothesis, we know the distribution of $X_{i-1}^{(n-1)}$ in terms of F_1 and F_2. Therefore, it remains to verify the recursion (5.2) for the answer (5.1). This is easily done by grouping binomial coefficients, summing over r, and using the hockey-stick identity. □

5.2. **Estimates from random walks.** We are interested in the asymptotics of the (expected) number of inversions $\mathrm{inv}(\mathbf{w})$ in the random permutation $\mathbf{w}$ obtained from the non-reduced pipe dream model. First, we use the following known bound in terms of a *displacement* (*disarray*) $\mathrm{dis}(w) := \sum_{i=1}^n |i-w_i| = \sum_{i=1}^n |i-w_i^{-1}|$:

Proposition 5.2 (Diaconis–Graham [DG77]). *For any permutation w, we have*

$$\frac{1}{2}\operatorname{dis}(w) \le \operatorname{inv}(w) \le \operatorname{dis}(w). \tag{5.3}$$

Taking the expectation of (5.3) and using linearity, we see that it suffices to understand the asymptotic behavior of $\mathbb{E}\left[\left|i - \mathbf{w}_i^{-1}\right|\right]$ for all i. In principle, the exact distribution of $\mathbf{w}_i^{-1}$ from Proposition 5.1 should allow us to compute this expectation. However, this is not straightforward. Instead, we use the random walk interpretation of each individual pipe:

Proposition 5.3. *Fix $\varepsilon > 0$ and let $i < (1-\varepsilon)n$. Then*

$$\mathbb{E}\left[\left|i - \mathbf{w}_i^{-1}\right|\right] = \sqrt{\frac{4i}{\pi}\frac{p}{1-p}} + O(1), \qquad n \to \infty.$$

Proof. Fix i. Let $J_i, J_{i-1}, \dots, J_1, J_0$ be the (random) column coordinates of the positions of the i-th pipe in row $i, i-1, \dots, 1, 0$. In particular, $J_i = 0$ and $J_0 = \mathbf{w}_i^{-1}$. For example, in the pipe dream in Figure 1, left, we have $J_3 = 0$, $J_2 = 3$, $J_1 = 3$, and $J_0 = 5$ for $i = 3$.

We aim to upper bound the probability that the pipe reaches the diagonal $i+j = n$ first time at row k_0, that is, $J_{k_0} = n - k_0$. Denote this event by R_{k_0}, and observe that $\mathbb{P}(R_a) \geqslant \mathbb{P}(R_b)$ for $a < b$. Before the pipe reaches the diagonal, the horizontal displacements $J_k - J_{k+1}$, $k_0 < k < i-1$, are iid (independent identically distributed), and are distributed as

$$\mathbb{P}\left(\{J_k - J_{k+1} = m\} \cap R_{k_0}\right) = p\mathbf{1}_{m=0} + (1-p)^2 p^{m-1}\mathbf{1}_{m\ge 1}, \qquad m \in \mathbb{Z}_{\geqslant 0}, \quad k_0 < k < i-1. \tag{5.4}$$

One readily checks that the expectation and variance of the random variable in the right-hand side are equal to 1 and $\frac{2p}{1-p}$, respectively. We can represent

$$J_{k_0} = J_{k_0} - J_{k_0+1} + J_{i-1} + \sum_{k=k_0+1}^{i-2} \left(J_k - J_{k+1}\right).$$

For the event R_{k_0} to occur, the above sum must be equal to $n - k_0 = i - k_0 + (n-i) > i - k_0 + n\varepsilon$. Since the expectations of the iid summands are equal to 1, by a standard large deviation estimate, this probability is upper bounded by $e^{-c_\varepsilon n}$ for suitable $c_\varepsilon(k_0) > 0$.[5] By monotonicity, we can choose these constants such that $c_\varepsilon(k_0) \geqslant C_\varepsilon := c_\varepsilon(0) > 0$ for all k_0. Taking the union over all k_0, we see that the probability that a pipe started at i ever reaches the diagonal is exponentially small.

Therefore, $J_0 = \mathbf{w}_i^{-1}$ is close (with exponentially small error in probability) to a sum of i iid random variables $J_k - J_{k+1}$. By the Central Limit Theorem, this sum is approximately normal with mean i and variance $2ip/(1-p)$. Subtracting i from $\mathbf{w}_i^{-1}$, taking the absolute value, and using the fact that $\mathbb{E}\left(|Z|\right) = \sqrt{2/\pi}$ for standard normal Z, we obtain the result. □

We can now bound the expected number of inversions in $\mathbf{w}$ on the scale $n^{3/2}$:

Theorem 5.4. *Fix $p \in [0,1)$. For every $\varepsilon > 0$ and sufficiently large n, we have*

$$\frac{2}{3\sqrt{\pi}}(1-\varepsilon)n^{3/2}\sqrt{\frac{p}{1-p}} \le \mathbb{E}[\operatorname{inv}(\mathbf{w})] \le \frac{4}{3\sqrt{\pi}}(1+\varepsilon)n^{3/2}\sqrt{\frac{p}{1-p}}. \tag{5.5}$$

[5] Note that if $i - k_0 \ll n$, the actual bound is even stronger than this, but we do not need this precision.

Proof. For $p = 0$, the permutation is identity with probability 1, so the bounds (5.5) hold trivially.

Let $p > 0$ and let us calculate $\mathbb{E}[\mathrm{dis}(\mathbf{w})]$ to apply Proposition 5.2. With Proposition 5.3 for $i < (1-\varepsilon)^{2/3}n$, we obtain for large n:

$$\mathbb{E}[\mathrm{dis}(\mathbf{w})] = \sum_{i=1}^{n} \mathbb{E}\big[\big|\mathbf{w}_i^{-1} - i\big|\big] \geq \sum_{i=1}^{(1-\varepsilon)^{2/3}n} \frac{2}{\sqrt{\pi}}\sqrt{\frac{p}{1-p}}\sqrt{i} \geq \frac{2}{\sqrt{\pi}}\sqrt{\frac{p}{1-p}}\frac{2}{3}n\sqrt{n}(1-\varepsilon),$$

where the last inequality is a simple Riemann sum approximation. The upper bound follows similarly, this time extending the Riemann sum to n. □

Numerical simulations suggest the following behavior of the number of inversions:

Conjecture 5.5. *For any $p \in [0,1)$, we have convergence in probability:*

$$\lim_{n\to\infty} \frac{\mathrm{inv}(\mathbf{w})}{n^{3/2}} = \varkappa\sqrt{\frac{p}{1-p}}. \tag{5.6}$$

Note that the bounds $2/(3\sqrt{\pi}) \approx 0.376$ and $4/(3\sqrt{\pi}) \approx 0.752$ in Theorem 5.4 are at the same time bounds on $\varkappa$. Simulations show that $\varkappa$ is close to 0.5, but is not exactly equal to it.[6]

The fact that the number of inversions lives on scale $n^{3/2}$ implies a trivial permuton limit of $\mathbf{w}$. Denote by id the deterministic identity permuton supported on the diagonal of $[0,1]^2$.

Proposition 5.6. *For any fixed $p \in [0,1)$, the random permutations $\mathbf{w} \in S_n$ converge in distribution to* id *as $n \to \infty$.*

Proof. For any $\tau \in S_k$ and $w \in S_n$, $k < n$, denote by $t(\tau, w)$ [Grü24, Section 3] the relative frequency of the pattern τ in w. This is simply the number of times the pattern τ appears in w, divided by $\binom{n}{k}$. In particular, $t(21, w) = \frac{\mathrm{inv}(w)}{\binom{n}{2}}$. We have for any $2 < \ell < n$ [Grü24, (9)]:

$$t(21, w) = \sum_{\tau \in S_\ell} t(21, \tau)\, t(\tau, w). \tag{5.7}$$

The term in the sum with $\tau = \mathrm{id}$ vanishes since $t(21, \mathrm{id}) = 0$. For our random permutations $\mathbf{w} \in S_n$, the left-hand side of (5.7) converges to zero in probability by Proposition 5.3 and Markov inequality:

$$\mathbb{P}\left(\mathrm{inv}(\mathbf{w}) \geqslant \delta n^2\right) \leqslant C_\delta\, n^{-\frac{1}{2}} \to 0, \qquad n \to \infty$$

for all $\delta > 0$. For a fixed ℓ, this implies that $t(\tau, \mathbf{w}) \to 0$, $n \to \infty$, in probability for all $\mathrm{id} \neq \tau \in S_\ell$, $\ell \geqslant 3$. We see that all relative frequencies converge to zero except for $t(\mathrm{id}, \mathbf{w}) \to 1$. Therefore, by [BBF+20, Theorem 2.5], we get the result. □

This completes the proof of Theorem 1.11 from the Introduction.

6. Maximal principal specializations of Grothendieck polynomials

6.1. **Grothendieck polynomials via bumpless pipe dreams.** In this subsection, we outline another combinatorial model for Schubert and Grothendieck polynomials based on bumpless pipe dreams. Some of these definitions and results go back to [Las02], and are described in detail in [Wei21] and [LLS23].

[6] After this article was posted to the `arXiv`, Defant settled this conjecture in [Def24] and showed that $\varkappa = \frac{2\sqrt{2}}{3\sqrt{\pi}}$.

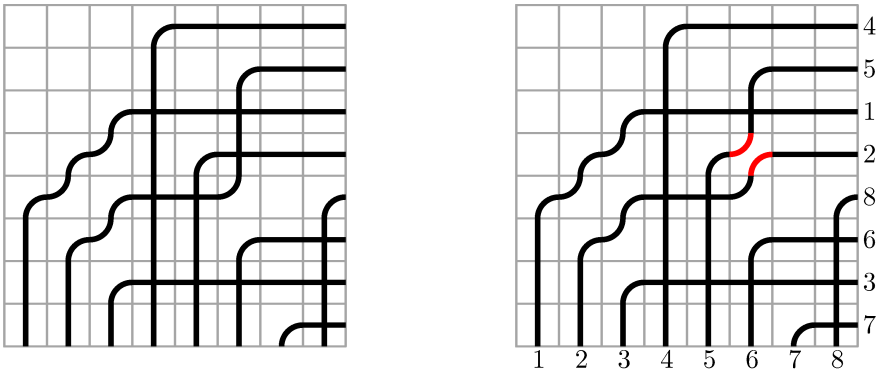

FIGURE 11. **Left**: Example of a (non reduced) bumpless pipe dream D. **Right**: The associated reduced bumpless pipe dream D' of D. In this case, D' is obtained by ignoring the second crossing of the pipes 2 and 5. The permutation is $w(D) = w(D') = 45128637$.

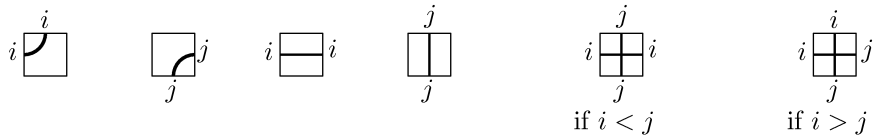

FIGURE 12. Labeling tiles in a bumpless pipe dream to read the associated permutation $w(D)$.

A *bumpless pipe dream* is a tiling D of the $n \times n$ square with six types of tiles:

SE bump, *NW bump*, *cross*, *empty*, *horizontal*, *vertical*. (6.1)

These tiles form a set of pipes labeled $1, \ldots, n$ going from the bottom boundary (left to right) to the right boundary. See Figure 11, left, for an illustration. We denote the set of all bumpless pipe dreams of size n by $\mathrm{BPD}(n)$.

Remark 6.1. Bumpless pipe dreams are the same as configurations of the six-vertex model in the $n \times n$ square with domain wall boundary conditions (see [Wei21, Section 3] or [Las02]). We refer to [ZJ09, Section 2] or [Res10] for background and many properties on the six-vertex model. This object is also sometimes called the *oscullating lattice paths* model [Beh08].

The same configurations can be identified with alternating sign matrices (ASMs) of size n, see [Bre99] for a detailed exposition, and [Kup96], [ZJ09, Section 2.5.6] for applications of the six-vertex model to the enumeration of ASMs.

Definition 6.2 (From bumpless pipe dreams to permutations; see [Wei21, Section 2.3])**.** A permutation $w(D)$ is associated to a bumpless pipe dream D by tracing the pipes from left to right, starting from the bottom boundary, and ignoring the second and subsequent crossings of each pair of pipes. See Figure 11, right, for a reading of the bumpless pipe dream in the left part of the figure which leads to $w(D)$. The local rules for labeling the tiles in a bumpless pipe dream (which produce the permutation $w(D)$) are given in Figure 12. Denote by $\mathrm{BPD}(w) \subset \mathrm{BPD}(n)$ the set of bumpless pipe dreams whose associated permutation is w.

Definition 6.3. A bumpless pipe dream is called *reduced* if no two pipes cross twice. Denote the set of reduced bumpless pipe dreams of size n by $\mathrm{RBPD}(n)$, and by $\mathrm{RBPD}(w) \subset \mathrm{RBPD}(n)$ the subset whose associated permutation is w.

Remark 6.4. Alternatively, just as in pipe dreams (see Remark 1.3), the permutation $w(D)$ from a non-reduced bumpless pipe dream can be defined using the Demazure product, see [Wei21, §2.3] for details.

For a bumpless pipe dream D (reduced or not), denote by $\mathrm{NWbump}(D)$ and $\mathrm{empty}(D)$ the set of NW bumps and empty tiles in D, respectively (see (6.1) for the notation). For a tile in a bumpless pipe dream, we denote its horizontal and vertical coordinates by (k, l), $1 \leqslant k, l \leqslant n$. Here k increases from left to right, and l increases from top to bottom.

Theorem 6.5 ([Wei21, Thm. 1.1])**.** *For any permutation $w \in S_n$, we have*

$$\mathfrak{G}_w^{\beta}(x_1, \ldots, x_n) = \beta^{-\ell(w)} \sum_{D \in \mathrm{BPD}(w)} \prod_{(k,l) \in \mathrm{empty}(D)} \beta x_k \prod_{(k,l) \in \mathrm{NWbump}(D)} (1 + \beta x_k). \tag{6.2}$$

In particular, for $\beta = 0$, we have for the Schubert polynomials:

$$\mathfrak{S}_w(x_1, \ldots, x_n) = \sum_{D \in \mathrm{RBPD}(w)} \prod_{(k,l) \in \mathrm{empty}(D)} x_k. \tag{6.3}$$

Corollary 6.6. *Recall the notation (1.10). We have*

$$v_n(\beta) = \sum_{D \in \mathrm{PD}(n)} \beta^{\#\,\mathrm{cross}(D) - \ell(w(D))}, \tag{6.4}$$

$$= \sum_{P \in \mathrm{BPD}(n)} \beta^{\#\,\mathrm{empty}(P) - \ell(w(P))} (1 + \beta)^{\#\,\mathrm{NWbump}(P)}, \tag{6.5}$$

where $w(D)$ and $w(P)$ are the permutations associated to the pipe dream D and bumpless pipe dream P, respectively.

Proof. These identities follow from the formulas for Grothendieck polynomials in Theorems 1.4 and 6.5. For (6.4), we immediately get

$$v_n(\beta) = \sum_w \mathfrak{G}_w^{\beta}(1^n) = \sum_{D \in PD(n)} \beta^{\#\,\mathrm{cross}(D) - \ell(w(D))}.$$

For (6.5), we have

$$\begin{aligned} v_n(\beta) &= \sum_w \mathfrak{G}_w^{\beta}(1^n) \\ &= \sum_{P \in BPD(n)} \beta^{-\ell(w(P))} \sum_{D \in \mathrm{BPD}(w)} \prod_{(k,l) \in \mathrm{empty}(D)} \beta \prod_{(k,l) \in \mathrm{NWbump}(D)} (1 + \beta) \\ &= \sum_{P \in BPD(n)} \beta^{\#\,\mathrm{empty}(P) - \ell(w(P))} (1 + \beta)^{\#\,\mathrm{NWbump}(P)}. \end{aligned}$$

This completes the proof. □

Remark 6.7. Gao and Huang [GH23] gave a bijection between reduced pipe dreams and reduced bumpless pipe dreams that preserves the corresponding weight of the diagrams in the corresponding expansions (1.3) and (6.3) of Schubert polynomials. This bijection was recently generalized

to the case of pipe dreams and bumpless pipe dreams with marked NW-bumps and Grothendieck polynomials by Huang–Shimozono–Yu [HSY24].

Remark 6.8. By the product formula for the number of alternating sign matrices of size n [Zei96], [Kup96], we have $\#\,\mathrm{BPD}(n) = \prod_{k=0}^{n-1} \frac{(3k+1)!}{(n+k)!}$. Moreover, since $\mathrm{RBPD}(n) \subset \mathrm{BPD}(n)$, we have

$$u_n(0) \le v_n(0) \le \prod_{k=0}^{n-1} \frac{(3k+1)!}{(n+k)!}.$$

From the asymptotics of the number of AMSs of order n (which is relatively straightforward using the product formula), we conclude that

$$\limsup_{n\to\infty} \frac{1}{n^2} \log_2 u_n(0) \le 0.37.$$

The asymptotic behavior of the number of bumpless pipe dreams (six-vertex model configurations) with periodic boundary is originally due to Lieb [Lie67]. The domain wall case with general six-vertex parameters is treated by Korepin–Zinn-Justin [KZJ00].

6.2. **Asymptotics of Grothendieck random permutations via domino tilings.** Consider a random bumpless pipe dream $\mathbf{D} \in \mathrm{BPD}(n)$ with the distribution

$$\mathbb{P}_{\text{2-ASM}}(\mathbf{D} = D) = 2^{-\binom{n}{2}} 2^{\#\,\mathrm{NWbump}(D)}, \qquad D \in \mathrm{BPD}(n). \tag{6.6}$$

Via the bijection with Alternating Sign Matrices (Remark 6.1), this distribution is equivalent to choosing each alternating sign matrix of size n with probability proportional to $2^{\#(\text{number of } -1\text{'s})}$. We call this distribution the *2-enumerated ASM model*, and it is equivalent (via a two-to-one bijection) to the *uniform* probability distribution on domino tilings of the Aztec diamond of size $n-1$. This connection, as well as the asymptotics of uniformly random domino tilings, has been a subject of extensive research in statistical mechanics and integrable probability, see, for example, [CEP96], [CKP01], and [EKLP92], [ZJ00], [FS06].

The results from the previous Section 6.1 immediately imply:

Corollary 6.9. *The Grothendieck random permutation $\mathbf{w} \in S_n$ with the parameter $p = \frac{1}{2}$ (see Section 1.4 for the definition) coincides with the permutation $w(\mathbf{D})$ associated (as in Definition 6.2) to the random bumpless pipe dream $\mathbf{D} \in \mathrm{BPD}(n)$ with the distribution (6.6).*

Remark 6.10. For general p, an analog of Corollary 6.9 would involve a more complicated weighting of bumpless pipe dreams (six-vertex configurations). This weighting is still in the free-fermion family of six-vertex weights. At the level of domino tilings, the p-weighting corresponds to a deformation of the uniform model in which vertical and horizontal dominoes have different weights. This model is also well-studied, for example, see [CJY15]. For simplicity, here we focus only on the case $p = \frac{1}{2}$.

Our asymptotic results for Grothendieck random permutations (Theorem 1.5) readily translate into results about the behavior of the permutations $w(\mathbf{D})$ coming from the 2-enumerated ASM model. On the other hand, the asymptotic behavior of the bumpless pipe dream $\mathbf{D}$ in various regimes has also been extensively studied, and some of these results can be brought back to Grothendieck random permutations. Let us present just one example leading to asymptotically Gaussian fluctuations:

Proposition 6.11 (Central limit theorem for the image of n)**.** *Let $\mathbf{w} \in S_n$ be the Grothendieck random permutation with $p = \frac{1}{2}$. Let $\mathbf{w}_n$ be the image of n under $\mathbf{w}$. We have*

$$\frac{\mathbf{w}_n - n/2}{\sqrt{n/4}} \xrightarrow{d} \mathcal{N}(0,1), \qquad n \to \infty. \tag{6.7}$$

Here $\mathcal{N}(0,1)$ is the standard normal distribution.

Proof. Let $\mathbf{l}_n$ be the position of the single NW bump in the rightmost column of $\mathbf{D}$. In Figure 11, we have $\mathbf{l}_n = 5$. By Corollary 6.9, $\mathbf{w}_n$ has the same distribution as $\mathbf{l}_n$. In the language of domino tilings (see the map in, e.g., [FS06]), $\mathbf{l}_n$ is the position of the first particle in the particle process associated to the domino tiling. By [JN06, Theorem 1.5], $\mathbf{l}_n$ satisfies a central limit theorem as in (6.7). Note that our standard deviation $\sqrt{n/4}$ matches the normalization in [JN06] as the latter work deals with GUE random matrices whose diagonal elements have variance 2. This completes the proof. □

Remark 6.12. Proposition 6.11 can also be proven directly by looking at the trajectory of the pipe of color n in the random pipe inside the staircase shape (Section 1.2), as this trajectory is a random walk.

6.3. **Exact formulas for elementary layered permutations.** We are now in a position to discuss principal specializations of Grothendieck polynomials on layered permutations. We begin with a few exact formulas, for which we need some notation.

Let $\mathsf{C}_n := \frac{1}{n+1}\binom{2n}{n}$ denote the nth *Catalan number* which counts the number of *Dyck paths* of size n. Let s_n denote the n-th *little Schröder number* [OEI, A001003] and S_n the n-th *large Schröder number* [OEI, A006318]. It is known that $\mathsf{S}_n = 2\mathsf{s}_n$ for $n \geq 1$.

The *Narayana polynomial* is defined as

$$\mathcal{L}_n(x) := \sum_{d \in \mathrm{Dyck}(n)} x^{v(d)},$$

where the sum is over Dyck paths of size n and $v(d)$ is the number of valleys of the path d. The coefficients of $\mathcal{L}_n(x)$ are the *Narayana numbers* $N(n,k) = \frac{1}{k}\binom{n}{k}\binom{n}{k-1}$ [OEI, A001263]. Note that $\mathsf{C}_n = \mathcal{L}_n(1)$ and $s_n = \mathcal{L}_n(2)$. The polynomials $\mathcal{L}_n(x)$ have the following generating function:

$$\sum_{n \geq 0} y^n \mathcal{L}_n(x) = \frac{1 - y(1+x) - \sqrt{(1-y(1+x))^2 - 4xy^2}}{2y}. \tag{6.8}$$

Consider the following *elementary layered permutation* (see also (1.12) for notation):

$$w_0(k;n) := \mathrm{id}_k \times w_0(n) = (1, \ldots, k, k+n, k+n-1, \ldots, k+1) \in S_{k+n}. \tag{6.9}$$

Recall the notation $\Upsilon_w(\beta)$ (1.9). A formula due to Fomin and Kirilov [FK97] relates the Schubert principal specialization $\Upsilon_{w_0(a;b)}(0)$ to Proctor's formula [Pro90] counting bounded plane partitions of staircase shape:

Theorem 6.13. *For nonnegative integers k and n, we have*

$$\Upsilon_{w_0(k;n)}(0) = \mathfrak{S}_{w_0(k;n)}(1, \ldots, 1) \;=\; \det[\mathsf{C}_{n-2+i+j}]_{i,j=1}^{k} \;=\; \prod_{1 \leq i < j \leq n} \frac{2k+i+j-1}{i+j-1}. \tag{6.10}$$

In [MPP22], an analogous formula for the $\beta = 1$ Grothendieck polynomials is proven:

Theorem 6.14 ([MPP22, Thm. 5.9]). *For nonnegative integers k and n, we have*

$$\Upsilon_{w_0(k;n)}(1) = \mathfrak{G}^{\beta=1}_{w_0(k;n)}(1,\dots,1) = 2^{-\binom{k}{2}} \det[\mathsf{s}_{n-2+i+j}]_{i,j=1}^{k} = 2^{-\binom{k+1}{2}} \det[\mathsf{S}_{n-2+i+j}]_{i,j=1}^{k}.$$

A general determinantal formula for all β may be derived from [HKYY19, Thm. 5.9]:

Theorem 6.15. *For nonnegative integers k and n, we have*

$$\Upsilon_{w_0(k;n)}(\beta) \;=\; (1+\beta)^{-\binom{k}{2}} \det[\mathcal{L}_{n+i+j-2}(1+\beta)]_{i,j=1}^{k}. \tag{6.11}$$

The determinants in Theorems 6.14 and 6.15 can be efficiently computed via the Dodgson condensation (the Desnanot–Jacobi identity). We use it to get the numerical data for $\beta = 1$ presented in Appendix A.

6.4. **Asymptotically maximal specializations for layered permutations.** Here we prove that principal specializations of $\beta = 1$ Grothendieck polynomials on layered permutations (see (1.13) for the definition) attain the asymptotically largest value. That is, we prove Theorem 1.14 from the Introduction.

Theorem 6.16. *Consider the compositions $b^{(n)} = (\dots, b_2, b_1)$ of n such that*

$$b_1 + \dots + b_{i-1} + (2+\sqrt{2})b_i \leqslant n \text{ for } i = 1, 2, \dots, \text{ while } b_1 + \dots + b_{i-1} \leqslant n-4,$$

and $b^{(n)}$ has $o(n)$ parts. Then for the layered permutations $w(b^{(n)})$ we have

$$\lim_{n\to\infty} \frac{1}{n^2} \log_2 \Upsilon_{w(b^{(n)})}(1) = \frac{1}{2},$$

which is asymptotically maximal.

Remark 6.17. In particular, one can take compositions to be geometric $b_i \sim (1-\alpha)\alpha^{i-1}n$, for any $\alpha \in [1/\sqrt{2}, 1)$.

In the rest of this Section 6.4, we prove Theorem 6.16. First, observe that the Grothendieck specializations enjoy the following basic factorization property:

Proposition 6.18. *Let $u \in S_k, w \in S_n$. We have*

$$\Upsilon_{u\times w}(\beta) = \Upsilon_u(\beta) \cdot \Upsilon_{\mathrm{id}_k \times w}(\beta),$$

where $u \times w$ is the block permutation defined by (1.12).

Proof. This follows from properties of pipe dreams corresponding to permutations of the form $u \times w$. See [Man01, Corollary 2.4.6] or [Mac91, (4.6)]. □

Let us denote (recall the notation (6.9))

$$F(k,n) \coloneqq \Upsilon_{w_0(k;n)}(1), \qquad G(k,n) \coloneqq 2^{\binom{k}{2}} \cdot F(k,n) = \det[\mathsf{s}_{n-2+i+j}]_{i,j=1}^{k}, \tag{6.12}$$

where the last equality follows from Theorem 6.14.

An important step in obtaining the asymptotics of $\Upsilon_w(1)$ for layered permutations is to understand the behavior of the function $F(k,n)$. A similar analysis [MPP22] was possible in the Schubert case ($\beta = 0$) thanks to an explicit product formula (Theorem 6.13). For other β's, we have determinantal (but not product) formulas (Theorem 6.14 and Theorem 6.15). However, in the case $\beta = 1$ we are able to asymptotically analyze these determinants via the correspondence with 2-enumerated ASMs.

Lemma 6.19. *Let $k \in (n/\sqrt{2}, n]$. We have*

$$\log_2 F(k, n-k) = \frac{n^2}{2} - \frac{k^2}{2} - O(n), \qquad n \to \infty. \tag{6.13}$$

In (6.13) and throughout the proofs below in this subsection, we assume that the constants in the $O(\cdot)$ notation are nonnegative.

Proof of Lemma 6.19. By (6.12), it suffices to show that for $k > n/\sqrt{2}$, we have

$$\det[\mathsf{s}_{n-k-2+i+j}]_{i,j=1}^{k} = 2^{\frac{n^2}{2} - O(n)}. \tag{6.14}$$

We employ the interpretation of the litte Schröder number s_m [OEI, A001003] as the number of Motzkin paths from $(0,0)$ to $(2m,0)$ (with steps $(1,1)$, $(1,-1)$, and $(2,0)$) which do not have horizontal steps at height 0. Let us call these paths the 0-*Schöder paths*, where 0 represents the lower boundary of the path. Then, by the Lindstrom–Gessel–Viennot lemma [KM59], [Lin73], [GV85] the determinant (6.14) counts k-tuples of nonintersecting 0-Schöder paths starting from $(-2i, 0)$ and ending at $(2(n-k+i-1), 0)$, respectively, where $i = 1, \dots, k$. Denote this space of configurations by $\mathcal{M}_{k,n-k}$. See Figure 13 for an illustration.

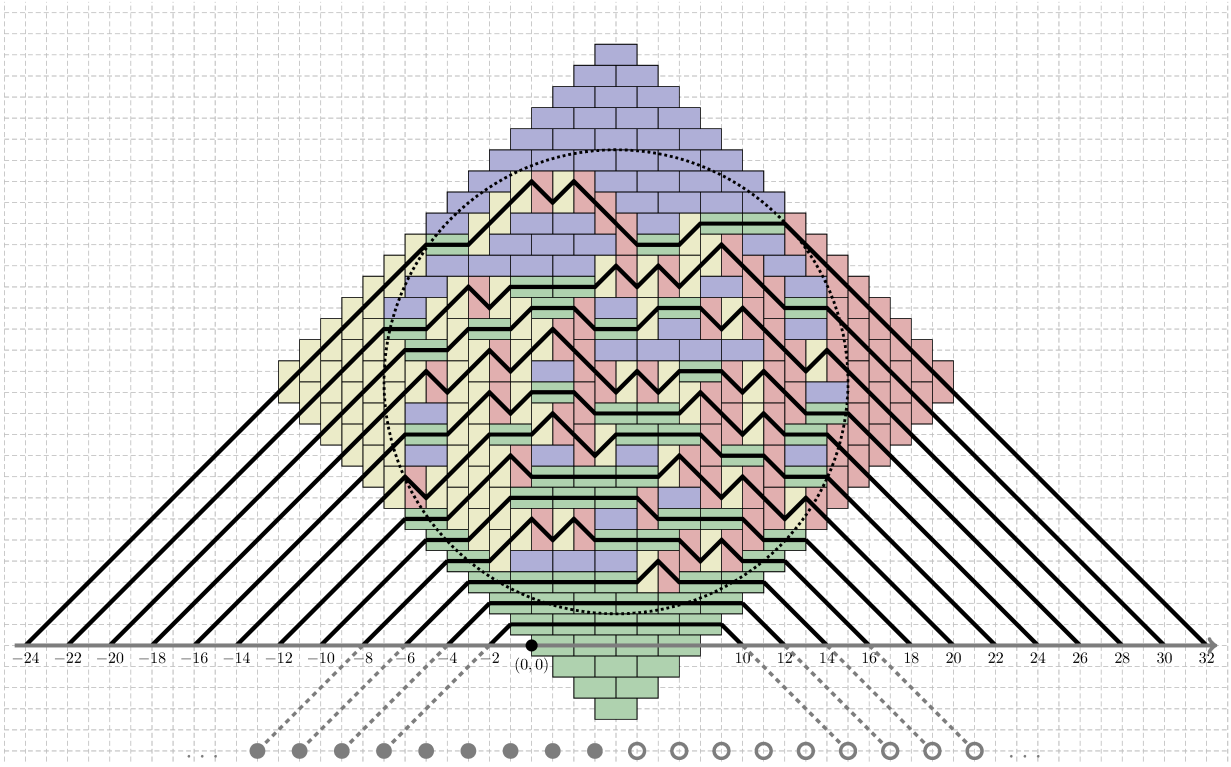

FIGURE 13. Nonintersecting 0-Schöder paths from $\mathcal{M}_{12,5}$, the corresponding Aztec diamond D_{n-1} of order $n-1 = 16$, and the arctic circle. The horizontal coordinate line is at the vertical height 0. The gray points at the bottom are the starting (filled) and ending (hollow) points of the $(k+1-n)$-Schröder paths representing the full domino tiling of the Aztec diamond. The dashed gray lines are the continuations of some of the paths from $\mathcal{M}_{k,n-k}$ into paths from the ensemble $\mathcal{S}_n$.

A well-known correspondence (e.g., see [EF05]) between domino tilings of the Aztec diamond and nonintersecting paths allows to interpret

$$\frac{\det[\mathsf{s}_{n-k-2+i+j}]_{i,j=1}^{k}}{2^{\binom{n}{2}}} \tag{6.15}$$

as a probability of a certain event in the uniformly random domino tiling of the Aztec diamond D_{n-1} of order $n-1$. Let us explain this identification in detail.

The total number of domino tilings of D_{n-1} is $2^{\binom{n}{2}}$. Domino tilings of D_{n-1} bijectively correspond to families of n nonintersecting paths, for which we may take the $(k+1-n)$-Schröder paths starting from $(n-k-2i, k+1-n)$, $i=1,\dots,n$, and ending at $(n-k+2(i-1), k+1-n)$, respectively, where $i=1,\dots,n$. Denote this ensemble of nonintersecting paths by $\mathcal{S}_n$, so $|\mathcal{S}_n| = 2^{\binom{n}{2}}$.

The k paths from $\mathcal{M}_{k,n-k}$ may be continued diagonally to coincide with the outermost k paths from the ensemble $\mathcal{S}_n$. This continuation procedure implies that the ratio $|\mathcal{M}_{k,n-k}|/|\mathcal{S}_n|$ given by (6.15) is equal to the probability that the $n-k$ paths in $\mathcal{S}_n \setminus \mathcal{M}_{k,n-k}$ are in their *lowest possible configuration*. See Figure 13 for an illustration.

The model of uniformly random domino tilings of the Aztec diamond develops an arctic circle [JPS98]. In particular, the configuration outside of the circle inscribed in the Aztec diamond (illustrated in Figure 13) is frozen (nonrandom). Qualitatively, by [CEP96, Proposition 13], this means that with probability $1-e^{-O(n)}$, the $n-k$ paths in $\mathcal{S}_n \setminus \mathcal{M}_{k,n-k}$ are indeed in their lowest possible configuration. Note that here we rely on the assumption $k > n/\sqrt{2}$, which guarantees that the top of the $n-k$ paths in $\mathcal{S}_n \setminus \mathcal{M}_{k,n-k}$ does not reach the arctic circle. This establishes (6.14), and completes the proof of Lemma 6.19. □

Remark 6.20. The recent work [CP24] provides asymptotics of $\log_2 F(k, n-k)$ for all k, not necessarily in the range $k > n/\sqrt{2}$. For $k < n/\sqrt{2}$, the leading term is strictly smaller than $\frac{n^2}{2}$, which agrees with the variational principle [CKP01, Theorem 1.3]. We do not need the regime $k < n/\sqrt{2}$ for Theorem 6.16.

Proof of Theorem 6.16. Let us denote $k_0 := n$ and

$$k_i := n - b_1 - \ldots - b_i, \quad i \geqslant 1,$$

so that $b_i = k_{i-1} - k_i$. We have by Proposition 6.18 and (6.9) that

$$\begin{aligned} \Upsilon_{w(\dots,b_2,b_1)}(1) &= \Upsilon_{w(\dots,b_3,b_2)}(1) \cdot F(n-b_1, b_1) \\ &= \prod_{i\geqslant 1} F(n-b_1-\ldots-b_i, b_i) = \prod_{i\geqslant 1} F(k_i, k_{i-1}-k_i). \end{aligned} \tag{6.16}$$

From the inequalities on the b_i's, we get

$$\frac{k_i}{k_{i-1}} = \frac{n-b_1-\ldots-b_i}{n-b_1-\ldots-b_{i-1}} \in (1/\sqrt{2}, 1).$$

Hence by Lemma 6.19, we have

$$\log_2 F(k_i, k_{i-1}-k_i) = \frac{k_{i-1}^2}{2} - \frac{k_i^2}{2} - O(k_{i-1}).$$

Therefore,

$$\frac{1}{n^2}\log_2 \Upsilon_{w(\dots,b_2,b_1)}(1,\dots,1) = \sum_{i\geqslant 1} \frac{1}{n^2}\log_2 F(k_i, k_{i-1}-k_i)$$

$$= \sum_{i\geqslant 1} \frac{1}{n^2}\left(\frac{k_{i-1}^2}{2} - \frac{k_i^2}{2} - O(k_{i-1})\right)$$
$$= \frac{1}{2} - \frac{1}{n^2} O\left(\sum_{i\geqslant 1} k_{i-1}\right).$$

Since $k_{i-1} = O(n)$ and there are $o(n)$ elements in our composition, we have

$$\sum_{i\geqslant 1} k_i = o(n^2), \text{ and so } \frac{1}{n^2} O\left(\sum_{i\geqslant 1} k_{i-1}\right) = o(1),$$

which completes the proof of Theorem 6.16. □

Remark 6.21 (Layered vs all permutations)**.** Recall the notation (1.10), (1.14). Theorem 6.16 establishes that on layered permutations, the Grothendieck specializations $\Upsilon_w(1)$ reach their asymptotic maximum: $u'_n(1) \sim 2^{\binom{n}{2}}$. However, it is not clear whether the absolute maximum, $u_n(1)$, is attained on layered permutations. Dennin [Den22, Fig. 9] verified that for $n \leqslant 9$, one has $u_n(1) = u'_n(1)$.

We present numerical data of optimal (i.e., achieving the exact, non-asymptotic maximum in $u'_n(1)$) layered permutations for $n \leq 500$ in Appendix A. We also comment on why these optimal layered permutations have parts whose behavior does not fall under the assumptions of Theorem 6.16.

6.5. **Bounds on the constant for Grothendieck specializations with general β.** In [MPP22], the authors conjectured that for β fixed there exists a limit

$$c(\beta) := \lim_{n\to\infty} \frac{1}{n^2} \log_2 v_n(\beta). \tag{6.17}$$

If the limit exists, it must satisfy for $\beta \geq 0$:

$$\frac{1}{4}\log_2(2+\beta) \leq c(\beta) \leq \frac{1}{2}\log_2(2+\beta), \tag{6.18}$$

see [MPP22, Section 7.12]. The limit (6.17) exists when $\beta = 1$, see (1.11), and we have $c(1) = \frac{1}{2}$. Here we improve the bounds (6.18) in certain regimes:

Proposition 6.22. *If the limit $c(\beta)$ (6.17) exists, then it must satisfy the following bounds. For $0 < \beta \leq 1$, we have*

$$\frac{1}{4}\max\{\log_2(2+\beta), 2\log_2(1+\beta)\} \leq c(\beta) \leq \frac{1}{2}\min\{\log_2(2+\beta), \log_2(1+1/\beta)\}.$$

For $\beta \geq 1$, we have

$$\frac{1}{4}\max\{\log_2(2+\beta), 2\log_2(1+1/\beta)\} \leq c(\beta) \leq \frac{1}{2}\log_2(1+\beta).$$

See Figure 14 for an illustration of the bounds.

Proof. For $0 < \beta \leq 1$ and $D \in \mathrm{PD}(n)$, we can bound $1 \leq \beta^{-\ell(w(D))} \leq \beta^{-\binom{n}{2}}$. Thus by (6.4), we have

$$\sum_{D\in\mathrm{PD}(n)} \beta^{\#\,\mathrm{cross}(D)} \leq v_n(\beta) \leq \beta^{-\binom{n}{2}} \sum_{D\in\mathrm{PD}(n)} \beta^{\#\,\mathrm{cross}(D)},$$

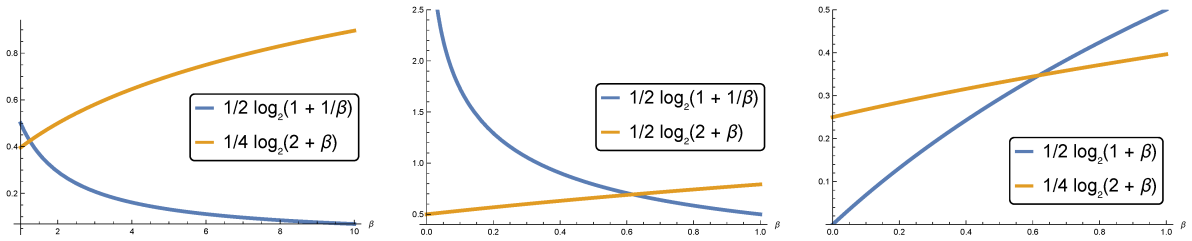

FIGURE 14. Comparing the bounds in Proposition 6.22 for $\beta > 1$ and $0 < \beta < 1$.

which leads to $(1+\beta)^{\binom{n}{2}} \le v_n(\beta) \le \left(\frac{1+\beta}{\beta}\right)^{\binom{n}{2}}$. Taking the logarithms and comparing with (6.18) gives the result.

For $\beta \ge 1$ and $D \in \mathrm{PD}(n)$, let us estimate $\beta^{-\binom{n}{2}} \le \beta^{-\ell(w(D))} \le 1$. Thus by (6.4), we have

$$\beta^{-\binom{n}{2}} \sum_{D \in \mathrm{PD}(n)} \beta^{\#\,\mathrm{cross}(D)} \le v_n(\beta) \le \sum_{D \in \mathrm{PD}(n)} \beta^{\#\,\mathrm{cross}(D)},$$

yielding $\left(\frac{1+\beta}{\beta}\right)^{\binom{n}{2}} \le v_n(\beta) \le (1+\beta)^{\binom{n}{2}}$, which leads to the desired bounds. □

7. Additional remarks and open problems

7.1. **Optimal permutations achieving the exact maxima $u_n(1)$ and $u_n(\beta)$.** This project was motivated by Stanley's original question from [Sta17] on determining the family of permutations w for which the Schubert specialization $\mathfrak{S}_w(1^n)$ is asymptotically maximal. This question as well as the asymptotic value remain widely open (see [MS16, Table 1] for data up to $n \le 10$). Dennin [Den22, Section 4.2, Fig. 8] extended this question to Grothendieck specializations $\mathfrak{G}_w^{\beta=1}(1^n)$, but one can ask the same question for general β. Presumably, answering this question would give rise to a family of optimal permutations w^β, which for $\beta = 0$ would answer the original Schubert specialization question.

Among the candidates for such a family w^β are the layered permutations [MS16], [MPP19] (see Appendix A for numerical evidence for $\beta = 1$). When $\beta = 1$, Dennin verified that layered permutations indeed achieve the maximum in $u_n(1)$ for $n \le 9$. Our results of Section 6.4 suggest that layered permutations are indeed good candidates as they at least attain the asymptotic maximum in $u_n(1)$.

To obtain the asymptotics of Grothendieck specializations on layered permutations for general β, one has to study the asymptotics of the following Hankel determinants:

$$F(k,n,\beta) := (1+\beta)^{-\binom{k}{2}} \det[\mathcal{L}_{n+i+j-2}(1+\beta)]_{i,j=1}^{k}, \tag{7.1}$$

where $\mathcal{L}_n(x)$ is the Narayana polynomial, see (6.8) and Theorem 6.15. For $\beta = 0$, these determinants admit a product formula and were analyzed in [MPP22]. We could access the special case $\beta = 1$ due to the connection to 2-enumerated ASMs and domino tilings. It would be interesting to find a deformation of the domino tiling model related to the determinants (7.1).

7.2. **Typical vs optimal permutations.** One of our main results, Theorem 1.5, concerns "typical" Grothendieck permutations. By comparing the permutation matrices in Figure 2, center, and Figure 4, left, we see that typical permutations are far from layered. However, it is likely that probabilities of typical Grothendieck random permutations also achieve the asymptotic maximum.

For our permutations, this is not yet a rigorous statement, as one has to prove the asymptotic uniformity of the probability weights of typical Grothendieck permutations.

7.3. **Measures on permutations generated by elementary transpositions.** Other Markov chains (and, more generally, stochastic processes on the symmetric group) have been studied where adjacent permutations are connected by an elementary transposition $s_i = (i, i+1)$, $i = 1, \dots, n-1$. These include the oriented swap process [AHR09], [BGR22], [Zha23a] which is a natural dynamics on permutations driven by independent nearest neighbor swaps, which swap only pairs of indices that has not been swapped before. The process starts from the identity and terminates at the full reversal permutation. Another model, random sorting networks [AHRV07], [GR19], [Dau22], is obtained by putting a uniform probability measure on all reduced words representing the full reversal permutation. Random sorting networks cannot be described by a simple Markov chain on permutations.

By design, both random sorting networks and the oriented swap process terminate at the full reversal permutation, and one is interested in the trajectories of individual elements. In contrast, out Grothendieck random permutations are obtained by running a Markov chain (reminiscent of the oriented swap process) for a set amount of "time", reading off the resulting permutation, and investigating its asymptotic properties. Despite the differences in the setup, in this work we observed certain asymptotic similarities between the Grothendieck random permutations and the models mentioned above.

7.4. **Local structure of Grothendieck permutations.** What is the local structure of the Grothendieck random permutations? In Figure 2, left and center, one can observe a certain local layered structure. Understanding this local structure goes beyond the permuton convergence. Can the local structure be understood in terms of descent statistics, major index, or pattern statistics other than the overall pattern counts? For instance, layered permutations are the ones maximizing the *packing density* of the pattern 132 [Kit11, Section 8.3.1]. Potential tools for this analysis may be found in [Bor20]. Alternatively, one could translate the local behavior of random domino tilings of the Aztec diamond [Joh05] to the local behavior of Grothendieck permutations.

7.5. **The RS shape of a Grothendieck permutation.** Applying the Robinson–Schensted (RS) correspondence to large random permutations, we numerically observe that the first column of the resulting Young diagram grows linearly with n, while all other rows and column are of order $\sqrt{n}$.[7] This behavior (except for the first column) is reminiscent of the limit shape phenomenon for Plancherel random partitions exhibiting the Vershik–Kerov–Logan–Shepp limit shape [VK77], [LS77]. It would be interesting to make these observations rigorous, and to find the limit shape for the Grothendieck random permutations. We are grateful to Philippe Biane for this suggestion.

7.6. **Random and maximal permutations for domain wall six-vertex model.** The Bumpless Pipe Dreams provide a surprising connection of Schubert calculus and K-theory to the six-vertex model, one of the central objects in statistical mechanics. The analysis of typical and maximal permutations for Schubert and Grothendieck specializations prompts the analogous questions about the six-vertex model.

Namely, consider the six-vertex model with domain wall boundary conditions and general Boltzmann weights a, b, c (for the 2-enumerated ASMs, we have $a = b = 1$ and $c = \sqrt{2}$). Represent a random configuration of the six-vertex model as a collection of pipes, and associate to it a random permutation $\mathbf{w}$ by resolving the intersections as in Definition 6.2. What is the behavior

[7] For layered permutations, all columns grow proportionally to n, while the rows are of order $\log n$.

of $\mathbb{E}[\mathrm{inv}(\mathbf{w})]$ and how does it vary depending on the weights of the six-vertex model? Do the permutations $\mathbf{w}$ have a permuton limit?

7.7. **q-analogues and generalized principal specialization.** Zhang [Zha23b] extended the analysis in [MPP19] to the *generalized principal Schubert specialization* $\mathfrak{S}_w(1, q, q^2, \ldots)$, when q is a root of unity. The analogue of layered permutations is the *multi-layered* ones [Zha23b, Section 4]. It would be interesting to extend our results to the Grothendieck specializations $\mathfrak{G}^{\beta}_w(1, q, q^2, \ldots)$ at a root of unity. However, having q complex makes connections to probabilistic models less clear.

Appendix A. Data for maximal specializations on layered permutations

A.1. **Dodgson condensation and data.** Principal specializations $\Upsilon_{w(b)}(\beta)$ of Grothendieck polynomials with general β on layered permutations (see Section 1.7 for notation) can be maximized using dynamic programming, similarly to how this is done for Schubert specializations in [MPP19]. To implement it, one needs an efficient way to compute the determinants $D_\beta(n,k) := \det[\mathcal{L}_{n+i+j-2}(1+\beta)]_{i,j=1}^{k}$ from Theorem 6.15. A recursion follows from the Dodgson condensation (Desnanot–Jacobi identity) [Dod66], [Mui06]:

Proposition A.1. *For $k, n \in \mathbb{Z}_{\geqslant 0}$, we have*

$$D_\beta(n,k) \;=\; \frac{1}{D_\beta(n+2,k-2)} \left(D_\beta(n+2,k-1) D_\beta(n,k-1) - D_\beta(n+1,k-1)^2 \right),$$

with initial conditions $D_\beta(n,0) = 1$, $D_\beta(n,1) = \mathcal{L}_n(1+\beta)$, and $D_\beta(0,k) = (1+\beta)^{\binom{k}{2}}$.

Proof. Let $M(n,k) = [\mathcal{L}_{n+i+j-2}(1+\beta)]_{i,j=1}^{k}$, so $D_\beta(n,k) = \det M(n,k)$. Clearly,

$$D_\beta(n,0) = 1, \qquad D_\beta(n,1) = \mathcal{L}_n(1+\beta).$$

For $n = 0$, the permutation $w_0(0;k) = 12\cdots k$ is the identity, and so $\mathfrak{G}^{\beta}_{w_0(0;k)} = 1$. By Theorem 6.15, we have

$$1 = \Upsilon_{w_0(n,k)}(\beta) = (1+\beta)^{-\binom{k}{2}} \det[\mathcal{L}_{i+j-2}(1+\beta)]_{i,j=1}^{k}.$$

Thus, $D_\beta(0,k) = \det M(0,k) = (1+\beta)^{\binom{k}{2}}$.

For $1 \leq i, j, p, q \leq k$, let $M_{i,j}^{p,q}$ denote the matrix obtained from M by deleting rows i and j and columns p and q. Similarly, let M_i^p be obtained from M by deleting row i and column p. By the Dodgson condensation, we have

$$\det(M(n,k)) \det(M(n,k)_{1,k}^{1,k}) \;=\; \det(M(n,k)_1^1) \det(M(n,k)_k^k) - \det(M(n,k)_1^k) \det(M(n,k)_k^1).$$

Observe that

$$M(n,k)_{1,k}^{1,k} = M(n+2,k-2), \quad M(n,k)_1^1 = M(n+2,k-1),$$
$$M(n,k)_k^k = M(n,k-1), \quad M(n,k)_1^k = M(n,k)_k^1 = M(n+1,k-1).$$

This implies the result. □

The implementation of the recursion for $D_\beta(n,k)$ combined with dynamic programming yields the data in Table 1. This data agrees with the asymptotic behavior $f(n) \to \frac{1}{2}$ obtained in Theorem 6.16.

n	$(\dots, b_2, b_1)$	$f(n)$
2	$(1,1)$	0.00000
3	$(1,2)$	0.17611
4	$(1,3)$	0.21621
5	$(1,1,3)$	0.24599
6	$(1,2,3)$	0.28068
7	$(1,2,4)$	0.31068
8	$(1,2,5)$	0.32354
9	$(1,3,5)$	0.33953
10	$(1,1,3,5)$	0.34821
11	$(1,1,3,6)$	0.35956
12	$(1,2,3,6)$	0.36955
13	$(1,2,4,6)$	0.37800
14	$(1,2,4,7)$	0.38614
15	$(1,2,4,8)$	0.39085
16	$(1,2,5,8)$	0.39618
17	$(1,3,5,8)$	0.40138
18	$(1,3,5,9)$	0.40550
19	$(1,1,3,5,9)$	0.40887
20	$(1,1,3,6,9)$	0.41252
21	$(1,1,3,6,10)$	0.41605
22	$(1,2,3,6,10)$	0.41946
23	$(1,2,4,6,10)$	0.42223
24	$(1,2,4,6,11)$	0.42517
25	$(1,2,4,7,11)$	0.42797
26	$(1,2,4,7,12)$	0.43021
27	$(1,2,4,8,12)$	0.43206
28	$(1,2,5,8,12)$	0.43392
29	$(1,2,5,8,13)$	0.43590
30	$(1,3,5,8,13)$	0.43780
40	$(1,2,4,6,10,17)$	0.45099
50	$(1,3,5,8,13,20)$	0.45956
60	$(1,1,3,6,10,15,24)$	0.46537
70	$(1,2,4,7,11,18,27)$	0.46983
80	$(1,2,5,8,13,20,31)$	0.47312
90	$(1,1,3,5,9,14,23,34)$	0.47573
100	$(1,2,3,6,10,16,25,37)$	0.47792
110	$(1,2,4,7,11,17,27,41)$	0.47975
120	$(1,2,4,8,12,19,30,44)$	0.48125

n	$(\dots, b_2, b_1)$	$f(n)$
130	$(1,3,5,8,13,21,32,47)$	0.48255
140	$(1,1,3,5,9,14,22,34,51)$	0.48367
150	$(1,1,3,6,10,15,24,36,54)$	0.48465
160	$(1,2,4,6,10,16,25,38,58)$	0.48552
170	$(1,2,4,7,11,17,27,41,60)$	0.48631
180	$(1,2,4,7,12,19,28,43,64)$	0.48701
190	$(1,2,5,8,12,20,30,45,67)$	0.48763
200	$(1,3,5,8,13,21,32,47,70)$	0.48820
210	$(1,3,5,9,14,22,33,49,74)$	0.48871
220	$(1,1,3,5,9,15,23,34,52,77)$	0.48917
230	$(1,1,3,6,10,15,24,36,54,80)$	0.48961
240	$(1,2,3,6,10,16,25,38,56,83)$	0.49001
250	$(1,2,4,6,10,17,26,39,59,86)$	0.49038
260	$(1,2,4,7,11,17,27,41,61,89)$	0.49072
270	$(1,2,4,7,12,18,28,42,63,93)$	0.49104
280	$(1,2,4,8,12,19,29,44,65,96)$	0.49134
290	$(1,2,5,8,12,20,30,45,68,99)$	0.49161
300	$(1,3,5,8,13,20,31,47,70,102)$	0.49187
310	$(1,3,5,8,14,21,32,48,72,106)$	0.49211
320	$(1,3,5,9,14,22,33,50,74,109)$	0.49234
330	$(1,1,3,5,9,14,23,34,52,76,112)$	0.49256
340	$(1,1,3,6,9,15,23,35,53,79,115)$	0.49276
350	$(1,1,3,6,10,15,24,36,55,81,118)$	0.49295
360	$(1,2,3,6,10,16,25,37,56,83,121)$	0.49314
370	$(1,2,4,6,10,16,25,38,58,85,125)$	0.49331
380	$(1,2,4,6,11,17,26,39,59,87,128)$	0.49347
390	$(1,2,4,7,11,17,27,41,60,89,131)$	0.49363
400	$(1,2,4,7,11,18,27,42,62,92,134)$	0.49378
410	$(1,2,4,7,12,18,28,43,64,94,137)$	0.49392
420	$(1,2,4,7,12,19,29,44,65,96,141)$	0.49406
430	$(1,2,5,8,12,19,30,45,67,98,143)$	0.49419
440	$(1,2,5,8,13,20,30,46,68,100,147)$	0.49431
450	$(1,3,5,8,13,20,31,47,70,102,150)$	0.49443
460	$(1,3,5,8,13,21,32,48,71,105,153)$	0.49454
470	$(1,3,5,8,14,21,33,49,73,107,156)$	0.49465
480	$(1,3,5,9,14,22,33,50,74,109,160)$	0.49476
490	$(1,1,3,5,9,14,22,34,51,76,111,163)$	0.49486
500	$(1,1,3,5,9,15,23,35,52,77,113,166)$	0.49495

TABLE 1. Tuples b of layered permutations $w(b)$ maximizing $u'_n(1)$ for $n = 2, \dots, 30$, and every 10 after up to 500. The third column is $f(n) := \frac{1}{n^2} \log_2 u'_n(1)$. The full table up to $n = 750$ is available on the `arXiv` as an ancillary `CSV` file.

A.2. **Optimal layered permutations and Theorem 6.16.** Observe that the optimal layered permutations given in Table 1 do not fall into the description of sequences given in Theorem 6.16. For example, for $n = 700$, the numerically optimal layered permutation has parts $b^{(700)}_{\text{opt}} = (1,3,5,9,14,21,33,49,73,107,157,228)$, whereas a sequence $b^{(700)}$ from Theorem 6.16 would satisfy the bound $b_1 = n - k \leqslant 700/(2+\sqrt{2}) \approx 205$ on its largest part. The parts of $b^{(700)}_{\text{opt}}$ are suspiciously close to the Fibonacci sequence (see Table 2). Let us explain this discrepancy.

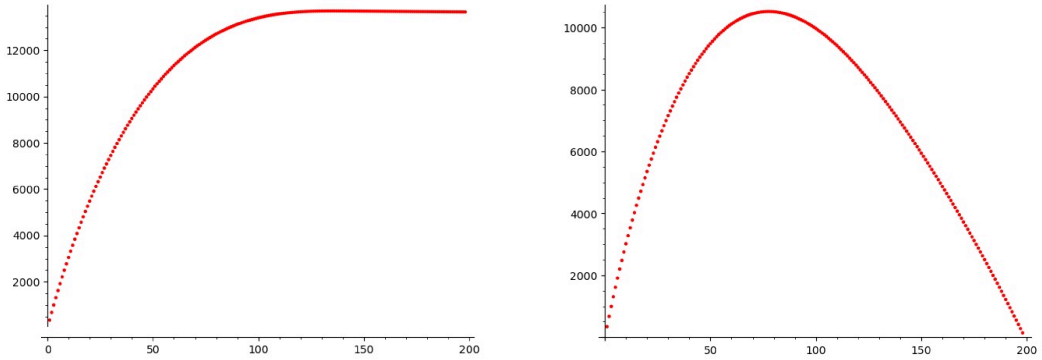

FIGURE 15. Plot of $\log_2 G(k, 200-k)$ (**left**) and $\log_2 F(k, 200-k)$ (**right**) for $k = 1, \dots, 200$. The maxima on the figures occurs at $k = 135$ and $k = 78$, respectively.

Optimal layered permutations can be constructed inductively via the optimization

$$\max_{b_1+b_2+\cdots=n} \Upsilon_{w(\dots,b_2,b_1)}(1) = \max_k \max_{b_2+b_3+\cdots=k} \bigl\{\Upsilon_{w(\dots,b_3,b_2)}(1) \cdot F(k, n-k)\bigr\},$$

where $b_1 = n-k$. Assume that $\max_{b_2+b_3+\cdots=k} \Upsilon_{w(\dots,b_3,b_2)}(1) = 2^{\binom{k}{2}} \cdot g(k)$, where $g(k) = 2^{-o(k^2)}$. To extract the first part b_1, we thus need to find

$$\max_k \bigl\{2^{\binom{k}{2}} \cdot g(k) \cdot F(k, n-k)\bigr\} = \max_k \bigl\{g(k) \cdot G(k, n-k)\bigr\},$$

see (6.12) for the notation. On the other hand, in the proof of Theorem 6.16 (in particular, see Lemma 6.19), we estimated the asymptotic behavior of $F(k, n-k)$, and found that the coefficient by n^2 in $\log_2 F(k, n-k)$ does not depend on k as long as $k > n/\sqrt{2}$. These two problems lead to different choices of k. See also the illustration in Figure 15.

n	1	1	2	3	5	8	13	21	34	55	89	144	233	377	610
k^*				1	2	3	5	8	13	21	34	56	90	147	237

TABLE 2. If n runs over the Fibonacci numbers, the optimal k^* maximizing $G(k, n-k)$ is close to the Fibonacci number of index 2 less. Note that k^* is not the same as $n - b_1$ in Table 1 due to the presence of the lower order term $g(k)$.

The discrepancy between optimal layered permutations and the ones appearing in Theorem 6.16 should be of order $o(n)$ in the large n limit. Indeed, assume that $k/n < 1/\sqrt{2}$. Then, as in the proof of Lemma 6.19 (see also Remark 6.20), one can show that $\log_2 F(k, n-k) \sim \alpha n^2 - k^2/2 - O(n)$ for some $\alpha < \frac{1}{2}$, so $2^{\binom{k}{2}} g(k) F(k, n-k) \sim 2^{\alpha n^2 - o(n^2)}$, which is not maximal. We believe that the discrepancy of the part sizes in optimal layered permutations is of order $o(n)$ as $n \to \infty$.

APPENDIX B. LIMIT SHAPE AND FLUCTUATIONS IN TASEP FROM CONTOUR INTEGRALS

In this section we compute the constants $\mathsf{c}, \mathsf{v}_1, \mathsf{v}_2$ from Definition 3.6, and show how to establish Theorem 3.7 by an asymptotic analysis of the correlation kernel. We omit tedious but standard estimates, as they are very similar to those in [Joh00, Section 3] or [Pet20].

B.1. **Fredholm determinant.** Recall that $\bar{\xi}_m(t) = \xi_m(t) - \xi_m(0)$ is the displacement of the m-th particle at time t. By Propositions 3.3 and 3.4, we have

$$\mathbb{P}_{\mathrm{TASEP}}(\bar{\xi}_m(t) \geqslant u) = \mathbb{P}(\lambda_m \geqslant u), \tag{B.1}$$

where λ_m is a point of the determinantal point process $X(\lambda) = \{\lambda_j + m - j\}_{j=1}^{m} \subset \mathbb{Z}_{\geqslant 0}$ with the correlation kernel (3.9):

$$K(u_1, u_2) = \frac{1}{(2\pi \mathbf{i})^2} \oiint \frac{dz\, dw}{z - w} \frac{w^{u_2}}{z^{u_1+1}} \left(\frac{z-p}{w-p}\right)^m \left(\frac{1-w}{1-z}\right)^t, \qquad u_1, u_2 \in \mathbb{Z}_{\geqslant 0}, \tag{B.2}$$

where the contours are positively oriented simple closed curves satisfying $p < |w| < |z| < 1$.

Lemma B.1. *The probability in the right-hand side of* (B.1) *is equal to the Fredholm determinant of the kernel K on $\{0, 1, \dots, u-1\}$:*

$$\mathbb{P}(\lambda_m \geqslant u) = \det\left[\mathrm{Id} - K\right]_{\leqslant u-1} := 1 + \sum_{\ell=1}^{\infty} \frac{(-1)^\ell}{\ell!} \sum_{i_1, \dots, i_\ell = 0}^{u-1} \det\left[K(i_a, i_b)\right]_{a,b=1}^{\ell}, \tag{B.3}$$

where Id *is the identity operator.*

Proof. The event $\{\lambda_m \geqslant u\}$ means that in the determinantal point process $X(\lambda)$, no particles are located in $\{0, 1, \dots, u-1\}$. It is a well-known property of determinantal point processes that this probability is given by a Fredholm determinant, see e.g. [Sos00, Theorem 2]. This statement can be traced back to the inclusion–exclusion principle (e.g., see [BOO00, Appendix A.3]). Note that the sum over ℓ in (B.3) is finite, as for $u > \ell$, the $\ell \times \ell$ determinant must have identical rows. Further details on Fredholm determinants may be found in [Sim05] or [Bor10]. □

Let us assume that $m = \lfloor L\mathsf{m} \rfloor$, $t = \lfloor L\mathsf{t} \rfloor$, $u = \lfloor L\mathsf{u} \rfloor$, where $L \to \infty$. By Lemma 3.5, it suffices to consider the case $\mathsf{t} \geqslant \mathsf{m}/p$, which we assume throughout the present Appendix B.

B.2. **Steepest descent and law of large numbers.** The asymptotic analysis of $K(u_1, u_2)$ is done by steepest descent (see, e.g., [Oko02, Section 3] for an accessible introduction). The integrand in (B.2) has the form

$$\frac{1}{z-w} \frac{w^{u_2}}{z^{u_1+1}} \left(\frac{z-p}{w-p}\right)^m \left(\frac{1-w}{1-z}\right)^t = \frac{\exp\left\{L\big(S(z; u_1/L) - S(w; u_2/L)\big) + O(1)\right\}}{z(z-w)}, \tag{B.4}$$

where

$$S(z; \mathsf{u}) := -\mathsf{u} \log z + \mathsf{m} \log(z-p) - \mathsf{t} \log(1-z). \tag{B.5}$$

The term $O(1)$ arises from dropping integer parts in m and t. It is negligible in the limit because the determinantal process will be scaled from discrete to continuous space.

The point λ_m is at the left edge of the determinantal process. Therefore, to catch its asymptotic location $\mathsf{u} = \mathsf{c}(\mathsf{m}, \mathsf{t})$, we need to find a *double critical point* of the function $z \mapsto S(z; \mathsf{u})$.

Remark B.2. Let us explain the need for the double critical point in more detail. By (3.8), we have $K(u, u) = \mathbb{P}(u \in X(\lambda))$, which is the density of the random point configuration $X(\lambda)$. The equation $S'(z; \mathsf{u}) = 0$ for single critical points is quadratic, and its discriminant is a function of p and our parameters $(\mathsf{m}, \mathsf{t}, \mathsf{u})$. Fox fixed m (viewed as a parameter of the determinantal process and not the scaled index on the last part λ_m), there are three possibilities depending on (t, u):

- If the discriminant is negative, then $K(u, u)$ converges to a value strictly between 0 and 1. Therefore, at the scaled time t around the scaled location u there is a random configuration of points from $X(\lambda)$ of density strictly between zero and one.

- If the discriminant is positive, then $K(u,u)$ converges to 0 or 1, and around u there is either a densely packed, or an empty region of points from $X(\lambda)$.
- The case of zero discriminant (double critical points) is at the transition between the two cases, and thus corresponds to the edge of the random configuration $X(\lambda)$.

Solving the double critical point equations $S'(z;\mathsf{u}) = S''(z;\mathsf{u}) = 0$ in z, u, we find

$$z_{cr} = \frac{\sqrt{p\mathsf{t}} - \sqrt{\mathsf{m}}}{\sqrt{\mathsf{t}/p} - \sqrt{\mathsf{m}}}, \qquad \mathsf{u}_{cr} = \frac{(\sqrt{p\mathsf{t}} - \sqrt{\mathsf{m}})^2}{1-p}. \tag{B.6}$$

Here out of two solutions to quadratic equations, we picked the one with the smaller u_{cr} which corresponds to the left edge of $X(\lambda)$. Note that the solution u_{cr} in (B.6) is the same as the constant $\mathsf{c}(\mathsf{m},\mathsf{t})$ from Definition 3.6, which is not a coincidence.

Let us deform the integration contours in the kernel (B.2) to pass near the double critical point z_{cr}. This point lies inside the interval $(0,p)$, while the original contours satisfy $p < |w| < |z| < 1$. Due to high multiplicity poles in the integrand, the w contour should not be deformed through p, and the z contour should not be deformed through 0 and 1.

We deform the contours as follows. First, deform w such that the new w contour goes around p and passes to the right of z_{cr}. Then, deform z through w, such that the new z contour goes around 0 and passes to the left of z_{cr}. Dragging z through w picks up a residue at $z = w$, which needs to be integrated over the new w contour. However, taking the residue at $z = w$ eliminated the pole at $w = p$, so the new single integral is zero. This implies that the contour deformation does not produce extra terms in the kernel. See Figure 16 for an illustration.

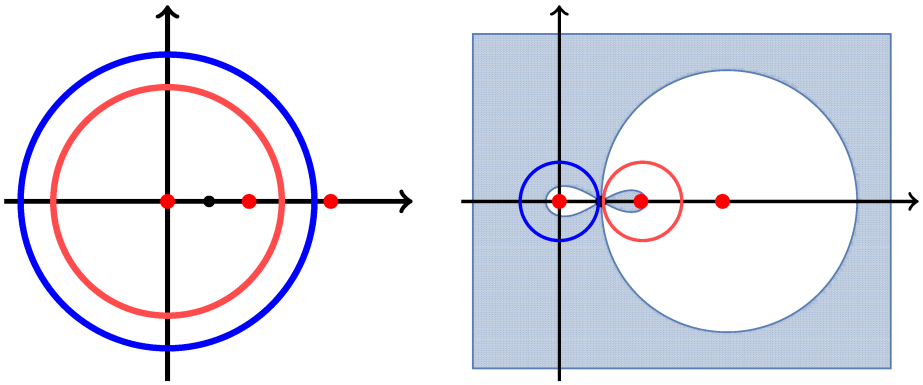

FIGURE 16. **Left**: Original contours in K (B.2). **Right**: Deformed contours passing through the critical point. All contours are positively oriented.
The highlighted region in the right plot is $\operatorname{Re}\big(S(z;\mathsf{u}_{cr}) - S(z_{cr};\mathsf{u}_{cr})\big) < 0$. The new z and w contour must lie inside (resp., outside) of this region for the contribution outside a neighborhood of z_{cr} to vanish in the limit. In this example, $p = 0.5$, $\mathsf{m} = 1$, $\mathsf{t} = 5$, so $z_{cr} \approx 0.27$ and $\mathsf{u}_{cr} \approx 0.68$. Large (red) dots show the points 0, p, and 1; the smaller dot is z_{cr}.

To arrive at the law of large numbers $\lambda_m/L \to \mathsf{c}(\mathsf{m},\mathsf{t})$ (recall that this is the same as u_{cr}), it remains to show that changing c by ε or $(-\varepsilon)$ makes the Fredholm determinant (B.3) go to 0 or 1, respectively. To show convergence to 1, it suffices to estimate $|K(u_1,u_2)| \leqslant e^{-\delta L}$ for $u_1, u_2 \leqslant L(\mathsf{c}-\varepsilon)$, which follows from the steepest descent analysis. To show convergence to 0, it suffices to look at the density function $K(u,u)$ for u around $L(\mathsf{c}+\varepsilon)$. In the limit, this density

is strictly positive, and so the event $\lambda_m \geqslant L(\mathsf{c}+\varepsilon)$ has probability tending to zero. We omit further details.

B.3. **Asymptotic fluctuations.** Consider the probabilities of fluctuations as in Theorem 3.7:

$$\mathbb{P}_{\mathrm{TASEP}}\left(\bar{\xi}_{\lfloor L\mathsf{m}-L^{1/3}\alpha\mathsf{v}_1\rfloor}(\lfloor L\mathsf{t}\rfloor)\geqslant L\mathsf{c}-L^{1/3}\beta\mathsf{v}_2\right)=\det\left[\mathrm{Id}-K^{L\mathsf{t},L\mathsf{m}-L^{1/3}\alpha\mathsf{v}_1}\right]_{\leqslant L\mathsf{c}-L^{1/3}\beta\mathsf{v}_2}+o(1). \tag{B.7}$$

Assume that m and t are fixed (recall that $\mathsf{c},\mathsf{v}_1,\mathsf{v}_2$ depend on them). In the right-hand side of (B.7), we dropped integer parts as they do not affect the limit to continuous space.

One can show that in the series (B.3) for the Fredholm determinant (B.7), terms where $i_a < L\mathsf{c}-sL^{1/3}$ for at least one $a=1,\dots,\ell$ (and s sufficiently large but finite), are negligible in the limit. Thus, it suffices to consider $\tilde{K}(\tilde{u}_1,\tilde{u}_2):=K^{L\mathsf{t},L\mathsf{m}-L^{1/3}\alpha\mathsf{v}_1}(L\mathsf{c}+\tilde{u}_1L^{1/3},L\mathsf{c}+\tilde{u}_2L^{1/3})$, where $\tilde{u}_1,\tilde{u}_2\in\mathbb{R}$. This computation will also produce the normalization constants v_1 and v_2 for the Tracy–Widom GUE fluctuations.

In $\tilde{K}$, deform the contours to pass near the double critical point $z_{cr}=z_{cr}(\mathsf{m},\mathsf{t})$ given by (B.6). The contribution outside a small neighborhood of z_{cr} vanishes in the limit. In the neighborhood, make a change of variables

$$z=z_{cr}+L^{-1/3}\frac{\tilde{z}}{\varrho},\qquad w=z_{cr}+L^{-1/3}\frac{\tilde{w}}{\varrho},$$

where $\varrho>0$ is to be determined. The new contour $\tilde{z}$ goes from $e^{-\frac{2\pi\mathbf{i}}{3}}\infty$ to -1 to $e^{\frac{2\pi\mathbf{i}}{3}}\infty$, and $\tilde{w}$ goes from $e^{-\frac{\pi\mathbf{i}}{3}}\infty$ to 0 to $e^{\frac{\pi\mathbf{i}}{3}}\infty$. The function (B.5) is Taylor expanded in L as

$$\begin{aligned}&L\left(S(z;\mathsf{c}+L^{-2/3}\tilde{u}_1)-S(z_{cr};\mathsf{c}+L^{-2/3}\tilde{u}_1)\right)\\&\qquad=-\frac{\tilde{z}^3}{3\varrho^3}\frac{p^{3/2}}{\sqrt{\mathsf{m}\mathsf{t}}}\frac{(\sqrt{\mathsf{t}/p}-\sqrt{\mathsf{m}})^4}{(1-p)^3z_{cr}}+\frac{\tilde{z}}{\varrho z_{cr}}\left(-\tilde{u}_1+\frac{\alpha\mathsf{v}_1(\sqrt{p\mathsf{t}/\mathsf{m}}-1)}{1-p}\right).\end{aligned}$$

Let us pick $\varrho>0$ such that the coefficient by $\tilde{z}^3$ is $(-1/3)$, that is,

$$\varrho=\frac{\sqrt{p}}{(1-p)\,z_{cr}}\frac{(\sqrt{p\mathsf{t}}-\sqrt{\mathsf{m}})^{2/3}(\sqrt{\mathsf{t}/p}-\sqrt{\mathsf{m}})^{2/3}}{(\mathsf{m}\mathsf{t})^{1/6}}.$$

We also have in the integrand:

$$\frac{dz\,dw}{z(z-w)}\sim-\frac{L^{-1/3}}{\varrho z_{cr}}\frac{d\tilde{z}\,d\tilde{w}}{\tilde{w}-\tilde{z}}.$$

Adding the difference $S(z_{cr};\mathsf{c}+L^{-2/3}\tilde{u}_2)-S(z_{cr};\mathsf{c}+L^{-2/3}\tilde{u}_1)$ inside the exponent in the integrand (B.4) does not change the correlation kernel, since it is a gauge transformation of the form $\tilde{K}(\tilde{u}_1,\tilde{u}_2)\mapsto\tilde{K}(\tilde{u}_1,\tilde{u}_2)\frac{f(\tilde{u}_2)}{f(\tilde{u}_1)}$, where $f(\cdot)$ is a nonvanishing function. Thus, we have

$$\tilde{K}(\tilde{u}_1,\tilde{u}_2)\frac{f(\tilde{u}_2)}{f(\tilde{u}_1)}\sim-\frac{L^{-1/3}}{\varrho z_{cr}}\int_{e^{-\frac{2\pi\mathbf{i}}{3}}\infty}^{e^{\frac{2\pi\mathbf{i}}{3}}\infty}d\tilde{z}\int_{e^{\frac{\pi\mathbf{i}}{3}}\infty}^{e^{-\frac{\pi\mathbf{i}}{3}}\infty}d\tilde{w}\,\frac{\exp\left[\frac{\tilde{w}^3}{3}-\frac{\tilde{z}^3}{3}+\tilde{z}U_1-\tilde{w}U_2\right]}{\tilde{w}-\tilde{z}}, \tag{B.8}$$

where

$$U_{1,2}:=\frac{1}{\varrho\,z_{cr}}\left(-\tilde{u}_{1,2}+\frac{\alpha\mathsf{v}_1(\sqrt{p\mathsf{t}/\mathsf{m}}-1)}{1-p}\right). \tag{B.9}$$

The integral in (B.8) together with the minus sign from the prefactor is equal to the celebrated Airy_2 kernel $\mathsf{A}(U_1, U_2)$ (e.g., see [Oko02, (40)]). The Tracy–Widom GUE cumulative distribution function is the Fredholm determinant of the Airy_2 kernel, that is, $F_2(r) = \det[\mathrm{Id} - \mathsf{A}]_{\geqslant r}$, $r \in \mathbb{R}$.

The additional prefactor $(L^{1/3}\varrho z_{cr})^{-1}$ in (B.8) combined with the sums in the pre-limit Fredholm determinant (B.3) turns them into Riemann integrals of the Airy_2 kernel. The normalization by ϱz_{cr} is absorbed by a change of variables:

$$\frac{1}{L^{1/3}\varrho z_{cr}} \sum_{i=\lfloor L^{1/3}\tilde{u}\rfloor \leqslant -L^{1/3}\beta \mathsf{v}_2} g(\tilde{u}) \sim \frac{1}{\varrho z_{cr}} \int_{-\infty}^{-\beta\mathsf{v}_2} g(\tilde{u})\, d\tilde{u} = \int_{\frac{1}{\varrho z_{cr}}\left(\beta\mathsf{v}_2 + \frac{\alpha \mathsf{v}_1(\sqrt{p\mathsf{t}/\mathsf{m}}-1)}{1-p}\right)}^{+\infty} \mathsf{g}(U)\, dU.$$

Here we incorporated the bound $L\mathsf{c} - L^{1/3}\beta\mathsf{v}_2$ from (B.7) into the bound for i, and shifted all indices by $L\mathsf{c}$. The function $g(\tilde{u})$ represents terms like $K(\cdot, i_a)K(i_a, \cdot)$ in the Fredholm determinant (B.3) arising when expanding the individual $\ell \times \ell$ determinants as sums over permutations. Here $\tilde{u}$ and i_a are related as $i_a = \lfloor L^{1/3}\tilde{u}\rfloor$. We also set $\mathsf{g}(U) = \mathsf{g}(\tilde{u})$.

We see that the following convergence of Fredholm determinants holds:

$$\lim_{L\to\infty} \det\left[\mathrm{Id} - K^{L\mathsf{t}, L\mathsf{m} - L^{1/3}\alpha\mathsf{v}}\right]_{\leqslant L\mathsf{c}} = \det\left[\mathrm{Id} - \mathsf{A}\right]_{\geqslant r}, \tag{B.10}$$

where

$$r = \frac{1}{\varrho z_{cr}}\left(\beta\mathsf{v}_2 + \frac{\alpha\mathsf{v}_1(\sqrt{p\mathsf{t}/\mathsf{m}} - 1)}{1-p}\right).$$

We see that setting

$$\begin{aligned} \mathsf{v}_1 = \mathsf{v}_1(\mathsf{m}, \mathsf{t}) &:= \frac{\varrho z_{cr}(1-p)}{\sqrt{p\mathsf{t}/\mathsf{m}} - 1} = \frac{\sqrt{p}\mathsf{m}^{1/3}}{\mathsf{t}^{1/6}} \frac{(\sqrt{\mathsf{t}/p} - \sqrt{\mathsf{m}})^{2/3}}{(\sqrt{p\mathsf{t}} - \sqrt{\mathsf{m}})^{1/3}}; \\ \mathsf{v}_2 = \mathsf{v}_2(\mathsf{m}, \mathsf{t}) &:= \varrho z_{cr} = \frac{\sqrt{p}}{(1-p)} \frac{(\sqrt{p\mathsf{t}} - \sqrt{\mathsf{m}})^{2/3}(\sqrt{\mathsf{t}/p} - \sqrt{\mathsf{m}})^{2/3}}{(\mathsf{m}\mathsf{t})^{1/6}} \end{aligned} \tag{B.11}$$

turns the right-hand side of (B.10) into the Tracy–Widom GUE distribution $F_2(\alpha + \beta)$. This completes the proof of Theorem 3.7.

References

[AD95] D. Aldous and P. Diaconis, *Hammersley's interacting particle process and longest increasing subsequences*, Probab. Theory Relat. Fields **103** (1995), no. 2, 199–213. ↑20

[AHR09] O. Angel, A. Holroyd, and D. Romik, *The oriented swap process*, Ann. Probab. **37** (2009), 1970–1998. arXiv:0806.2222. ↑39

[AHRV07] O. Angel, A. E. Holroyd, D. Romik, and B. Virág, *Random Sorting Networks*, Adv. Math. **215** (2007), 1–27. arXiv:math/0609538 [math.PR]. ↑39

[BB21] A. Borodin and A. Bufetov, *Color-position symmetry in interacting particle systems*, Ann. Probab. **49** (2021), no. 4, 1607–1632. arXiv:1905.04692 [math.PR]. ↑14

[BB93] N. Bergeron and S. Billey, *RC-graphs and Schubert polynomials*, Experiment. Math. **2** (1993), no. 4, 257–269. MR1281474 ↑4

[BBCS18] J. Baik, G. Barraquand, I. Corwin, and T. Suidan, *Pfaffian Schur processes and last passage percolation in a half-quadrant*, Ann. Probab. **46** (2018), no. 6, 3015–3089. arXiv:1606.00525 [math.PR]. ↑9

[BBCW18] G. Barraquand, A. Borodin, I. Corwin, and M. Wheeler, *Stochastic six-vertex model in a half-quadrant and half-line open asymmetric simple exclusion process*, Duke Math. J. **167** (2018), no. 13, 2457–2529. arXiv:1704.04309 [math.PR]. ↑9

[BBF+20] F. Bassino, M. Bouvel, V. Féray, L. Gerin, M. Maazoun, and A. Pierrot, *Universal limits of substitution-closed permutation classes*, J. Eur. Math. Soc. **22** (2020), no. 11, 3565–3639. arXiv:1706.08333 [math.PR]. ↑6, 23, 24, 29

[Beh08] R. E. Behrend, *Osculating paths and oscillating tableaux*, Electron. J. Combin. **15** (2008), no. 1, R7. arXiv:math/0701755 [math.CO]. ↑30

[BF14] A. Borodin and P. Ferrari, *Anisotropic growth of random surfaces in 2+1 dimensions*, Commun. Math. Phys. **325** (2014), 603–684. arXiv:0804.3035 [math-ph]. ↑16, 19

[BFH+23] B. Brubaker, C. Frechette, A. Hardt, E. Tibor, and K. Weber, *Frozen pipes: lattice models for Grothendieck polynomials*, Algebraic Combinatorics **6** (2023), no. 3, 789–833 (en). ↑4

[BGG73] I.N. Bernstein, I.M. Gelfand, and S.I. Gelfand, *Schubert cells, and the cohomology of the spaces G/P*, Russian Math. Surveys **28** (1973), no. 3, 1–26. ↑5

[BGR22] A. Bufetov, V. Gorin, and D. Romik, *Absorbing time asymptotics in the oriented swap process*, Ann. Appl. Probab. **32** (2022), no. 2, 753–763. ↑39

[BOO00] A. Borodin, A. Okounkov, and G. Olshanski, *Asymptotics of Plancherel measures for symmetric groups*, Jour. AMS **13** (2000), no. 3, 481–515. arXiv:math/9905032 [math.CO]. ↑43

[Bor10] F. Bornemann, *On the numerical evaluation of Fredholm determinants*, Math. Comp. **79** (2010), no. 270, 871–915. arXiv:0804.2543 [math.NA]. ↑43

[Bor11] A. Borodin, *Determinantal point processes*, Oxford handbook of random matrix theory, 2011. arXiv:0911.1153 [math.PR]. ↑19

[Bor20] J. Borga, *Local convergence for permutations and local limits for uniform ρ-avoiding permutations with $|\rho| = 3$*, Probab. Theory Relat. Fields **176** (2020), no. 1, 449–531. arXiv:1807.02702 [math.PR]. ↑39

[BR05] A. Borodin and E.M. Rains, *Eynard–Mehta theorem, Schur process, and their Pfaffian analogs*, J. Stat. Phys **121** (2005), no. 3, 291–317. arXiv:math-ph/0409059. ↑19

[Bre99] D. M. Bressoud, *Proofs and Confirmations: The Story of the Alternating-Sign Matrix Conjecture*, Cambridge University Press, 1999. ↑30

[BS22] V. Buciumas and T. Scrimshaw, *Double Grothendieck Polynomials and Colored Lattice Models*, Int. Math. Res. Not. **2022** (2022), no. 10, 7231–7258. ↑4

[Buf20] A. Bufetov, *Interacting particle systems and random walks on Hecke algebras*, arXiv preprint (2020). arXiv:2003.02730 [math.PR]. ↑8

[BW20] A. Borodin and M. Wheeler, *Observables of coloured stochastic vertex models and their polymer limits*, Probab. Math. Phys. **1** (2020), 205–265. arXiv:2001.04913 [math.PR]. ↑14

[BW22] A. Borodin and M. Wheeler, *Colored stochastic vertex models and their spectral theory*, Astérisque **437** (2022). arXiv:1808.01866 [math.PR]. ↑13, 15

[CEP96] H. Cohn, N. Elkies, and J. Propp, *Local statistics for random domino tilings of the Aztec diamond*, Duke Math. J. **85** (1996), no. 1, 117–166. arXiv:math/0008243 [math.CO]. ↑7, 32, 36

[CJY15] S. Chhita, K. Johansson, and B. Young, *Asymptotic domino statistics in the Aztec diamond*, Ann. Appl. Probab. **25** (2015), no. 3, 1232–1278. arXiv:1212.5414 [math.PR]. ↑32

[CKP01] H. Cohn, R. Kenyon, and J. Propp, *A variational principle for domino tilings*, Jour. AMS **14** (2001), no. 2, 297–346. arXiv:math/0008220 [math.CO]. ↑7, 32, 36

[Cor12] I. Corwin, *The Kardar-Parisi-Zhang equation and universality class*, Random Matrices Theory Appl. **1** (2012), 1130001. arXiv:1106.1596 [math.PR]. ↑2, 8, 20

[CP24] F. Colomo and A.G. Pronko, *Scaling limit of domino tilings on a pentagonal domain*, arXiv preprint (2024). arXiv:2407.07849 [math-ph]. ↑36

[Dau22] D. Dauvergne, *The Archimedean limit of random sorting networks*, J. Amer. Math. Soc. **35** (2022), 1215–1267. arXiv:1802.08934 [math.PR]. ↑39

[Def24] Colin Defant, *Random subwords and pipe dreams*, 2024. ↑9, 29

[Dem74] M. Demazure, *Désingularisation des variétés de Schubert généralisées*, Ann. Sci. École Norm. Supér. **7** (1974), no. 1, 53–88. ↑4, 5

[Den22] H. Dennin, *Pattern bounds for principal specializations of β-Grothendieck Polynomials*, arXiv preprint (2022). arXiv:2206.10017 [math.CO]. ↑2, 37, 38

[DG77] P. Diaconis and R. L. Graham, *Spearman's footrule as a measure of disarray*, J. R. Stat. Soc. Ser. B **39** (1977), no. 2, 262–268. ↑28

[DMO05] M. Draief, J. Mairesse, and N. O'Connell, *Queues, stores, and tableaux*, J. Appl. Probab. **42** (2005), no. 4, 1145–1167. arXiv:0707.4104 [cs.DM]. ↑16, 19

[Dod66] C. L. Dodgson, *Condensation of Determinants, Being a New and Brief Method for Computing their Arithmetical Values*, Proc. R. Soc. Lond. **15** (1866), 150–155. ↑40

[DW08] A.B. Dieker and J. Warren, *Determinantal transition kernels for some interacting particles on the line*, Annales de l'Institut Henri Poincaré **44** (2008), no. 6, 1162–1172. arXiv:0707.1843 [math.PR]. ↑16

[EF05] S.-P. Eu and T.-S. Fu, *A Simple Proof of the Aztec Diamond Theorem*, Electron. J. Combin. **12** (2005), no. 1, R18. arXiv:math/0412041 [math.CO]. ↑36

[EKLP92] N. Elkies, G. Kuperberg, M. Larsen, and J. Propp, *Alternating-sign matrices and domino tilings*, Jour. Alg. Comb. **1** (1992), no. 2-3, 111–132 and 219–234. ↑7, 32

[FK94] S. Fomin and A.N. Kirillov, *Grothendieck polynomials and the Yang-Baxter equation*, Proc. formal power series and alg. comb, 1994, pp. 183–190. ↑4

[FK96] S. Fomin and A.N. Kirillov, *The Yang-Baxter equation, symmetric functions, and Schubert polynomials*, Discrete Mathematics **153** (1996), no. 1-3, 123–143. ↑4

[FK97] S. Fomin and A.N. Kirillov, *Reduced words and plane partitions*, J. Algebraic Combin. **6** (1997), no. 4, 311–319. MR1471891 ↑33

[FS06] P.L. Ferrari and H. Spohn, *Domino tilings and the six-vertex model at its free-fermion point*, J. Phys. A **39** (2006), no. 33, 10297. arXiv:cond-mat/0605406 [cond-mat.stat-mech]. ↑7, 32, 33

[GH23] Y. Gao and D. Huang, *The canonical bijection between pipe dreams and bumpless pipe dreams*, Int. Math. Res. Not. IMRN **21** (2023), 18629–18663. MR4665632 ↑31

[GR19] V. Gorin and M. Rahman, *Random sorting networks: local statistics via random matrix laws*, Probab. Theory Relat. Fields **175** (2019), 45–96. arXiv:1702.07895 [math.PR]. ↑39

[Grü24] R. Grübel, *Ranks, copulas, and permutons*, Metrika **87** (2024), 155–182. arXiv:2206.12153 [math.ST]. ↑6, 7, 23, 24, 29

[GV85] I. Gessel and G. Viennot, *Binomial determinants, paths, and hook length formulae*, Adv. Math. **58** (1985), no. 3, 300–321. ↑35

[HKM+13] C. Hoppen, Y. Kohayakawa, C. G. Moreira, B. Ráth, and R. M. Sampaio, *Limits of permutation sequences*, J. Comb. Theory Ser. B **103** (2013), no. 1, 93–113. arXiv:1103.5844 [math.CO]. ↑6, 23, 24

[HKPV06] J.B. Hough, M. Krishnapur, Y. Peres, and B. Virág, *Determinantal processes and independence*, Probability Surveys **3** (2006), 206–229. arXiv:math/0503110 [math.PR]. ↑19

[HKYY19] B. H. Hwang, J. S. Kim, M. Yoo, and S. M. Yun, *Reverse plane partitions of skew staircase shapes and q-Euler numbers*, J. Combin. Theory Ser. A **168** (2019), 120–163. arXiv:1711.02337 [math.CO]. ↑34

[HSY24] D. Huang, M. Shimozono, and T. Yu, *Marked Bumpless Pipedreams and Compatible Pairs*, arXiv preprint (2024). arXiv:2407.18160 [math.CO]. ↑12, 32

[HT15] T. Halpin-Healy and K. Takeuchi, *A KPZ cocktail-shaken, not stirred...*, J. Stat. Phys **160** (2015), no. 4, 794–814. arXiv:1505.01910 [cond-mat.stat-mech]. ↑20

[Jim86] M. Jimbo, *Quantum R matrix for the generalized Toda system*, Commun. Math. Phys. **102** (1986), 537–547. ↑13

[JN06] K. Johansson and E. Nordenstam, *Eigenvalues of GUE minors*, Electron. J. Probab. **11** (2006), no. 50, 1342–1371. arXiv:math/0606760 [math.PR]. Erratum: Electron. J. Probab. 12 (2007), 1048–1051. ↑33

[Joh00] K. Johansson, *Shape fluctuations and random matrices*, Commun. Math. Phys. **209** (2000), no. 2, 437–476. arXiv:math/9903134 [math.CO]. ↑19, 42

[Joh05] K. Johansson, *The arctic circle boundary and the Airy process*, Ann. Probab. **33** (2005), no. 1, 1–30. arXiv:math/0306216 [math.PR]. ↑39

[JPS98] W. Jockusch, J. Propp, and P. Shor, *Random domino tilings and the arctic circle theorem*, arXiv preprint (1998). arXiv:math/9801068 [math.CO]. ↑36

[Kit11] S. Kitaev, *Patterns in permutations and words*, Monographs in Theoretical Computer Science. An EATCS Series, Springer, Heidelberg, 2011. With a foreword by Jeffrey B. Remmel. MR3012380 ↑39

[KM59] S. Karlin and J. McGregor, *Coincidence probabilities*, Pacific J. Math. **9** (1959), 1141–1164. ↑35

[Kup96] G. Kuperberg, *Another proof of the alternative-sign matrix conjecture*, Intern. Math. Research Notices **1996** (1996), no. 3, 139–150. ↑30, 32

[KZJ00] V. Korepin and P. Zinn-Justin, *Thermodynamic limit of the six-vertex model with domain wall boundary conditions*, Journal of Physics A: Mathematical and General **33** (2000), no. 40, 7053. ↑32

[Las02] A. Lascoux, *Chern and Yang through ice*, 2002. Unpublished manuscript. ↑7, 29, 30

[Las90] A. Lascoux, *Anneau de Grothendieck de la variété de drapeaux*, Modern Birkhäuser Classics, Birkhäuser Boston, 1990. ↑4, 5

[Lie67] E.H. Lieb, *Residual entropy of square ice*, Physical Review **162** (1967), no. 1, 162–172. ↑32

[Lig05] T. Liggett, *Interacting Particle Systems*, Springer-Verlag, Berlin, 2005. ↑15

[Lig76] T. Liggett, *Coupling the simple exclusion process*, Ann. Probab. (1976), 339–356. ↑15

[Lin73] B. Lindström, *On the vector representations of induced matroids*, Bulletin of the London Mathematical Society **5** (1973), no. 1, 85–90. ↑35

[LLS23] T. Lam, S. J. Lee, and M. Shimozono, *Back stable K-theory Schubert calculus*, Int. Math. Res. Not. IMRN **24** (2023), 21381–21466. arXiv:2108.10202 [math.CO]. ↑4, 29

[LS77] BF Logan and L.A. Shepp, *A variational problem for random Young tableaux*, Adv. Math. **26** (1977), no. 2, 206–222. ↑39

[LS82] A. Lascoux and M.-P. Schützenberger, *Structure de Hopf de l'anneau de cohomologie et de l'anneau de Grothendieck d'une variété de drapeaux*, C. R. Acad. Sci. Paris Sér. I Math. **295** (1982), no. 11, 629–633. ↑5

[Mac91] I.G. Macdonald, *Notes on Schubert Polynomials*, Université du Québec à Montréal, 1991. ↑34

[Man01] L. Manivel, *Symmetric functions, Schubert polynomials and degeneracy loci*, SMF/AMS Texts and Monographs, vol. 6, American Mathematical Society, Providence, RI; Société Mathématique de France, Paris, 2001. Translated from the 1998 French original by J. R. Swallow. ↑34

[MP17] K. Matveev and L. Petrov, *q-randomized Robinson–Schensted–Knuth correspondences and random polymers*, Annales de l'IHP D **4** (2017), no. 1, 1–123. arXiv:1504.00666 [math.PR]. ↑19

[MPP19] A. H. Morales, I. Pak, and G. Panova, *Asymptotics of principal evaluations of Schubert polynomials for layered permutations*, Proc. Amer. Math. Soc. **147** (2019), 1377–1389. arXiv:1805.04341 [math.CO]. ↑2, 11, 38, 40

[MPP22] A. H. Morales, I. Pak, and G. Panova, *Hook Formulas for Skew Shapes IV. Increasing Tableaux and Factorial Grothendieck Polynomials*, J. Math. Sci. **261** (2022), 630–657. ↑2, 33, 34, 37, 38

[MS16] G. Merzon and E. Smirnov, *Determinantal identities for flagged Schur and Schubert polynomials*, Eur. J. Math. **2** (2016), 227–245. arXiv:1410.6857 [math.CO]. ↑11, 38

[Mui06] T. Muir, *The theory of determinants*, 2nd ed., Vol. 1, Macmillan, London, 1906. ↑40

[OEI] OEIS Foundation Inc. and Sloane, N.J.A., *The On-Line Encyclopedia of Integer Sequences*. Available at http://oeis.org. ↑4, 33, 35

[Oko01] A. Okounkov, *Infinite wedge and random partitions*, Selecta Math. **7** (2001), no. 1, 57–81. arXiv:math/9907127 [math.RT]. ↑18, 19

[Oko02] A. Okounkov, *Symmetric functions and random partitions*, Symmetric functions 2001: Surveys of developments and perspectives, 2002. arXiv:math/0309074 [math.CO]. ↑43, 46

[Pet20] L. Petrov, *PushTASEP in inhomogeneous space*, Electron. J. Probab. **25** (2020), no. 114, 1–25. arXiv:1910.08994 [math.PR]. ↑42

[Pet25] L. Petrov, *Grothendieck shenanigans - simulation of random permutations from staircase reduced word*, 2025. Available at: https://lpetrov.cc/simulations/2025-01-26-grothendieck-shenanigans/, Accessed on: 2025-01-26. ↑6

[Pro90] R. Proctor, *New symmetric plane partition identities from invariant theory work of De Concini and Procesi*, European J. Combin. **11** (1990), no. 3, 289–300. MR1059559 ↑33

[QS15] J. Quastel and H. Spohn, *The one-dimensional KPZ equation and its universality class*, J. Stat. Phys **160** (2015), no. 4, 965–984. arXiv:1503.06185 [math-ph]. ↑20

[Res10] N. Reshetikhin, *Lectures on the integrability of the 6-vertex model*, Exact Methods in Low-dimensional Statistical Physics and Quantum Computing, 2010, pp. 197–266. arXiv:1010.5031 [math-ph]. ↑30

[Ros81] H. Rost, *Nonequilibrium behaviour of a many particle process: density profile and local equilibria*, Z. Wahrsch. Verw. Gebiete **58** (1981), no. 1, 41–53. ↑20

[Sim05] B. Simon, *Trace ideals and their applications: Second edition*, Mathematical Surveys and Monographs, vol. 120, AMS, 2005. ↑43

[Sos00] A. Soshnikov, *Determinantal random point fields*, Russian Mathematical Surveys **55** (2000), no. 5, 923–975. arXiv:math/0002099 [math.PR]. ↑19, 43

[Sta17] R. Stanley, *Some schubert shenanigans*, arXiv preprint (2017). arXiv:1704.00851 [math.CO]. ↑1, 38

[TW93] C. Tracy and H. Widom, *Level-spacing distributions and the Airy kernel*, Physics Letters B **305** (1993), no. 1, 115–118. arXiv:hep-th/9210074. ↑20

[VK77] A.M. Vershik and S.V. Kerov, *Asymptotics of the Plancherel measure of the symmetric group and the limiting form of Young tableaux*, Doklady AN SSSR **233** (1977), no. 6, 1024–1027. English translation: Soviet Mathematics Doklady **18** (1977), 527—531. ↑39

[VK86] A. Vershik and S. Kerov, *The characters of the infinite symmetric group and probability properties of the Robinson-Shensted-Knuth algorithm*, SIAM J. Alg. Disc. Math. **7** (1986), no. 1, 116–124. ↑16, 19

[Wei21] A. Weigandt, *Bumpless pipe dreams and alternating sign matrices*, J. Comb. Theory Ser. A **182** (2021), 105470. arXiv:2003.07342 [math.CO]. ↑4, 7, 29, 30, 31

[Zei96] D. Zeilberger, *Proof of the alternating sign matrix conjecture*, Electron. J. Combin **3** (1996), no. 2, R13. ↑32

[Zha23a] L. Zhang, *Shift-invariance of the colored TASEP and finishing times of the oriented swap process*, Adv. Math. **415** (2023), 108884. arXiv:2107.06350 [math.PR]. ↑39

[Zha23b] N. Zhang, *Principal specializations of Schubert polynomials, multi-layered permutations and asymptotics*, 2023. arXiv:2311.04487 [math.CO]. ↑40

[ZJ00] P. Zinn-Justin, *Six-vertex model with domain wall boundary conditions and one-matrix model*, Phys. Rev. E **62** (2000), no. 3, 3411. arXiv:math-ph/0005008. ↑7, 32

[ZJ09] P. Zinn-Justin, *Six-Vertex, Loop and Tiling models: Integrability and Combinatorics* (2009). arXiv:0901.0665 [math-ph]. ↑30

A. H. Morales, Université du Québec à Montréal, Montreal, QC, Canada and University of Massachusetts Amherst, Amherst, MA, USA
E-mail: morales_borrero.alejandro@uqam.ca

G. Panova, University of Southern California, Los Angeles, CA, USA
E-mail: gpanova@usc.edu

L. Petrov, University of Virginia, Charlottesville, VA, USA
E-mail: lenia.petrov@gmail.com

D. Yeliussizov, Kazakh–British Technical University, Almaty, Kazakhstan
E-mail: yeldamir@gmail.com